ION-MOLECULE REACTION KINETICS OF A SERIES OF 5-MEMBERED AND 6-MEMBERED

CYCLIC MOLECULES: SIGNIFICANCE TO THE INTERSTELLAR MEDIUM AND TITAN'S

ATMOSPHERE

by

LILLIAN DALILA MATHEWS

(Under the Direction of Nigel G. Adams)

ABSTRACT

The importance of cyclic species in both the interstellar medium (ISM) and

Titan's atmosphere has been realized since benzene was positively identified in both

environments. In the ISM, benzene is likely involved in the formation of multi-ring

species such as polycyclic aromatic hydrocarbons (PAHs). These PAHs are considered to

be responsible for the unidentified infrared bands (UIR) detected in the ISM.   In

addition, the haze that obscures the surface of Titan is thought to be composed partially

of PAHs. PAHs are thought to be formed from the very abundant benzene present in

the atmosphere.   Nitrogen is also abundantly available in the atmosphere of Titan and

is sure to be incorporated into the rings as they develop. Indeed, a mass corresponding

to that of pyridine (C_5H_5N), a nitrogen analogue of benzene, has been detected by the

Ion Neutral Mass Spectrometer aboard the Cassini Orbiter as it passed through Titan's

atmosphere. Because of the importance of cyclic species in this atmosphere and that of

the ISM, and because of the lack of kinetic data available, a selected ion flow tube (SIFT)

has been used to study the ion-neutral reactions of a series of ions with several five and six member cyclic molecules that are of interest to both environments. Rate coefficients and product distributions were determined for each reaction at 298 K. The ions N_2^+, N^+, O^+, O_2^+, NH_3^+, NH_4^+, H_3O^+, Ne^+, Ar^+, and Kr^+ were reacted with piperidine, pyridine, and pyrimidine. The stability of each cyclic molecule was investigated as a function of the recombination energy of the various ions. $C_4H_4^+$ was reacted with hydrogen cyanide to determine if this ion-neutral reaction was a plausible formation route for pyridine in the ionosphere of Titan. CH_3^+ and $C_3H_3^+$ were reacted with cyclohexane, piperidine, pyrrolidine, 1,4-dioxane, benzene, toluene, pyridine, pyrimidine, pyrrole, and furan. For both CH_3^+ and $C_3H_3^+$ association product channels were present. This provides a mechanism for increasing the complexity of cyclic species and possibly even conversion from a single ring to a multi-ring molecule. The relevance of these data to Titan and the ISM is discussed.

INDEX WORDS: Selected Ion Flow Tube, Ion-Molecule Reactions, Nitrogen
                heterocycle, Oxygen heterocycle, Interstellar Medium,
                Association, Titan's ionosphere,

ION-MOLECULE REACTION KINETICS OF A SERIES OF 5-MEMBERED AND 6-MEMBERED

CYCLIC MOLECULES: SIGNIFICANCE TO THE INTERSTELLAR MEDIUM AND TITAN'S

ATMOSPHERE

by

LILLIAN DALILA MATHEWS

B.S., The University of Montevallo, 2004

A Dissertation Submitted to the Graduate Faculty of The University of Georgia in Partial

Fulfillment of the Requirements for the Degree

DOCTOR OF PHILOSOPHY

ATHENS, GEORGIA

2010

ION-MOLECULE REACTION KINETICS OF A SERIES OF 5-MEMBERED AND 6-MEMBERED

CYCLIC MOLECULES: SIGNIFICANCE TO THE INTERSTELLAR MEDIUM AND TITAN'S

ATMOSPHERE

by

LILLIAN DALILA MATHEWS

Major Professor: Nigel G. Adams

Committee: Geoffrey D. Smith
                 I. Jonathan Amster

Electronic Version Approved:

Maureen Grasso
Dean of the Graduate School
The University of Georgia
May 2010

DEDICATION

To my mother. You instilled in me the importance of an education and never let me give up. You always believed I could do anything I put my mind to and I wish you were here to witness the end result of your encouragement and faith in me. I miss and love you and promise you this is not the end of my quest for knowledge.

In Memoriam of Lula Belle Fondren 1955-2006

ACKNOWLEDGEMENTS

Last and most importantly I want to thank those I love the most- my family. Dad, thank you for the brains and monetary support all of these years. Lena, thank you for the beach vacations and silly phone calls. Ashley, thank you for moving to Athens so I wouldn't be alone and for being such a wonderful friend. Mary, thank you for the encouraging phone calls and for not getting mad when I forget the four hour time difference and call you at 6 in the morning. You three are the best sisters a girl could have. Brad and Kristie, thank you for always being there for me. Donna, thank you for all the encouragement, especially toward the end, and for being the best Aunt in the world! Carol, thank you for being a great role model and a constant source of strength. Wayne and Kathy, thank you for all of your love and support. Finally, to my wonderful husband, Charles, thank you for listening to me talk about chemistry constantly and still loving me.

TABLE OF CONTENTS

LIST OF TABLES

LIST OF FIGURES

CHAPTER 1

INTRODUCTION AND BACKGROUND

1.1 INTRODUCTION

Improvements in the telescopes used to observe interstellar molecules have provided a wealth of information on the species present in many interstellar environments. Radio telescopes are used for ground based observations and the recent completion of the Robert C. Byrd Green Bank Telescope, the overhaul of the Very Large Array to replace the electronics and receivers of the 1970's and the construction of the Atacma Large Millimeter/Submillmeter Array in Chile all are advancing the field of astrochemistry[1-3]. The new improvements mean that the telescopes can detect weaker signals than before and thus have added to the list of species identified. Improvements to ground based telescopes have and will continue to allow the search of a larger range of radio wavelengths permitting many more species to be identified.

To detect signals emitted in all but radio waves it has been necessary to escape the obscuring effect of the Earth's troposphere. In order to make observations in the infrared without the cost of a spacecraft telescope, the Kuiper Airborn Observatory (KAO)[4], which was comprised of a telescope mounted on a C-1471A jet, began flying from Ames in 1971. KAO missions ended in 1995 and a new airborne observatory named the Stratospheric Observatory for Infrared Astronomy or SOFIA is now under

final testing. SOFIA consists of a Boeing 747 airplane with a telescope capable of detecting in the infrared[5]. Like KOA, SOFIE will operate at an altitude of 40,000 feet to eliminate interference from molecules lower in the atmosphere.

When sufficiently funded the deployment of a space based telescope is ideal. The space based Hubble mission has proved very successful by observing many stellar objects with a spectral range that extends from the ultraviolet into the near infra-red. While the Hubble is still in use, plans are being made to deploy the James Webb Space Telescope in 2014 which will allow observation further into the infrared and hopefully detect the first bright objects formed in the early universe right after the big bang. The James Webb mission will also focus on the processes that lead to the birth of stars and formation of planetary systems as well as the determination of the chemical properties of stellar systems that might contain species related to the origins of life[6]. These two specific missions will provide an abundance of information about the chemical species present.

Titan, the largest moon of Saturn, is also under detailed investigation. It is the only planetary satellite known to have an extensive atmosphere. To investigate Saturn and its satellites more closely, the Cassini-Huygens mission was developed in the 1980s. The payload was launched in 1997 and reached orbit around Saturn the summer of 2004. As the Cassini orbiter makes its orbits of Saturn it has passed and will continue to pass through Titan's upper atmosphere where data are collected on the chemical species present. These data have proved that a complex chemistry is occurring throughout Titan's atmosphere with many large organic species present[7-11]. In addition,

the visual and infrared mapping spectrometer (VIMS) aboard Cassini indicates that liquid is present on the surface[12] and radar measurements of Titan's rotation indicates a large ocean hidden deep within the surface[13]. A liquid medium allows the mixing of different chemical species and bodes well for the creation of more complex species that are possibly biologically active.

Just knowing which molecules are present in the different interstellar environments and planetary atmospheres is not enough. To really understand the processes that create these environments, it is necessary to investigate how each species was formed and how all of the species present interact. This is done through sophisticated chemical models that employ hundreds of known and/or potential molecules and hundreds of reaction pathways[14-18]. For these models to be valid, the reaction pathways need to be studied in a laboratory setting where the rate coefficients of the reactions and product distributions can be determined[19,20].

Several different types of reactions are routinely included in the models[21]. The models generally start with the ionization of the most abundant atoms or molecules present. Once a species is ionized it can undergo ion-neutral, ion-ion, and electron recombination reactions. Neutral-neutral reactions can also occur though these are usually not as rapid as ion reactions unless one of the neutral molecules is a radical species[22]. The type of environment being modeled dictates which reactions are most important. For example, models of the ISM begin with the cosmic ray ionization of H_2 since this is the most abundant molecule present. The temperature of the ISM is around 10-20 K while the density is usually quite low (~ 10^4 molecules cm^{-3})[21]. Reactions

important to include in models of this system are electron recombination of positive ions and ion-neutral reactions such as condensation reactions and radiative association reactions. In models of the ISM, the identities of the chemical species present are accurately known from the spectroscopic data obtained by the astronomers. Models of the ISM are compared to these data and varied until the chemistry in the model is consistent with the spectral lines observed.

In contrast, models of Titan's atmosphere begin with the ionization of N_2 and CH_4 by solar radiation and energetic electrons from Saturn's magnetosphere. The temperature profile of the atmosphere is largely isothermal at a temperature of 170 K. The density is much higher than that in the ISM with a pressure range of 1.5 bar at the surface reducing to 10^{-12} bar at 1400 km above the surface. Reactions important to include in the model are electron recombination and ion-neutrals reactions such as proton transfer, charge transfer and collisionally stabilized association reactions. The higher pressures allow collisional association to occur at the gas kinetic rate and thus their inclusion in the models becomes very important. The model predictions are compared to mass spectra obtained from the Cassini orbiter. Very little spectroscopic data are available for Titan in contrast to the ISM. Therefore, the chemical species included in the Titan models are largely educated guesses following from the known neutral composition of nitrogen and methane. The chemical reactions in the model are varied until the observed number density at each mass peak in the mass spectrum is achieved. This allows for a great deal of uncertainty and spectroscopic data for Titan's atmosphere are much needed.

For modeling of both the ISM and Titan to be successful, it is important to have relevant laboratory data and in particular to know the stability and reactivity of various molecules. In the present study, rate coefficients and ion product distributions have been determined for several cyclic molecules and several gas phase formation routes have been investigated. These new data are used to understand the chemistry of cyclic molecules in the gas phase. Such studies will give information such as what conditions are needed for these molecules to be abundant thus increasing the likelihood of their detection.

1.2 SCOPE OF DISSERTATION

With the discovery of benzene (c-C_6H_6) in the interstellar medium (ISM)[23,24] and in the atmosphere of Titan[25-27] interest has recently turned to how complex organic molecules are formed in these environments. This interest for Titan has increased largely due to the data collected by the Cassini orbiter[25,28-32]. The Ion Neutral Mass Spectrometer (INMS) aboard Cassini has detected a variety of positive ions from 1-99 amu which are believed to include a large number of nitrogen containing species[14,33].The Cassini Plasma Spectrometer (CAPS) detected large positive ions[9] in the range of 100- 350 amu as well as massive negative ions[34-36] up to 8000 amu. Analysis of these data has revealed that ion-neutral reactions are more important than previously thought. Also, there are expected to be large multi-ring molecules in Titan's atmosphere such as polyaromatic hydrocarbons (PAHs) and polyaromatic nitrogen heterocycles (PANHs) which along with aerosols and tholins are responsible for the thick layer of orange haze obstructing the view of Titan's surface[9,10,37]. Interestingly, the

5

INMS detected a peak at 79 amu that could possibly correspond to protonated benzene or charged pyridine[7] and a peak at 80 amu that could correspond to protonated pyridine. Benzene has been detected in the atmosphere by the Composite InfraRed Spectrometer (CIRS) and on the surface of Titan by the Huygens gas chromatograph mass spectrometer[26]. Therefore, the possibility of protonated benzene must be considered but the formation of nitrogen containing linear and cyclic molecules is also possible due to the large amount of N_2 in Titan's atmosphere. With this discovery, it becomes very important to study the reactions that form these cyclic species and how the ions present react with these various cyclic species. This chemistry has been neglected until now and kinetic data in the literature are scarce.

This dissertation begins by studying the reactivity and stability of three nitrogen containing heterocyclic molecules. Pyridine, pyrimidine and piperidine were reacted with several ions of differing recombination energy to determine how readily the rings fragmented as well as what product ions were produced upon fragmentation. Rate coefficients and ion product distributions for the reactions were determined. Cyclic molecules, especially those containing heteroatoms, have been largely overlooked by most of the astrochemical community. However, as the Cassini Mission proves, this should change. As more modelers began to realize that they will need the information being provided in our studies. The second study was prompted by the results of the first study of the nitrogen heterocyclic species. The product distributions obtained in the first study revealed possible routes to formation of pyridine.   In the product distribution, a neutral HCN is expected whenever a $C_4H_4^+$ ion is formed. Consequently,

since HCN is a very stable molecule, it is not surprising that is present in both the interstellar medium and the atmosphere of Titan. Based on the concept of microreversibility, the reverse reaction was studied in an attempt to identifiy a possible route of formation for pyridine. A third study involved reactions with CH_3^+, a central ion in both the ISM and Titan's atmosphere. It is known to be formed in the ISM by the radiative association[38] of $C^+ + H_2$ to form CH_2^+ which then reacts rapidly with H_2 to form CH_3^+. It is formed in Titan[15] by either the dissociative charge transfer reaction of $N_2^+ + CH_4$ or by the action of energetic electrons or solar radiation upon CH_4. The CH_3^+ ion was reacted with several cyclic species with varying amounts of saturation and of π electrons as well as different heteroatoms such as those of nitrogen and oxygen. Several trends were discovered in the product distributions and the routes to formation of the product ion are discussed. The fourth study was similar to the third in that the same neutral rings were used while the reactant ion was changed to $C_3H_3^+$. Much like the methyl cation, $C_3H_3^+$ is also an important ion in both the ISM and Titan's atmosphere. $C_3H_3^+$ is formed in the interstellar medium[39] by the radiative association reaction of $C_3H^+ + H_2$. It is formed on Titan[15] through the condensation reaction of $CH_3^+ + C_2H_2$. Of particular interest with $C_3H_3^+$ is that two stable isomers are present, both the propargyl cation and the cyclopropargyl cation. The reactivity of both isomers was explored in this study with product distributions and rate coefficients reported. In the fifth study the CH_3^+ reactions with benzene and pyridine was studied in more depth. The major constituents of Titan are N_2 (98%), CH_4 (1-2%) and a few tenths of a percent of H_2. The sequential reactions of CH_3^+ + Benzene/Pyridine + $N_2/CH_4/H_2$ were studied to

7

monitor how the product ions would react with main constituents of Titan's ionosphere. In this chapter the data obtained in both the CH_3^+ and $C_3H_3^+$ study are discussed in regards to the significance it plays in the scheme of Titan's atmospheric chemistry. The structures of all of the neutral cyclic molecules used in these studies are shown in Figure 1.1.
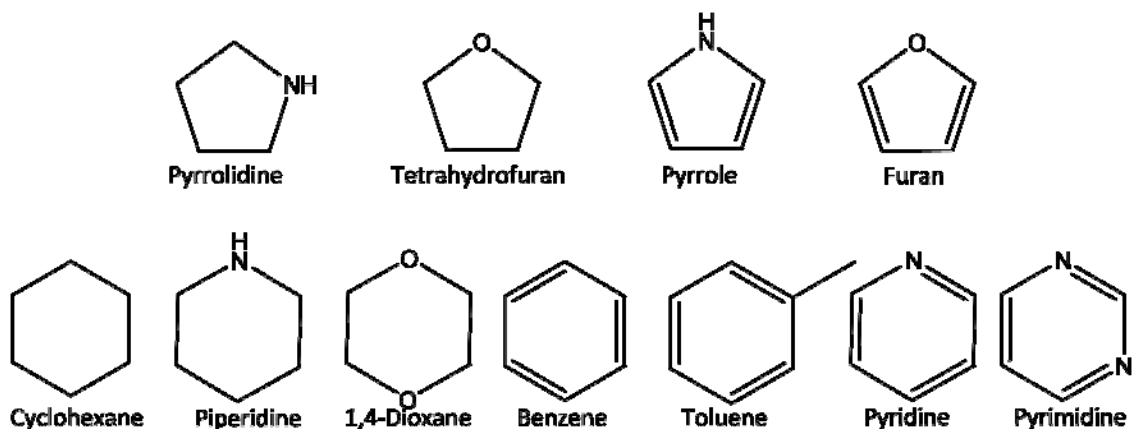
Figure 1.1 The structure of all of the cyclic neutral molecules used in the ion-neutrals reactions.

1.3 REFERENCES

1.   Wooten, A. "ALMA and Synergies with the GBT in Interstellar Astrochemistry"; 2009 Center for Chemistry of the Universe Workshop, 2009, Green Bank, West Virginia.

2.   Ruffle, P. Robert C. Byrd Green Bank Telescope; Vol. 2010.

3.   NROA. Atacama Large Millimeter/Submillimeter Array, 2007; Vol. 2010.

4.   Kuiper Airborne Observatory, 2010; Vol. 2010.

5.   Meyer, B.; Cappuccio, M. SOFIA Science Center: Stratospheric Observatory for Infrared Astronomy, 2010; Vol. 2010.

6.   Masetti, M.; Gardner, J. P. The James Webb Space Telescope, 2010; Vol. 2010.

7.   Cravens, T. E.; Robertson, I. P.; Waite, J. H.; Yelle, R. V.; Kasprzak, W. T.; Keller, C. N.; Ledvina, S. A.; Nieman, H. B.; Luhmann, J. G.; McNutt, R. L.; Ip, W.-H.; de la Haye, V.; Mueller-Wodarg, I.; Wahlund, J.-E.; Anicich, V. G.; Vuitton, V. *Geophys. Res. Lett.* **2006**, *33*, L07105.

8.   Cravens, T. E.; Yelle, R. V.; Wahlund, J.-E.; Shemansky, D. E.; Nagy, A. F. Composition and Structure of the Ionosphere and Thermosphere. In *Titan from Cassini-Huygens*; Brown, R. H., Lebreton, J.-P., Waite, J. H., Eds.; Springer: Dordrecht, 2009; pp 259.

9.   Waite, J. H., Jr.; Young, D. T.; Cravens, T. E.; Coates, A. J.; Crary, F. J.; Magee, B.; Westlake, J. *Science* **2007**, *316*, 870.

10. Atreya, S. *Science* **2007**, *316*, 843.

11. Wahlund, J.-E.; Galand, M.; Mueller-Wodarg, I.; Cui, J.; Yelle, R. V.; Crary, F. J.; Mandt, K.; Magee, B.; Waite Jr., J. H.; Young, D. T.; Coates, A. J.; Garnier, P.; Aagren, K.; Andre, M.; Eriksson, A. I.; Cravens, T. E.; Vuitton, V.; Gurnett, D. A.; Kurth, W. S. *Planet. Space Sci.* **2009**, *57*, 1857.

12. Brown, R. H.; Soderblom, L. A.; Soderblom, J.; Clark, R.; Jaumann, R.; Barnes, J.; Sotin, C.; Buratti, B.; Baines, K.; Nicholson, P. *Nature* **2008**, *454*, 607.

13. Lorenz, R. D.; Stiles, B. W.; Kirk, R. L.; Allison, M. D.; Persi del Marmo, P.; Less, L.; Lunine, J. I.; Ostro, S. J.; Hensley, S. *Science* **2008**, *319*, 1649.

14. Vuitton, V.; Yelle, R. V.; McEwan, M. J. *Icarus* **2007**, *191*, 722.

15. Keller, C. N.; Anicich, V.; Cravens, T. E. *Planet. Space Sci.* **1998**, *46*, 1157.

16. Anicich, V.; McEwan, M. J. *Icarus* **2001**, *154*, 522.

17. Anicich, V.; McEwan, M. J. *Planet. Space Sci.* **1997**, *45*, 897.

18. Cravens, T. E.; Vann, J.; Clark, J.; Yu, J.; Keller, C. N.; Brull, C. *Adv. Space Res.* **2004**, *33*, 212.

19. Anicich, V.; Wilson, P.; McEwan, M. J. *Amer. Soc.Mass Spectrom.* **2003**, *14*, 900.

20. Vuitton, V.; Doussin, J.-F.; Benilan, Y.; Raulin, F.; Gazeau, M.-C. *Icarus* **2006**, *185*, 287.

21. Duley, W. W.; Williams, D. A. *Interstellar Chemistry*; Academic Press: New York, 1984.

22.   Smith, I. W. M. *International Journal Of Mass Spectrometry and Ion Processes* **1995**, *149/150*, 231.

23.   Cernicharo, J.; Heras, A. M.; M., T. A. G. G.; Pardo, J. R.; Herpin, F.; Guelin, M.; Waters, L. B. F. M. *Ap. J.* **2001**, *546*, L123.

24.   Kuan, Y.-J.; Yan, C.-H.; Charnley, S. B.; Kisiel, Z.; Ehrenfreund, P.; Huang, H.-C. *Mon. Not. Roy. Astr. Soc.* **2003**, *345*, 650.

25.   Coustenis, A.; Salama, A.; Schultz, B.; Lellouch, E.; Encrenaz, T.; Gautier, D.; Feuchtgruber, H. *Icarus* **2003**, *161*, 383.

26.   Vuitton, V.; Yelle, R. V.; Cui, J. *Journal of Geophysical Research* **2008**, *113*, E05007(1.

27.   Wilson, E. H.; Atreya, S. K.; Coustenis, A. *J. Geophys. Res.* **2003**, *108(E2)*, 5014.

28.   de Kok, R.; Irwin, P. G. J.; Teanby, N. A.; Lellouch, E.; Bezard, B.; Vinatier, S.; Nixon, C. A.; Fletcher, L.; Howett, C.; Calcutt, S. B.; Bowles, N. E.; Flasar, F. M.; Taylor, F. W. *Icarus* **2007**, *186*, 354.

29.   Vinatier, S.; Bezard, B.; Fouchet, T.; Teanby, N. A.; De Kok, R.; Irwin, P. G. J.; Conrath, B.; Nixon, C. A.; Romani, P. N.; Flasar, F. M.; Coustenis, A. *Icarus* **2007**, *188*, 120.

30.   Yelle, R. V.; Borggren, N.; de la Haye, V.; Kasprzak, W. T.; Nieman, H.; Muller-Wodarg, I.; Waite Jr., J. H. *Icarus* **2006**, *182*, 567.

31.   Teanby, N. A.; Irwin, P. G. J.; De Kok, R.; Vinatier, S.; Bezard, B.; Nixon, C. A.; Flasar, F. M.; Calcutt, S. B.; Bowles, N. E.; Fletcher, G.; Howett, C.; Taylor, F. W. *Icarus* **2007**, *186*, 364.

32.   Coustenis, A.; Achterberg, R. K.; Conrath, B.; Jennings, D. E.; Marten, A.; Gautier, D.; Nixon, C. A.; Flasar, F. M.; Teanby, N. A.; Bezard, B.; Samuelson, R.; Carlson, R. C.; Lellouch, E.; Bjoraker, G. L.; Romani, P. N.; Taylor, F. W.; Irwin, P. G. J.; Fouchet, T.; Hubert, A.; Orton, G. S.; Kunde, V.; Vinatier, S.; Mondellini, J.; Abbas, M. M.; Courtin, R. *Icarus* **2007**, *189*, 35.

33.   Vuitton, V.; Yelle, R. V. *ApJ* **2006**, *647*, L175.

34.   Coates, A. J.; Crary, F. J.; Lewis, G. R.; Young, G. T.; Waite, J. H.; Sittler, E. C. *Geophys. Res. Letts.* **2007**, *34*, L22103.

35. Coates, A.; Wellbrock, A.; Lewis, G. R.; Jones, G. H.; Young, D. T.; Crary, F. J.; Waite, J. H. *Planet. Space Sci.* **2009**, *doi:10.1016/j.pss.2009.05.05.009*.

36. Vuitton, V.; Lavvas, P.; Yelle, R. V.; Galand, M.; Wellbrock, A.; Lewis, G. R.; Coates, A. J.; Wahlund, J.-E. *Planet. Space Sci.* **2009**, *57*, 1558.

37. Carrasco, N.; Schmitz-Afonso, I.; Bonnet, J.-Y.; Quirico, E.; Thissen, R.; Dutuit, O.; Bagag, A.; Laprevote, O.; Bush, A.; Guilani, A.; Adande, G.; Ouni, F.; Hadamcik, E.; Szopa, C.; Cernogora, G. *J. Phys. Chem. A* **2009**, *113*, 11195.

38. Dalgarno, A. Chemisty of Molecular Clouds. In *Structure and Dynamics of the Interstellar Medium*; Tenoria-Tagle, G., Moles, M., Melnick, J., Eds.; Springer-Verlag: Granada, Spain, 1989; pp 3.

39. Smith, D. *Chem. Rev.* **1992**, *92*, 1473.

CHAPTER 2

EXPERIMENTAL

2.1 THE SELECTED ION FLOW TUBE (SIFT)

The advent of the SIFT opened up a new world in the study of gas phase reaction kinetics of ions. Its predecessor, the flowing afterglow (FA), was an invaluable tool for studying the chemistry occurring in a plasma[1], however, the advantage of the SIFT allows for the separation of the ion of interest from the environment that creates the ion[2,3]. This ensures that the reaction being study is that of the ion and neutral alone, not those of the ion, neutral, parent gas, and electrons found in the plasmas of the FA. This separation allows accurate ion product distributions and rate coefficients to be determined without complicated data analysis. While the concept for the SIFT seems uncomplicated, for it to work properly requires the parallel operation of several analogue and digital electronic components, pumps, pressure gauges, flow controllers, specialized software and more. To discuss the SIFT effectively it is best to break it down into four major components: ionization source, the SIFT chamber, the flow tube, and the detection chamber. All of the peripherals connect through to one of these four areas. A schematic of the SIFT can be seen in Figure 2.1.
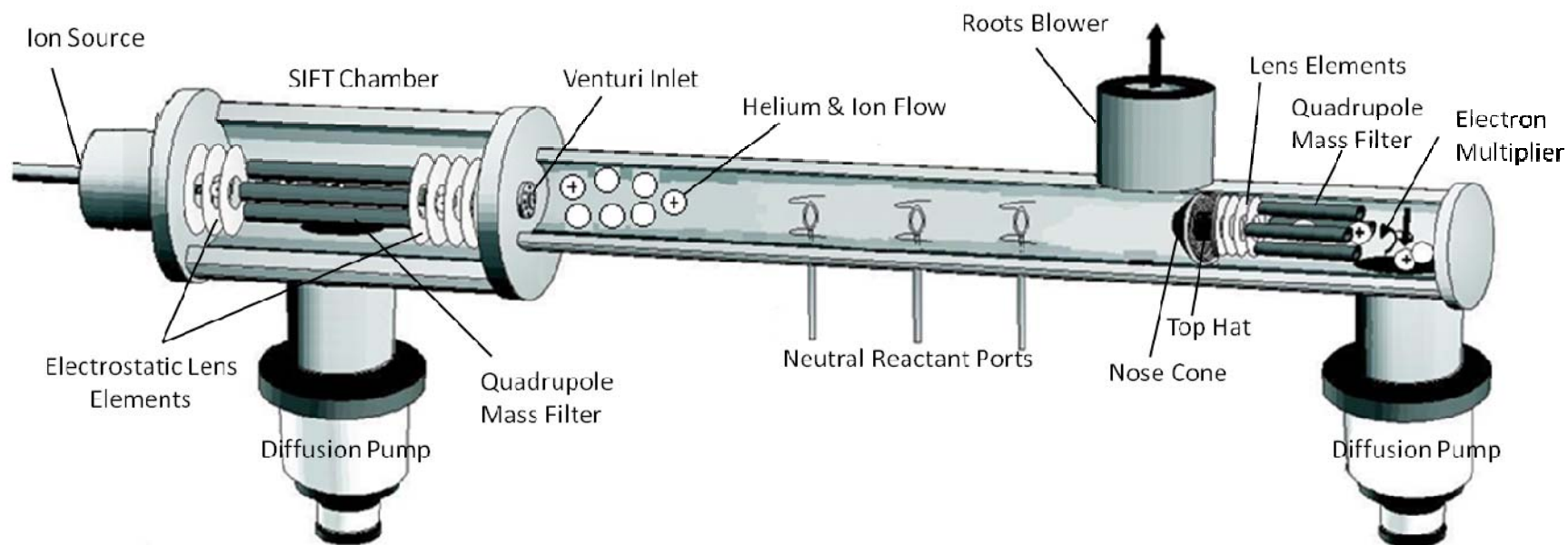
Figure 2.1 A schematic diagram of the University of Georgia's SIFT. Ions are produced from the source gas and the appropriate ion mass is selected by the upstream quadrupole mass filter. These ions are then transported downstream by a supersonic flow of helium where they can react with the neutral reactant gas in the flow tube. A sample of the primary and product ions enter through an orifice in the nose cone where they encounter another quadrupole mass filter.   An electron multiplier and ion counting system is used to monitor the ion signals of both the primary ion and the product ions.

2.1.1 Physical Description

The selected ion flow tube used in this study is composed of a stainless steel flow tube of approximately 171 cm from ion injection to nose cone. There are several ports located along the flow tube. Of the several possible uses for these ports, the main function is to the supply neutral reactant gas. The three ports used for this purpose are located 83.6 cm, 59.6 cm and 29.8 cm from the nose cone providing the choice of three different reaction lengths/times. The inside diameter of the flow tube at the reaction zone is 8.4 cm. The SIFT chamber meets the flow tube at one end of a V junction so the chamber is off axis from the remainder of the flow tube. The other end of the V junction connects to a small flowing afterglow that is used to help diagnose problems with the system.

2.1.2 Ionizations Source

The three ionization sources most commonly used to create ions are a microwave plasma source, a high pressure electron impact source (HPIS) and a low pressure electron impact source (LPIS). The operation will be discussed for the generation of positive ions. The microwave plasma source is used most often for the formation of noble gas ions. This source provides the highest density of ions but tends to produce too much fragmentation with molecular gases. The microwave source is composed of a glass tube (½ inch diameter) with two glass to metal seals. One of the seals connects to a metal flange which in turn connects to the SIFT chamber. The second glass to metal seal is connected to a ¼ inch stainless steel tube which is used to provide source gas

through a series of Swagelok connections. Once the gas enters the glass tube, it is ionized by a microwave cavity that fits around the glass tube and is connected to a standard klystron source to generate the microwaves. The plasma is initiated using a Tesla coil. The plasma is confined to the glass tube by an orifice disk containing a 1 mm diameter aperture at the flange end of the source. The orifice disk is maintained at +20 V with respect to the flow tube which provides the ion injection energy into the flow tube. The positive ions are drawn from the orifice disk by a series of electrostatic lens elements that also focus the ions into a quadrupole mass filter.

The HPIS is used to produce ions that are formed by secondary reactions of the parent ion with the neutral parent gas. For example, the ionization of methane gives CH_3^+ as one of the source ions and these can react with neutral methane in the source to produce $C_2H_5^+$. Other ions are also formed but the quadrupole mass filter in the SIFT chamber can be tuned to pass only one ion mass (e.g. $C_2H_5^+$). To create the high pressure environment for secondary reactions the source gas enters the HPIS into a box structure, as seen in Figure 2.2. The box has two additional openings. The opening on the end allows electrons from a heated filament to enter the box to ionize the source gas. The electrons are accelerated into the box by an electrode placed directly across from this opening and placed at a positive potential. The second opening is on top of the box and allows the ions created to escape into the SIFT chamber. The positive ions are repelled by an electrode at a positive potential placed at the bottom of the box and
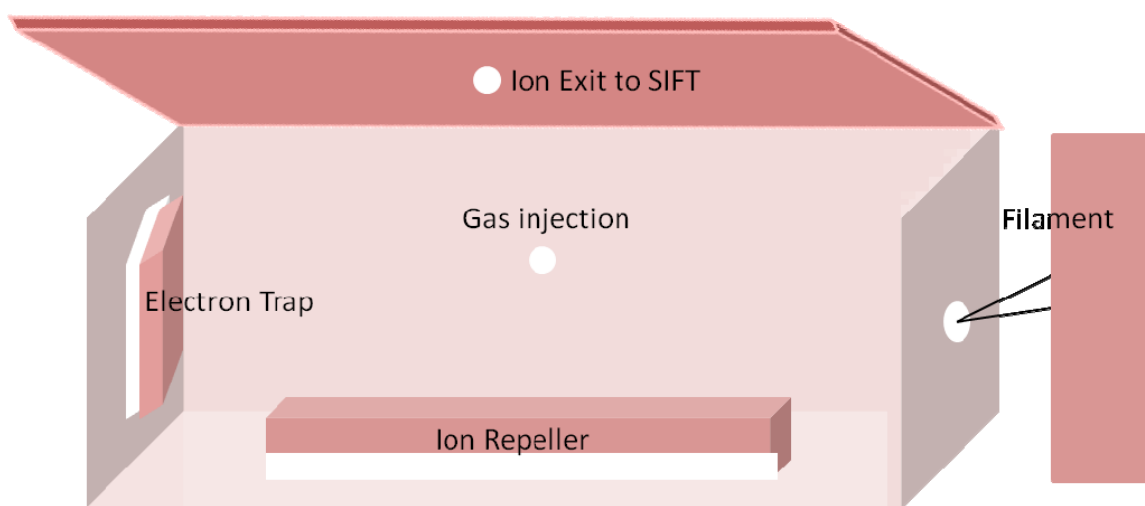
Figure 2.2 Schematic of a high pressure ionization source shown through one side of the box. During normal operation the top is attached to the box and a positive potential is supplied to provide energy for the ions exiting the box. The electron trap and ion repeller are isolated from the box potential by ceramic spacers.

this helps them exit the box. Once the ions exit the high pressure region of the source they are focused by electrostatic lenses into the quadrupole mass filter.

The LPIS, as seen in Figure 2.3, is the most common way to create primary ions by electron impact. Typically, electrons with an energy of 70 eV are produced via resistive heating of filaments and allowed to come in contact with the source gas. The construction of the source is very open compared to the microwave source and the HPIS with no barrier between the inlet of the neutral gas and the SIFT chamber. The main components of the LPIS are the filament assembly which holds four filaments, a circular filament cage that fits over the filament assembly, the grid and the extractor. The grid is an electrode with a protruding cylinder of fine mesh wires. A hole in the bottom of the wire cylinder allows the gas inlet to pass through so gas is injected in the middle of the wire cylinder. The four filaments surround the grid without touching it. As electrons are ejected from the filament they are accelerated toward the grid which is set at a positive potential. There the electrons interact with the gas molecules and ionization occurs. The filament cage is maintained at a potential more negative than the filaments and grid to constrain the electrons within the grid for efficient ionization of the gas. The extractor lens is held at a more negative potential than the grid to extract the positive ions for entry into the SIFT chamber.

The HPIS and LPIS are controlled by an Extrel Ionizer Controller. The controller regulates the voltages supplied to the electrodes and the current flowing through the filaments. A current of 1 mA is generally used to heat the filaments and eject electrons.

Extractor Lens

Grid/ Ion Energy

Cage
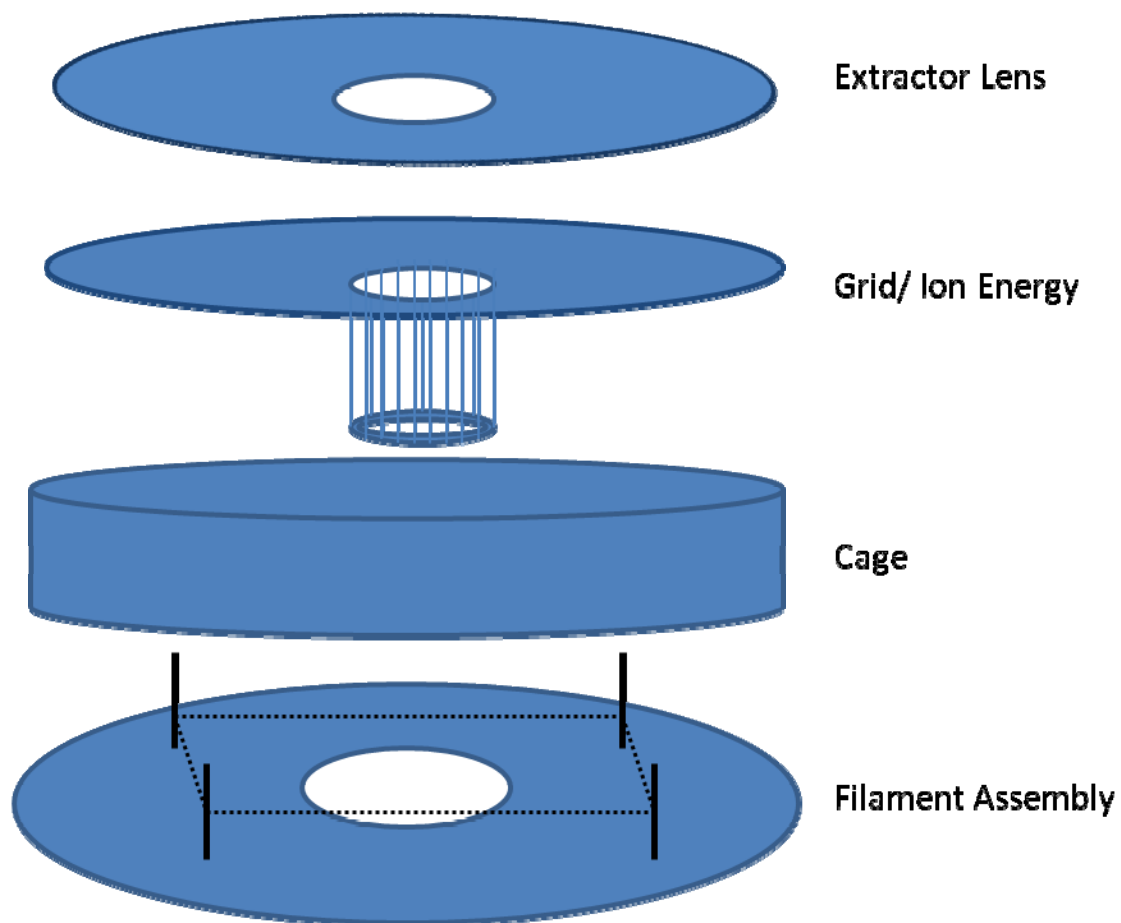
Filament Assembly

Figure 2.3 Schematic of a low pressure ionization source. A tube (not shown) running through the center of the filament assembly into the grid supplies the source gas.

This electron energy is varied until a maximum ion signal is obtained. The electron energy is typically between 70 and 100 eV. In the LPIS, there are two electrodes that are supplied with potentials: the ion energy and the extractor. For a fixed ion energy, the extractor potential is varied until the ion current is maximized. When using the HPIS there are three electrodes that can be varied to maximize the ion current: the ion energy, the electron trap, and the ion repeller.

2.1.3 SIFT Chamber

The SIFT chamber begins where the ionization source ends. The chamber contains a stack of electrostatic lens elements, a quadrupole mass filter, another set of electrostatic lens elements and terminates at the SIFT disk. The pressure in the SIFT chamber is monitored by an Alpert-Bayard Ionization Gauge and is maintained at 1 x 10^{-7} to 5 x 10^{-8} torr when no gases are flowing by a Varian Diffstak 6" oil diffusion pump which is backed by a Edwards rotary vane mechanical pump. When gases are flowing in the source the pressure in the SIFT chamber typically is 1 x 10^{-5} to 1 x 10^{-4} torr. Once the ions exit the ionization source they encounter three electrostatic lens elements. These lens elements extract the ions from the source and focus them on axis into the quadrupole. The ions enter the quadrupole where ions with the selected mass to charge (m/z) pass through the quadrupole. The ions exit the quadrupole and another set of electrostatic lens elements focus them into a 1 mm orifice in the SIFT disk (SD). The SD has a small voltage applied to draw the ions through the orifice and into the flow tube. The current that reaches the SD is monitored by a piccoameter and is indicative of how

many ions pass through the quadrupole. The signal to the SD and then through the orifice is maximized by tuning the various lens elements.

2.1.4 Flow Tube/ Reactions Zone

The ions entering the flow tube through the SD orifice are immediately carried downstream by a supersonic flow of helium. The helium enters the tube through a series of venture type inlets that encircle the SD orifice. A short distance downstream from the SD the ions encounter an electrode. This is a copper disk attached to a vacuum flange and inserted into the flow tube. The copper disk lies flush with the side of the tube to minimize any obstruction when not in use. When in use the electrode is at a -20 V potential to attract the ions. The electrode is used to measure the current of ions coming through the orifice in the SD. The potential on the various lens elements in the SIFT chamber are varied to get the greatest number of ion through the orifice. This electrode is important for two reasons. First, a large current to the SD does not always mean they are focused properly through the orifice. It could mean that the ions are colliding with the SD, producing a large current in that manner. Tuning to the electrode ensures that the ions are injected into the flow tube. Secondly, the electrode can be used as a diagnostic tool when there is low or no signal downstream. It is necessary to know that ions are exiting the SIFT chamber and narrows the troubleshooting area considerably.

Once the current is maximized to the electrode its potential is turned off and the electrode is grounded. The ions then can continue downstream undisturbed by an

attractive potential.   As the ions travel with the helium they experience multiple collisions ($\sim 10^{-7}$) with the helium carrier gas. These collisions help to thermalize any kinetically and internally excited ions so that only thermalized ions react with the neutral reactant gas. The neutral gas is introduced into the flow tube through one of three ports and the flow is measured by a capillary flow system.

After the neutral gas is introduced into the flow tube the ion and the neutral have a defined time to react depending on the port that the neutral was introduced through and the velocity of the ions. Once the ion and neutral have traversed the reaction length, they and the product ions encounter the nose cone on which a ⅓ mm diameter orifice is located. A portion of the ions is sampled through the orifice while the remainder is evacuated with the helium from the flow tube through a roots blower. The nose cone has a small voltage applied to attract the ions through the orifice to the detection system. The orifice is kept purposely small to allow the flow tube pressure to stay high ($\sim$0.500 torr) while keeping the detections system pressure low ($\sim 1 \times 10^{-5}$ torr) enough to operate the downstream quadrupole mass filter.

2.1.5 Detection Chamber

Once the ions enter the detection chamber through the nose cone orifice they encounter an electrostatic lens element shaped like a top hat. The top hat is placed very close to the nose cone (1 mm) to maximize field penetration into the flow tube which minimizes charge build up at the orifice.   After the top hat, a set of four electrostatic lens elements guide and focus the ions into the downstream quadrupole

mass filter. An electron multiplier and ion counting system is used to monitor the ion signal of both the primary ions and the product ions. The low pressure in the detection system is maintained by 6" and 4" Varian diffusion pumps. The diffusion pumps are backed by a Welch DuoSeal pump. The pressure in the detection system is monitored by a Bayard-Alpert Ionization gauge. The electron multiplier is a channeltron type design (Photonis). A voltage of negative 2-2.8 kV is supplied to the multiplier by a high voltage power supply. Before the voltage reaches the multiplier it passes through an in house circuit constructed to allow detection of either positive or negative ions (note only positive ion operation is discussed above). The circuit and the operational instructions can be seen in Figure 2.4. The electron signal pulse coming from the multiplier first passes through a 90.5 MHZ notch filter to remove interference from the UGA student radio station. The signal pulses at this point are very small so they must pass through a pre-amplifier before being counted by a gated ion counter and collected via a computer interface.

2.2 DATA COLLECTION

Before data collection can begin the downstream quadrupole and lens elements must be tuned to maximize the detected ion counts. Both components are controlled by an Extrel program (Merlin). After tuning the elements it is possible to obtain a signal representing the number of counts at a mass to charge ratio from the gated ion counter. This signal is collected by an in house kinetics program. Once the primary ion peak is identified and maximized, the products can be generated by introducing the neutral gas
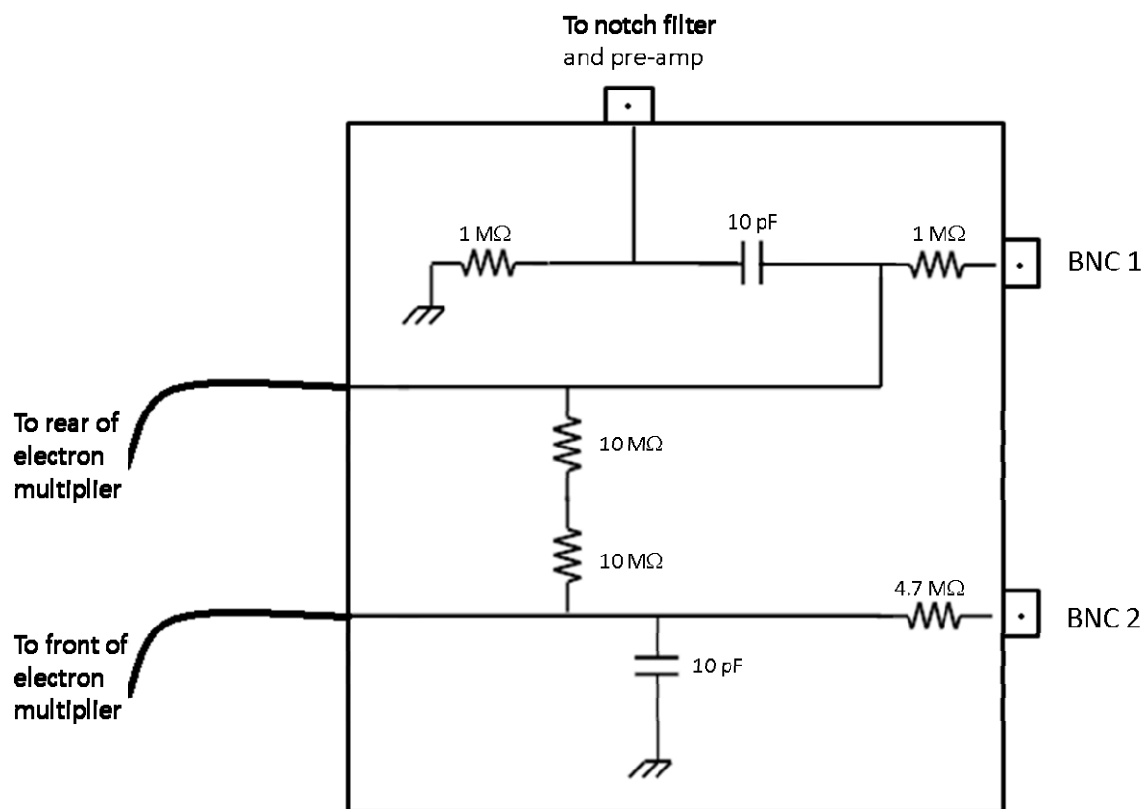
Figure 2.4 An in house circuit designed to allow for detection of either positive or negative ions by the electron multiplier. For positive ion detection, BNC 2 is connected to a high voltage power supply (-2 kV) and BNC 1 is connected to ground. For negative ion detection, BNC 1 is connected to a high voltage power supply (2 kV) and BNC 2 is connected to ground.

through one of the neutral gas inlet ports. A mass scan program is used to determine the product ion peaks that are present and their exact masses. During the kinetic experiments the counts of the primary ion and product ions are followed as a function of neutral flow. A graph is then generated with counts for a selected time interval plotted on the ordinate and neutral flow in standard cubic centimeters per a minute (sccm) on the abscissa. Once an appropriate neutral flow range has been investigated a spectrum is saved, as shown in Figure 2.5, for later analysis. Immediate analysis of the rate coefficient for the primary ions can be accomplished using the built in kinetics program or the data can be analyzed manually as explained below.

2.3 DATA ANALYSIS AND THEORY

The data collected are analyzed to determine the rate coefficient for the reaction of the primary ion and the product ion distribution. To determine the rate coefficient it is necessary to consider the kinetics of the generic reaction

$$A^+ + B \xrightarrow{k} C^+ + D \tag{2.1}$$

where k is the rate coefficient for the reaction. A full analysis of this reaction including diffusion components is given in reference 2. Note that in flow tube experiments, diffusive loss of the ion can be ignored providing there is a viscous flow and pressure in the tube remains constant (~ 0.5 torr). This allows for the simplified rate equation

$$\frac{d[A^+]}{dt} = -k[A^+][B] \tag{2.2}$$
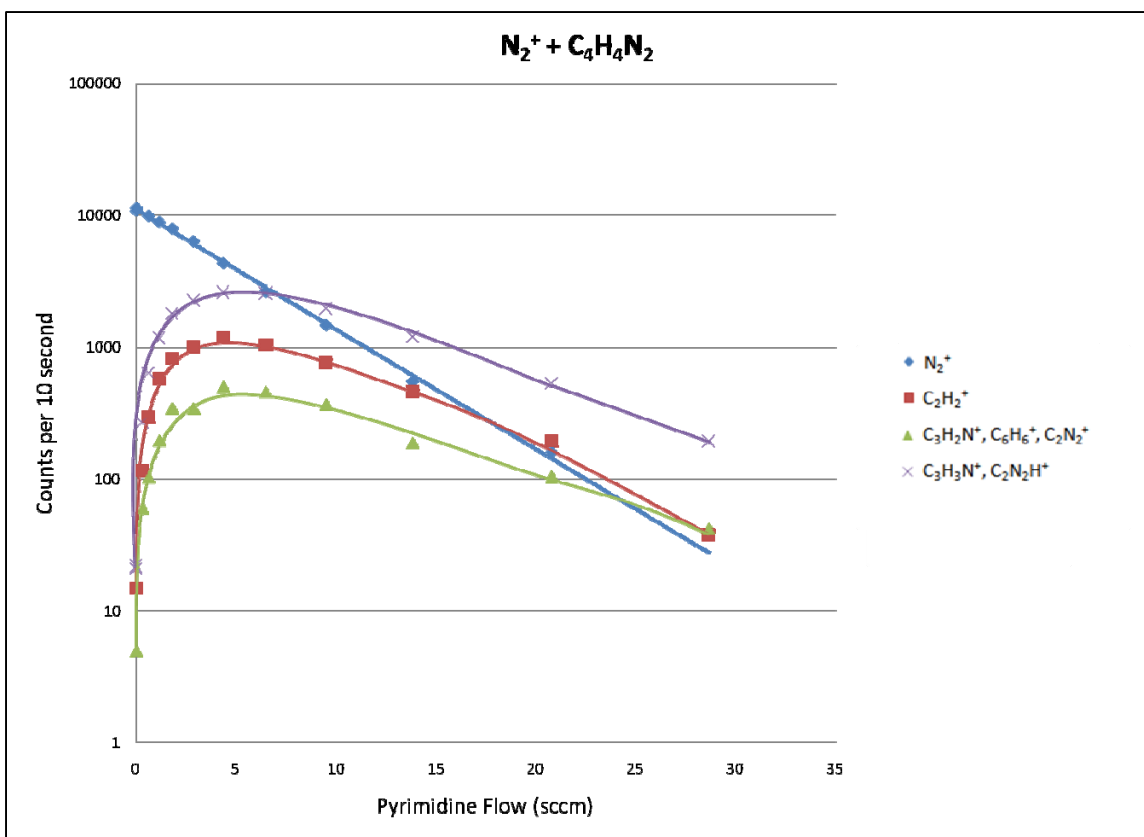
Figure 2.5 Decay of N_2^+ and rise of the product ions for the N_2^+ reaction with pyrimidine. All three of the products show signs of reacting further with the pyrimidine.

In addition, in SIFT experiments the concentration of the ion is much lower than the concentration of the neutral, [B] >> [A$^+$]. Thus [B] can be considered a constant for integration purposes and the rate is described as a pseudo-first-order rate equation[4]

$$\int \frac{d[A^+]}{[A^+]} = \int -k[B]dt \qquad (2.3)$$

and integration gives the simplified expression

$$\ln[A^+] = -k[B]t + c \qquad (2.4)$$

This is recognized as the equation for a line where at t= 0 then [B]= 0 and the y-intercept, c, equals the initial concentration of the primary ion, $\ln[A^+]_o$. The slope of the line is –kt where

$$t = \frac{z}{v_i} \qquad (2.5)$$

z is the reaction distance determined by the port through which the neutral gas enters and the velocity of the ions is represented by v_i. Typically, z equals 83.6 cm as the longest port is generally used for the maximum reaction time. To determine the velocity of the ions, it is important to consider the flow dynamics of the helium carrier gas. The velocity of the helium carrier gas can be determined from

$$v_{He} = \frac{Q}{\bar{p}\pi r^2} \qquad (2.6)$$

where Q is the flow of helium gas in torr L s^{-1}, $\bar{p}$ is the average pressure (torr) in the center of the flow tube, and r is the radius of the tube. The velocity of the ions, v_i, has been experimentally shown to be generally between 1.45-1.65v_{He} between 80-300 K.

For the University of Georgia SIFT it has been determined to be $1.51v_{He}$. From these equations the rate coefficient can be readily determined by plotting ln [A$^+$] versus [B]. An error of ±20% is typically associated with the measurement though when sticky gases are used the error can increases to ± 30%.

Like the primary ion, the product ions are monitored as a function of neutral flow. Because only the m/z is monitored the identification of the primary ions must occur through chemical intuition and through knowledge of the neutral gas formula. However, there are times when more than one chemical formula can generate a given mass peak. In these cases, reaction with isotopically labeled species can help with the identification. When this is not possible, consideration of the reaction energetics (for example by determining the heat of formation for the reaction) can aid in determining the identity if the formation of one of the chemical formula is unfavorable (e.g. endothermic). However, the thermochemical data must be available in the literature and in many cases it is not. To this end, all possible formulae must be considered. Once identification of the masses is complete, it is worthwhile to determine the product percentages. Knowing which product is the major product channel provides valuable information on how the ion and neutral react and through which reaction mechanism. Then the percent signal of each product channel can be determined at each flow by[5]

$$\%S_i^+ = \frac{S_i^+}{\sum_{j=1}^{k} S_j^+} \times 100 \tag{2.7}$$

where S_i^+ is the signal of the product channel i. The percentages are then plotted versus the neutral flow and extrapolated to zero neutral flow using a line fitting program. The

y-intercept of the fitted lines for the various product ions are determined as the product

distribution and this eliminates the effect of secondary reactions. An example of this

can be seen in Figure 2.6.
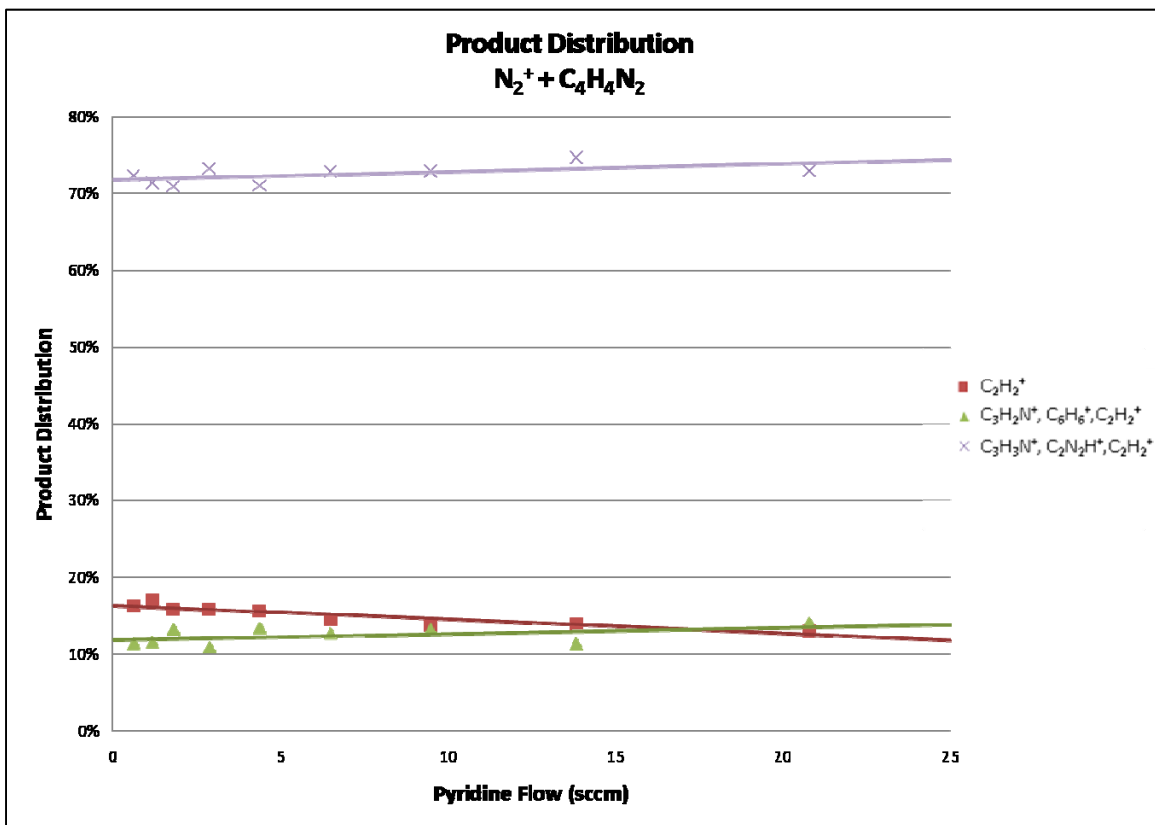
Figure 2.6 Percent product distribution for the reaction of N_2^+ with pyridine. Points at flows less than 0.5 sccm have been omitted from the plot since with sticky gases, such as pyridine, the time to equilibrate prevents accurate measurements.

2.4 REFERENCES

1.   Adams, N. G.; Church, M. J.; Smith, D. *J.Phys.D.* **1975**, *8*, 1409.

2.   Adams, N. G.; Smith, A. D. Flowing Afterglow and SIFT. In *Techniques for the Study of Ion-Neutral Reactions*
        Farrar, J. M., Saunders, J. W. H., Eds.; Wiley-Interscience: New York, 1988; pp 165.

3.   Adams, N. G.; Smith, D. *Int. J. Mass Spectrom. Ion Phys.* **1976**, *21*, 349.

4.   Smith, D.; Adams, N. G. The Selected Ion Flow Tube (SIFT): Studies of Ion-Neutral Reactions. In *Advances in Atomic and Molecular Physics*; Bates, D. R., Bederson, B., Eds.; Academic Press: New York, 1988; Vol. 24; pp 1.

5.   Decker, B. K. Reactions of Sulfurated Ions in Thermal Plasmas and Reaction Dynamics by Gas-Phase Infrared Emission Spectroscopy, University of Georgia, 1999.

CHAPTER 3

STUDIES OF REACTIONS OF A SERIES OF IONS WITH NITROGEN CONTAINING

HETEROCYCLIC MOLECULES USING A SELECTED ION FLOW TUBE

3.1 ABSTRACT

A series of reactions between NH_3^+, O_2^+, O^+, Kr^+, N^+, N_2^+, Ar^+, Ne^+, NH_4^+ and H_3O^+ and three heterocyclic molecules (pyridine, pyrimidine and piperidine) were studied using a Selected Ion Flow Tube (SIFT) at 298 K. The stability of each ring was investigated through reactivity and the rate coefficients and ion product distributions were determined for each reaction. Most of the reactions proceed by charge transfer or proton transfer when energetically possible, with varying degrees of fragmentation. Based on microreversibility, gas phase formation routes are suggested for the production of ionized pyridine and pyrimidine. If these reverse reactions proceed with no or small activation energy barriers, this would be of interest for formation of heterocyclic rings in the interstellar medium and in the Titan atmosphere. Dissociation mechanisms leading to the major fragment product ions in both the pyridine and pyrimidine reactions have been studied and provide information about the site of interaction between the ions and molecules.

3.2 INTRODUCTION

Many cyclic organic molecules have been discovered in interstellar gas clouds (ISC), with both homocyclic and heterocyclic variants being detected, and possibly also in the Titan atmosphere. This is important, because many biological molecules are heterocyclic and the presence of heterocyclics in these extraterrestrial regions could suggest this as a source of prebiotic materials, which can then be transported by comets and meteors to planets in evolving stellar systems and act as nutrients for life. For example, thymine ($C_5H_6N_2O_2$), cytosine ($C_4H_5N_3O$) and uracil ($C_4H_4N_2O_2$), three of the

31

nucleotides of DNA and RNA are composed partially of the heterocyclic base pyrimidine. The organic rings that have been detected so far include c-C_3H_2[1], c-C_2H_4O[2,3], c-C_3H[4] , c-C_2H_3N and c-C_2H_5N[5] and c-C_3H_2O[6] along with c-C_6H_6 being found in ISC[7] and possibly in Titan's atmosphere[8,9]. Polycyclic aromatic hydrocarbons (PAHs) are another class of molecule that are thought to be present in the interstellar medium. It is believed that these types of molecules are responsible for some of the diffuse interstellar bands (DIBs) seen in ISC though this is yet to be verified. Also, just recently, it was suggested by Hudgins et. al. that the 6.2 μm interstellar emission line seen in infrared emission spectra of interstellar clouds is due to the substitution of a nitrogen atom into the endoskeleton of these PAHs (generating PANHs) [10].

To add to the information available on this topic, this study focuses on the ion-molecule reactions of three different nitrogen containing heterocyclic compounds; Pyrimidine ($C_4H_4N_2$), Pyridine (C_5H_5N), and Piperidine ($C_5H_{11}N$), as shown in Figure 3.1.

Pyrimidine   Pyridine   Piperidine
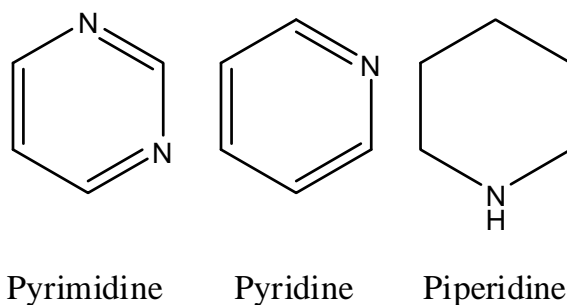
Figure 3.1. Structural diagrams of several heterocyclic molecules as indicated.

The study was undertaken to determine the stability of the heterocyclics with the deposition of varying amounts of energy as determined by the recombination energy of the various ions (ranging from 10 to 22 eV) used in reactions with the neutrals.

The presence of pyrimidine and pyridine in the ISC was first investigated in the early 1970s with little success[11]. More recently, these two molecules, and other nitrogen containing molecules like these, were the focus of interstellar searches by Kuan et al.[5,12]. Of the several different regions of the interstellar medium surveyed, only one line that potentially indicates the presence of pyrimidine was detected. The interstellar feature W51 e1/e2 provided this single line that coincides perfectly with the $J \leq 55$ band head of pyrimidine. However, the detection of one line is by no means considered a positive identification, but it is possible that several conditions conspire to make the other expected lines undetectable. Since large ring molecules are predicted to be unstable in these regions, they will have low relative abundances and hence the population of rotationally excited states is anticipated to be low. Also, the presence of spectral lines from other chemical species can interfere with the observation of expected lines especially where they are close to the limit of detectability. Thus, it is important to note that the absence of spectral features may not necessarily be due to the absence of the target molecule. Pyridine has also been targeted but with no positive identification to date[5,12]. Laboratory data on the stability of both pyrimidine and pyridine against UV radiation has been collected and both molecules are expected to survive only in UV shielded environments such as hot cores[13].

Titan's atmosphere has been extensively probed with the Cassini Ion and Neutral Mass Spectrometer (INMS). An ion peak at a mass to charge ratio, m/z, of 79 was detected that could be due to protonated benzene or possibly ionized pyridine[14]. Since pyridine has a large proton affinity, efficient proton transfer reactions with ions such as the dominant $HCNH^+$ should occur yielding an abundant ion with an m/z of 80. The INMS data[14] indicate the m/z of 79 as being comparable with the m/z of 80 (indeed dominating it in the altitude region of 1400 to 1600 km) and thus an identification of m/z =79 as ionized pyridine is highly unlikely. However, it is known that Titan's ionosphere is composed mostly of nitrogen with hydrocarbons, so the formation of nitrogen containing linear and cyclic molecules is likely to be facile. Even though the mass to charge ratios are accurately known, the identifications are not certain. Chemical modeling is a valuable means of better interpreting the mass spectral data. For modeling to be successful, it is essential for relevant laboratory kinetic data to be available. As a contribution to this effort, the stability and reactivity of various rings were probed in the present study. Rate coefficients and ion product distributions have been determined for a series of charge transfer reactions in which varying amounts of energy were deposited in the heterocyclic rings. In addition to establishing the relative stabilities, these studies suggested several gas phase formation routes to heterocyclic ion production. These new data will be valuable in understanding the chemistry of the molecules in the gas phase and will give information on the conditions that are needed for these molecules to form in ISC and the Titan atmosphere. Probing regions with

these conditions will improve the likelihood of the detection and identification of these molecules.

3.3 EXPERIMENTAL

The reactions of pyridine (C_5H_5N), pyrimidine ($C_4H_4N_2$) and piperidine ($C_5H_{11}N$) with ions of various recombination energies (RE): NH_3^+, O_2^+, O^+, Kr^+, N^+, N_2^+, Ar^+, Ne^+ (10-22 eV) and NH_4^+ and H_3O^+ were studied using a selected ion flow tube (SIFT). The technique has been described in detail before[15,16] and will not be discussed in depth here. Two different types of ion sources were used to produce the ions of interest. A high-pressure electron impact source was generally used to generate polyatomic ions, while a microwave discharge cavity was used when producing atomic ions because it provided a larger number density of ions in the flow tube. The ions of interest were selected using a quadrupole mass filter and focused through a 1 mm orifice into the flow tube. There the ions were carried downstream in a helium gas flow injected into the tube at supersonic flow through a Venturi type inlet. The pressure in the flow tube was maintained at ~0.5 torr by the helium flow, which was exhausted from the flow tube by a Roots pump. Downstream of the ion injection port, and after the thermalization of the ions, the reactant neutrals were introduced into the flow tube. A small portion of the reactant and product ions were then sampled at the end of the reaction region through a pinhole orifice in the detection nose cone, while the rest was evacuated by the Roots pump. A quadrupole mass spectrometer and an electron multiplier counting system located after the nose cone were used to quantitatively identify the ions by the mass to charge ratio.

The three reactant species used in this study are liquids at room temperature and it proved to be difficult to work with the neat vapors. When trying to determine accurate neutral flows, problems arose due to the gases sticking to the walls of the flow tube and it was not possible to stabilize flows and thus get linear semi logarithmic decays for the primary ion. To eliminate these problems, one percent mixtures of the reactant neutral in helium were used, keeping the reactant pressure below its saturated vapor pressure to minimize condensation. No evidence for dimerization was detected, which we have observed in other experiments with liquids of similar vapor pressures[17].

 Pyridine was obtained from Sigma Aldrich with a manufactured purity of 99.9+%.   Both pyrimidine and piperidine were obtained from Alfa Aesar with manufactured purities of 99%.   The liquids were further purified by several cycles of freeze-pump-thaw before use, in order to eliminate dissolved gases. Rate coefficients and percentage product ion distributions were determined using standard techniques[18]. The rate coefficients are accurate to ± 20%, while the product distributions are accurate to ± 5 in the percentage. All measurements were made at 298 K.

3.4 RESULTS

Ion product distributions for the reactions of pyridine, pyrimidine and piperidine are given in Table 3.1. These have been corrected for mass discrimination in the detection quadrupole mass filter. Mass discrimination factors were determined by monitoring the ion counts as a function of the downstream mass filter resolution. At low resolution, the ion counts became independent of resolution and, under these

Table 3.1 Product Distribution (%) in the Reactions of Pyridine, Pyrimidine, and Piperidine with ions indicated

Reactant Ion	Pyridine Ion Product	%	Pyrimidine ion product	%	Piperidine ion product	%
Ne$^+$ (21.56 eV)	C$_4$H$_3$$^+$, C$_3NH^+$	54	C$_2$H$_2$$^+$	46	C$_2$H$_4$$^+$, CH$_2N^+$	18
	C$_4$H$_2$$^+$, C$_3N^+$	21	C$_3$H$_2$N$^+$, C$_4$H$_4$$^+$, C$_2N_2$$^+$	32	C$_3$H$_6$$^+$, C$_2H_4N^+$	14
	C$_5$H$_5$N$^+$	13	C$_3$NH$^+$,C$_4$H$_3$$^+$	11	C$_3$H$_5$$^+$, C$_2H_3N^+$	13
	C$_4$H$_4$$^+$	12	C$_3$H$_3$N$^+$, C$_2$N$_2$H$^+$	7	C$_2$H$_5$$^+$, CH$_3N^+$	11
			C$_4$H$_3$N$_2$$^+$	<4	C$_2$H$_6$$^+$, H$_4CN^+$	10
					C$_3$H$_3$$^+$, C$_2NH^+$	7
					C$_4$H$_6$$^+$, C$_3H_4N^+$	6
					C$_4$H$_7$$^+$, C$_3H_5N^+$	6
					C$_4$H$_8$$^+$, C$_3H_6N^+$	6
					C$_3$H$_7$$^+$, C$_2H_5N^+$	5
					C$_2$H$_3$$^+$, HCN$^+$	4
Ar$^+$ (15.76 eV)	C$_4$H$_4$$^+$	66	C$_3$H$_3$N$^+$, C$_2$N$_2$H$^+$	54	C$_4$H$_8$$^+$, C$_3H_6N^+$	26
	C$_5$H$_4$N$^+$	15	C$_2$H$_2$$^+$	21	C$_2$H$_5$$^+$, CH$_3N^+$	19
	C$_4$H$_5$$^+$, C$_3H_3$N $^+$	12	C$_3$H$_2$N$^+$, C$_4$H$_4$$^+$, C$_2N_2$$^+$	22	C$_4$H$_7$$^+$, C$_3H_5N^+$	10
	C$_3$H$_3$$^+$, C$_2NH^+$	7	C$_4$H$_4$N$_2$$^+$	<4	C$_2$H$_6$$^+$,CH$_4N^+$	9
					C$_2$H$_4$$^+$, CH$_2N^+$	8
					C$_3$H$_5$$^+$, C$_2H_3N^+$	8
					C$_3$H$_6$$^+$, C$_2H_4N^+$	7
					C$_3$H$_8$$^+$,C$_2H_6N^+$	4
					C$_5$H$_{11}$N$^+$	4
					C$_4$H$_9$$^+$, C$_3H_7N^+$	3
					C$_3$H$_7$$^+$, C$_2H_5N^+$	2

Reactant Ion	Pyridine Ion Product	%	Pyrimidine ion product	%	Piperidine ion product	%
N_2^+ (15.58 eV)	l-$C_4H_4^+$	43	$C_3H_3N^+$, $C_2N_2H^+$	71	$C_4H_8^+$, $C_3H_6N^+$	32
	c-$C_4H_4^+$	43	$C_2H_2^+$	17	$C_2H_5^+$, CH_3N^+	15
	$C_4H_5^+$, $C_3H_3N^+$	14	$C_3H_2N^+$, $C_4H_4^+$, $C_2N_2^+$	12	$C_2H_4N^+$, $C_3H_6^+$	12
					$C_4H_7^+$, $C_3H_5N^+$	10
					$C_4H_9^+$, $C_3H_7N^+$	8
					$C_2H_5N^+$, $C_3H_7^+$	7
					$C_3H_8^+$, $C_2H_6N^+$	7
					$C_3H_5^+$, $C_2H_3N^+$	5
					$C_5H_{11}N^+$	4
N^+ (14.53 eV)	$C_4H_4^+$	54	$C_3H_3N^+$, $C_2N_2H^+$	64	$C_4H_8^+$, $C_3H_6N^+$	30
	$C_5H_5N^+$	46	$C_4H_4N_2^+$	31	$C_3H_8^+$, $C_2H_6N^+$	19
			$C_2H_2^+$	<2	$C_2H_4N^+$, $C_3H_6^+$	13
			$C_3H_2N^+$, $C_2N_2^+$, $C_4H_4^+$	<3	$C_4H_7^+$, $C_3H_5N^+$	13
					$C_2H_5N^+$, $C_3H_7^+$	12
					$C_3H_5^+$, $C_2H_3N^+$	9
					$C_5H_{11}N^+$	4
Kr^+ (14 eV)	l-$C_4H_4^+$	70	$C_3H_3N^+$, $C_2N_2H^+$	91	$C_4H_8^+$, $C_3H_6N^+$	44
	c-$C_4H_4^+$	30	$C_3H_2N^+$, $C_2N_2^+$, $C_4H_4^+$	<3	$C_4H_9^+$, $C_3H_7N^+$	31
			$C_3H_4N^+$	<3	$C_2H_5^+$, CH_3N^+	15
			$C_4H_4N_2^+$	<3	$C_2H_6^+$, CH_4N^+	7
					$C_2H_4^+$, CH_2N^+	3

Reactant Ion	Pyridine Ion Product	%	Pyrimidine ion product	%	Piperidine ion product	%
O^+ (13.62 eV)	$C_4H_4^+$	100	$C_3H_3N^+$, $C_2N_2H^+$	100	-	-
O_2^+ (12.07eV)	$C_5H_5N^+$	100	$C_4H_4N_2^+$	100	$C_5H_{10}N^+$	48
					$C_5H_{11}N^+$	17
					$C_3H_8^+$, $C_2H_6N^+$	14
					$C_3H_7^+$, $C_2H_5N^+$	10
					$C_4H_9^+$, $C_3H_7N^+$	10
					$C_5H_{10}^+$, $C_4H_8N^+$	3
NH_3^+ (10.07eV)	$C_5H_5N^+$	100	-	-	-	-
H_3O^+ (6.4 eV)	$C_5H_5NH^+$	100	$C_4H_4N_2H^+$	100	$C_5H_{11}NH^+$	91
					$C_5H_{10}N^+$	9
NH_4^+ (4.8 eV)	$C_5H_5NH^+$	100	$C_4H_4N_2H^+$	100	$C_5H_{11}NH^+$	100

Recombination energies of the reactant ions are given beside their identification[19]. The ionization energies of the heterocyclic molecules are 9.26, 9.33 and 8.03 eV respectively[19].

conditions; it was assumed that the transmission was mass independent. This was confirmed in individual reactions by determining the total ion count rate as a function of reactant gas flow after correction for mass discrimination and this was constant implying the discrimination had been accounted for correctly.

Reactions involving NH_4^+ and H_3O^+ proceed only by proton transfer. In these cases, charge transfer is endothermic and is not expected to be a product channel, consistent with observations. With all other reactant ions, charge transfer (both dissociative and non-dissociative) is energetically possible and was detected as the main product channel.

The rate coefficients were also measured for all of the reactions and are provided in Table 3.2. The dilution of the reactant neutral was taken into account with each rate coefficient being corrected accordingly. Most of the reactions proceed at the gas kinetic rate to within experimental error. Theoretical rate coefficients were calculated using combined variational transition state theory and classical trajectory theory[20]. Reaction efficiencies for all reactions were at or near unity.

3.4.1 Pyridine

The reactions of pyridine (ionization energy, IE 9.26 eV) with ions of low recombination energies, NH_3^+ (RE 10.07) and O_2^+ (RE 12.07), resulted only in non-dissociative charge transfer. When the more energetic ion, O^+ (RE 13.62 eV), was used, fragmentation of the ring became favored. Here the only product channel generates an ion at m/z 52. To determine if this was $C_4H_4^+$ or $C_3H_2N^+$, reactions with C_5D_5N were performed. Then, this product ion mass was observed to move to

Table3.2 Experimental rate coefficients, k_{exp}, for the reactions between the three neutral molecules and the indicated ions are listed followed by the theoretical rate coefficients, k_{theor}, calculated using combined variational transition state theory and classical trajectory theory[20]. Data needed to calculate the theoretical rate coefficients were obtained from the literature[21].

Primary Ion	k_{exp} $(10^{-9} cm^3 s^{-1})$	k_{theor} $(10^{-9} cm^3 s^{-1})$	*Efficiency
C_5H_5N			
Ne^+	3.4	3.18	1.07
Ar^+	2.3	2.47	0.93
N_2^+	2.7	2.79	0.97
N^+	3.4	3.68	0.92
Kr^+	1.92	1.99	0.97
O^+	4.4	3.48	1.26
O_2^+	3.1	2.66	1.17
NH_3^+	3.6	3.4	1.06
H_3O^+	4.4	3.25	1.35
NH_4^+	3.5	3.32	1.05
$C_4H_4N_2$			
Ne^+	2.9	3.34	0.87
Ar^+	2.7	2.59	1.04
N_2^+	2.9	2.94	0.99
N^+	4.8	3.87	1.24
Kr^+	2.1	2.09	1
O^+	3.6	3.66	0.98
O_2^+	2.6	2.8	0.93
NH_3^+	2.8	3.57	0.78
H_3O^+	4.3	3.41	1.26
NH_4^+	3.1	3.49	0.89
$C_5H_{11}N$			
Ne^+	2.29	2.07	1.11
Ar^+	1.7	1.6	1.06
N_2^+	1.7	1.82	0.93
N^+	2.30	2.41	0.95
Kr^+	1.05	1.26	0.83
O_2^+	2.23	2.75	0.81
NH_3^+	2.3	2.22	1.04
H_3O^+	1.97	3.35	0.59

*The reaction efficiency, k_{exp}/k_{theor}, is also included. All rate coefficients are expressed in units of $10^{-9} cm^3 s^{-1}$.

56 amu ($C_4D_4^+$) proving that the product was entirely $C_4H_4^+$, a common fragment of unsaturated, cyclic hydrocarbon dissociation[22] in both ion-molecule reactions and electron impact ionization. This is important because HCN is the neutral that results from this fragmentation and it is particularly stable and abundant in ISC and in Titan's ionosphere. It is interesting to note that the major product in the reactions with Kr^+(RE 14 eV), N^+(14.53 eV), N_2^+ (15.58 eV) and Ar^+ (15.76 eV) is also $C_4H_4^+$. As can be seen from Table 1, other dissociative and non-dissociative product channels are observed but $C_4H_4^+$ is by far the most abundant product ion. It is only when pyridine reacts with the energetic Ne^+ (RE 21.56 eV) that the $C_4H_4^+$ product channel is less significant because of the increasing fragmentation. In the Ne^+ reaction, in addition to the expected dissociative channels, the non-dissociative charge transfer is surprisingly a significant product.

Note that in these studies, there are often two possible ion products with the same mass. In one case, we were able to distinguish the product by isotopic labeling. For other reactions involving the isotopic pyridine, conflicting product masses made it impossible to determine the absolute identity of the product. Thermodynamic considerations also were used in an attempt to settle on the identity of the product ions. In all but a few cases, each possible ion product was energetically possible and thus this method could not be used to establish the ion identity. Another concern is the possibility of several isomers. In the case of $C_4H_4^+$, it is generally accepted that two linear isomers and two cyclic isomers are stable enough to form[23]. Reactions of $C_4H_4^+$ with benzene were used to determine if this molecular ion was cyclic or linear.

It had been previously determined that the linear form of $C_4H_4^+$ reacts with benzene in a charge transfer reaction while the cyclic form is unreactive[24,25]. The $C_4H_4^+$ product of the reaction of Ar^+ and pyridine studied in this manner showed that 70% of the $C_4H_4^+$ was linear and 30% was cyclic. When benzene was reacted with the $C_4H_4^+$ product of the N_2^+ reaction, it was determined that a 50:50 mix of the linear and cyclic isomer was present. This study unfortunately does not provide enough information to determine which of the two linear and which of the two cyclic isomers are formed. However, following from thermodynamic considerations and the neutralization-reionization mass spectrometry study of Zhang et al.[22], it is assumed the two isomers with the lowest energy configuration are generated. Therefore, the linear isomer is identified as the vinyl acetylene cation and the cyclic isomer as the methylene cyclopropene cation. Because of the complexity of the study, other reactions resulting in $C_4H_4^+$ as a product were not studied further to determine the identity of the isomer(s) present. Some of the other products also have isomers, such as cyclic and linear $C_3H_3^+$ that can be determined by following the rate of reactions with CO,[25] but due to the difficulty in interpreting the data these structures were not investigated.

3.4.2 Pyrimidine

Pyrimidine (IE 9.33 eV) was studied not only because of its biological importance but also to see how product channels differ when an additional nitrogen was present in the ring. Here an additional lone pair of electrons is gained, but the aromaticity is still preserved. As with pyridine, the reactions with O_2^+ resulted only in

non-dissociative charge transfer. In the reactions of O^+, Kr^+, N^+, N_2^+ and Ar^+, an ion, $C_3H_3N^+$, is produced with the neutral product corresponding to HCN, as occurred with pyridine. It is possible for the ion mass to correspond to $C_2N_2H^+$ but there was no information available in this case to calculate the energetics. However, following from the isotope substitution in the pyridine case, the most likely ion identity is $C_3H_3N^+$ produced with the neutral HCN. The energetic reaction with Ne^+ proceeded with much fragmentation and the major product channel was $C_2H_2^+$.

3.4.3 Piperidine

Piperidine is quite different from the other two molecules because it is saturated and has no delocalized π electrons. The lack of aromaticity suggested that this molecule would fragment more easily and considerably more fragmentation was observed. The products of the O_2^+ reaction resulted in both dissociative (unlike the other molecules) and non-dissociative charge transfer. As Table 1 shows, the reactions of Kr^+, N^+, N_2^+ and Ar^+ all had an ion with an m/z of 56 as the main product. This corresponds to $C_4H_8^+$ and/or $C_3H_6N^+$, both being energetically possible. Also it is interesting to note that, in this case, the reaction with the more energetic Ne^+ produced a different primary product ion from the four lower energy ions: Kr^+, N^+, N_2^+ and Ar^+ (m/z 56 product was present only as a 6% product).

3.5 DISSCUSSION

When comparing the stability of the three reactant molecules, it is clear that piperidine is the least stable as indicated by the large amount of fragmentation that occurs even at lower energies. This is expected considering piperidine is not

aromatic, unlike pyridine and pyrimidine. One interesting similarity among all three molecules is the consistency of the primary product channel for reactions with ions of recombination energies of about 14 to 16 eV. The reactions were compared to the reactions of a similar set of ions previously studied with benzene[25]. In this comparison it is important to note that even though benzene is more stable, i.e. requiring around 2 eV more energy to produce fragment ions, once sufficient energy is available, more product fragments are produced than in either of the equivalent reactions involving pyridine or pyrimidine. This could be due to the particularly stable ions and neutral combinations formed when pyridine and pyrimidine initially fragment; these are not all available to the benzene reactions.

Because of the limited number of ion-molecule reactions that have been studied involving these molecules, very few direct comparisons could be made to literature data. However, there was a study that provided electron impact (EI) fragmentation data for pyridine over a range of energies (10-200 eV) [26]. It might be thought that these data can be directly compared with our product distribution; however, in the EI study the dominant process through the entire energy range was non-dissociative charge transfer with the fragmentation producing $C_4H_4^+$ as the next most important channel. The importance of the $C_4H_4^+$ channel increased as the energy of the electrons was increased. Overall, there were more fragment ions observed in the EI experiments when compared to ion-molecule reactions with similar energies. Even though less fragmentation is observed in the ion-molecule reactions, it is worth noting that the non-dissociative charge transfer is only dominant

at energies below 12 eV. The differences between these two studies show the reaction mechanisms are very different, as might be expected. Also, in the EI studies, it was possible to identify all of the isobaric masses. This information can reasonably be used to determine the identity of the masses in question in the present work.

Comparison was also possible with some much earlier studies in the literature[27,28], although these were over a range of kinetic energies (1 to 300 eV). Plots of the literature distributions versus kinetic energy were made and extrapolated to zero kinetic energy to give a better comparison with the present data. They are listed in Table 3.3 for comparison to the 298K values obtained in this study. The literature values for the reactions of Ne^+, Ar^+ and Kr^+ with pyridine and Ar^+ and Kr^+ with pyrimidine all agree very well. The major product is always the same though the actual percentage differs to some degree. The previous studies show slightly more fragmentation though most of the additional products are only a small contribution. This difference could be partially due to the inaccuracy of extrapolated product distributions and the difference in experimental techniques. Two more recent papers detail the reactions of H_3O^+ and O_2^+ with both pyridine and piperidine [29,30] as studied using a SIFT.   As shown in Table 3.3 the product distributions in the literature agree very well with the values obtained in this study.

The site at which the ion interacts with the neutral molecule was also considered. In electron impact ionization, the loss of the electron of lowest ionization energy is expected[31] and the same can reasonably be expected of electron transfer in

46

Table 3. 3   Comparison of product distribution results from this study with literature.

Reactant Ion	Pyridine This Work		Literature		Pyrimidine This Work		Literature		Piperidine This Work		Literature	
Ne^+	$C_4H_3^+$	54 %	$C_4H_3^+$	40 %	--	--	--	--	--	--	--	--
	$C_4H_2^+$	21 %	$C_4H_2^+$	26 %	--	--	--	--	--	--	--	--
	$C_5H_5N^+$	13 %	$C_4H_4^+$	11 %	--	--	--	--	--	--	--	--
	$C_4H_4^+$	12 %	$C_2H_2^+$	8 %	--	--	--	--	--	--	--	--
			$C_3H_3^+$	5 %	--	--	--	--	--	--	--	--
			$C_2H_3^+$	5 %	--	--	--	--	--	--	--	--
Ar^+	$C_4H_4^+$	66 %	$C_4H_4^+$	42 %	$C_3H_3N^+$	54 %	$C_2H_2^+$	56 %	--	--	--	--
	$C_5H_4N^+$	15 %	$C_5H_4N^+$	25 %	$C_2H_2^+$	21 %	$C_3H_2N^+$	24 %	--	--	--	--
	$C_3H_3N^+$	12 %	$C_4H_3^+$	13 %	$C_3H_2N^+$	22 %	$C_3H_3N^+$	20 %	--	--	--	--
	$C_3H_3^+$	7 %	$C_4H_2^+$	8 %	$C_4H_4N_2^+$	≤ 4 %			--	--	--	--
			$C_3H_3N^+$	7 %					--	--	--	--
			$C_3H_3^+$	5 %					--	--	--	--
Kr^+	l-$C_4H_4^+$	70 %	$C_4H_4^+$	77 %	$C_3H_3N^+$	91 %	$C_3H_3N^+$	87 %	--	--	--	--
	c-$C_4H_4^+$	30 %	$C_5H_4N^+$	14 %	$C_3H_2N^+$	≤ 3 %	$C_4H_3N_2^+$	6 %	--	--	--	--
			$C_3H_3^+$	4 %	$C_3H_4N^+$	≤ 3 %	$C_3H_2N^+$	3 %	--	--	--	--
			$C_4H_5^+$	4 %	$C_4H_4N_2^+$	≤ 3 %	$C_2H_2^+$	3 %	--	--	--	--
			$C_5H_5N^+$	1 %			$C_4H_4N_2^+$	1 %	--	--	--	--
H_3O^+	$C_5H_5NH^+$	100 %	$C_5H_5NH^+$	100 %	--	--	--	--	$C_5H_{11}NH^+$	91%	$C_5H_{11}NH^+$	90%
									$C_5H_{10}N^+$	9%	$C_5H_{10}N^+$	10%
O_2^+	$C_5H_5N^+$	100 %	$C_5H_5N^+$	100 %	--	--	--	--	$C_5H_{10}N^+$	46%	$C_5H_{10}N^+$	55%
									$C_5H_{11}N^+$	17%	$C_5H_{11}N^+$	15%
									$C_3H_8^+,C_2H_6N^+$	14%	$C_3H_8^+,C_2H_6N$	10%
									$C_3H_7^+,C_2H_5N^+$	10%	$C_3H_7^+, C_2H_5N^+$	10%
									$C_4H_9^+,C_3H_7N^+$	10%	$C_4H_9^+, C_3H_7N^+$	5 %
									$C_5H_{10}^+,C_4H_8N^+$	3%	$C_5H_{10}^+, C_4H_8N^+$	5%

References for literature product distribution values: a[27], b[28], c[30], d[29]. Values for *a* and *b* were extrapolated to thermal energies.

ion-molecule reactions. Recognizing the expected radical site then allows the most likely product ion fragments to be identified. In turn, the observed product fragments can provide information about the actual radical site and therefore information about the interaction of the ion and molecule. In the reactions of pyridine and pyrimidine, it is reasonable to expect the ion to interact with the electrons located in the highest occupied molecular orbital (HOMO), which in both cases involves the lone pair on the nitrogen atom. When considering well-known fragmentation mechanisms starting from the radical site on the nitrogen, an expected major product ion would be $C_3H_3N^+$ for reactions with both pyridine and pyrimidine. However, for reactions involving pyridine, the experimental data show $C_3H_3N^+$ to be present in only two reactions and then only as a minor product. As stated before, the major product in almost all pyridine reactions exhibiting dissociative charge transfer is $C_4H_4^+$. The only way for this product to form is to have the radical site on a specific carbon atom in the ring, as seen in Figure 3.2. However, for pyrimidine, the major dissociative product is $C_3H_3N^+$. This could occur from either the radical site location on the nitrogen or on one of the carbons, as shown in Figure 3.3. A study in which the electronic structure of pyrimidine was investigated stated that the molecular orbital involved in producing the fragment as having some nitrogen influence[28]. However, a similar study by the same group on the electronic structure of pyridine described the orbital involved in the fragmentation as being strongly carbon-carbon bonding[27]. Apparently according to these studies, the addition of the second
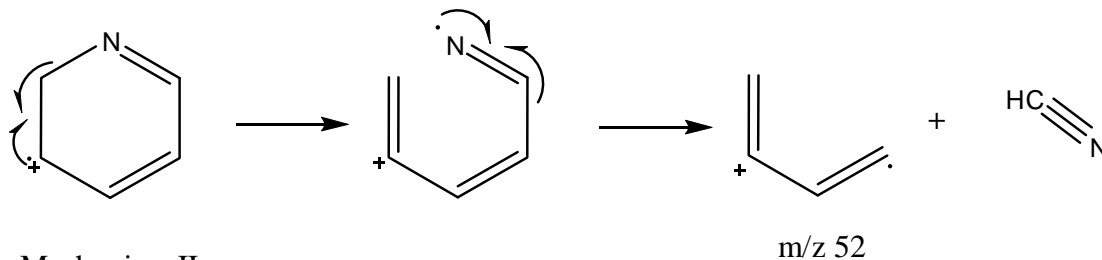
Mechanism I

Figure 3.2 Proposed pyridine dissociation mechanisms that give the experimentally observed product $C_4H_4^+$ at an m/z of 52.

Mechanism I
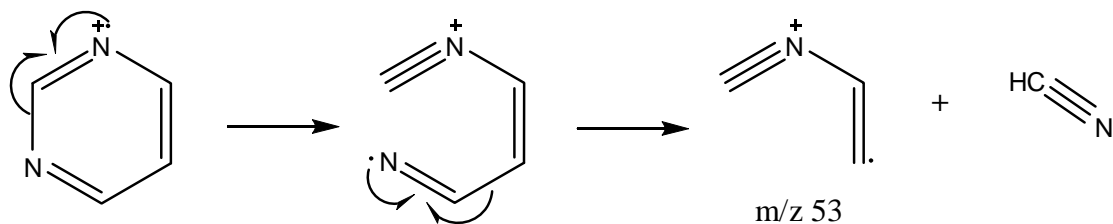
Mechanism II
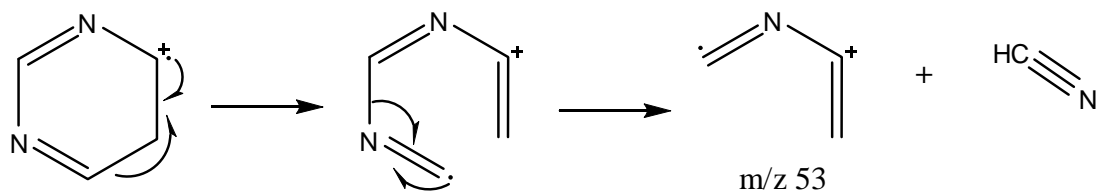
Figure 3.3 Proposed pyrimidine dissociation mechanisms that give the experimentally observed product $C_3H_3N^+$ at an m/z of 53. In Mechanism II it is also possible to generate $C_3H_3N^+$ with the radical located on either of the two carbons below the carbon radical shown.

49

nitrogen changes the radical site. However, since both molecules have similar HOMO's, it seems strange that the radical site in the pyridine reactions would reside on a carbon atom and in the pyrimidine reactions on the nitrogen atom. It is not clear why Asbrink et al. [28] make the assumption that the orbital involved in ionization and fragmentation involves the nitrogen atom in the case of pyrimidine but not for pyridine, especially since it is possible to get the same fragmentation product if the radical is located on a carbon atom in the pyrimidine dissociation.

Apart from these data, experimentally it should be possible to determine if the nitrogen is important in the interaction of the ion and molecule. Since pyrimidine has one more nitrogen than pyridine, and hence an additional reaction site, the overall reactions involving pyrimidine should be more efficient if the reaction is taking place at the nitrogen atom. Unfortunately, all of the rate coefficients were at or near gas kinetic rate so an additional reaction site could have no effect on the rate. A study of these reactions at a higher temperature might be valuable since it would be likely to slow down the reaction and allow differences in reactivity to be distinguished. Then, it would be possible to determine if the addition of a second nitrogen increases the rate of reaction as expected.

To better understand the interaction between the ions and neutrals involved in this study, some preliminary theoretical calculations were performed. Intrinsic reaction coordinate calculations were used to determine if the ion preferred to approach the neutral from above the plane of the molecule, essentially interacting with the delocalized π electrons, or from the plane of the molecule approaching

50

either a nitrogen lone pair or a carbon atom. Calculations were performed at the UB3LYP/6-31G* level using Gaussian 03[32] and followed the interaction of Ne$^+$ with both pyridine and pyrimidine. In both cases when approaching the carbon atom in plane, the carbon is blocked by a peripheral hydrogen atom, therefore the calculations measure the interaction of the ion and hydrogen. Both calculations showed the interaction with the π electrons was higher in energy than the interaction with the nitrogen or hydrogen. The interactions of Ne$^+$ with both pyridine and pyrimidine showed a slightly stronger interaction with the hydrogen than with the nitrogen. It is possible that the lower energy arises from the fact that hydrogen atom has a smaller Bohr radius than nitrogen, so at the same neutral-ion distance, there is less electron repulsion for the attack on the H-atom and thus the interaction of Ne$^+$ with hydrogen is lower in energy. This preliminary calculation does not support the conclusion drawn from these experiments that the ion interacts with the π electrons and therefore the radical site appears to be located on a carbon atom in the ring.

3.6 CONCLUSIONS

This study has addressed two very different but important observations. The first concerns the astrochemical importance of pyridine and pyrimidine, and the second regards the dissociation mechanism of the molecules. It is possible that heterocyclic molecules such as pyridine and pyrimidine are present in ISC. Several attempts have been made to identify both species there, but these species have proven to be elusive. Should these molecules exist, one possible route to their formation is identified through these experiments. Pyridine could be synthesized in

the gas phase through the association reaction of $C_4H_4^+$ with HCN, while pyrimidine might be formed by the reaction of $C_3H_3N^+$ with HCN providing there are no significant barriers to inhibit the reactions. Note that such barriers could be overcome to some degree by the ion-induced dipole and ion-permanent dipole interactions. It is proposed to check this in future studies. Fragmentation patterns of all of the ringed compounds have proven them to be stable enough to exist in protected regions of ISC.

The second point of interest involves the site of ionization and mechanisms of reaction with the neutral molecules. It is expected that the lone pair of electrons on the nitrogen would be the most likely site for the initial removal of an electron. However, for pyridine, the electron impact study and this ion-molecule study have proved that the major product is not consistent with this conclusion and instead the electron most likely is taken from the π delocalized electrons. From the experimentally observed products, the radical site must be on the second or third carbon atom relative to the nitrogen. Concerning pyrimidine, even though a previous study attributes the radical site to the nitrogen atom, it is also possible for the major product to be generated from a radical on any carbon atom in the ring except for the lone carbon atom between the two nitrogen atoms. From the information gathered on the pyridine reactions this seems a likely possibility.

3.7 ACKNOWLEDGEMENTS

3.8 REFERENCES

1.   Thaddeus, P.; Vrtilek, J. M.; Gottlieb, C. A. *Ap. J.* **1985**, *299*, L63.

2.   Dickens, J. E.; Irvine, W. M.; Ohashi, A.; al, e. *Ap. J.* **1997**, *489*, 753.

3.   Charnley, S. B.; Kuan, Y.-J.; Huang, C.; Botta, O.; Butner, H. M.; Cox, D. P.; Despois, D.; Ehrenfreund, P.; Kisiel, Z.; Lee, H. S.; Markwick, A. J.; Peeters, Z.; Rodgers, M. T. *Adv. Space Res.* **2005**, *36*, 137.

4.   Yamamoto, S.; Saito, S.; Ohishi, M.; Suzuki, H.; Ishikawa, N.; Kaifu, N.; Murakami, A. *Ap. J.* **1987**, *322*, L55.

5.   Kuan, Y.-J.; Charnley, S. B.; Huang, H.-C.; Kisiel, Z.; Ehrenfreund, P.; Tseng, W.-L.; Yan, C.-H. *Adv. Space Res.* **2004**, *33*, 31.

6.   Hollis, J. M.; Remijan, A.; Jewell, P. R.; Lovas, F. J. *Ap. J.* **2006**, *642*, 933.

7.   Cernicharo, J.; Heras, A. M.; M., T. A. G. G.; Pardo, J. R.; Herpin, F.; Guelin, M.; Waters, L. B. F. M. *Ap. J.* **2001**, *546*, L123.

8.   Wilson, E. H.; Atreya, S. K.; Coustenis, A. *J. Geophys. Res.* **2003**, *108(E2)*, 5014.

9.   Waite, J. H.; Nieman, H.; Yelle, R. V.; Kasprzak, W. T.; Cravens, T. E.; Luhmann, J. G.; McNutt, R. L.; Ip, W.-H.; Gell, D.; de la Haye, V.; Muller-Wordag, I.; Magee, B.; Borggren, N.; Ledvina, S.; Fletcher, G.; Walter, E.; Miller, R.; Scherer, S.; Thorpe, R.; Xu, J.; Block, B.; Arnett, K. *Science* **2005**, *308*, 982.

10.   Hudgins, D. M.; Bauschlicher, C. W.; Allamandola, L. J. *Ap. J.* **2005**, *632*, 316.

11.   Simon, M. N.; Simon, M. *Ap. J.* **1973**, *184*, 757.

12.   Kuan, Y.-J.; Yan, C.-H.; Charnley, S. B.; Kisiel, Z.; Ehrenfreund, P.; Huang, H.-C. *Mon. Not. Roy. Astr. Soc.* **2003**, *345*, 650.

13.   Peeters, Z.; Botta, O.; Charnley, S. B.; Kisiel, Z.; Kuan, Y.-J.; Ehrenfreund, P. *Astron. Astrophys.* **2005**, *433*, 583.

14.   Cravens, T. E.; Robertson, I. P.; Waite, J. H.; Yelle, R. V.; Kasprzak, W. T.; Keller, C. N.; Ledvina, S. A.; Nieman, H. B.; Luhmann, J. G.; McNutt, R. L.; Ip, W.-H.; de la Haye, V.; Mueller-Wodarg, I.; Wahlund, J.-E.; Anicich, V. G.; Vuitton, V. *Geophys. Res. Lett.* **2006**, *33*, L07105.

15.   Adams, N. G.; Smith, D. *Int. J. Mass Spectrom. Ion Phys.* **1976**, *21*, 349.

16.   Adams, N. G.; Smith, A. D. Flowing Afterglow and SIFT. In *Techniques for the Study of Ion-Neutral Reactions*
Farrar, J. M., Saunders, J. W. H., Eds.; Wiley-Interscience: New York, 1988; pp 165.

17.   Jackson, D. M.; Stibrich, N. J.; McLain, J. L.; Fondren, L. D.; Adams, N. G.; Babcock, L. M. *Int. J. Mass Spectrom.* **2005**, *247*, 55.

18.   Smith, D.; Adams, N. G. The Selected Ion Flow Tube (SIFT): Studies of Ion-Neutral Reactions. In *Advances in Atomic and Molecular Physics*; Bates, D. R., Bederson, B., Eds.; Academic Press: New York, 1988; Vol. 24; pp 1.

19.   Linstrom, P. J.; Mallard, W. G. NIST Chemistry WebBook. In *NIST Standard Database 69*; National Institute of Standards and Technology: Gaithersburg MD, 20899, June 2005.

20.   Su, T.; Chesnavich, W. J. *J. Chem. Phys.* **1982**, *76*, 5183.

21.   *CRC Handbook of Chemistry and Physics*; 77 ed.; Lide, D. R., Ed.; CRC Press, Inc.: New York, 1996-1997.

22.   Zhang, M.-Y.; Carpenter, B. K.; McLafferty, F. W. *J. Am. Chem. Soc.* **1991**, *113*, 9499.

23.   Adams, N. G.; Smith, D. *J. Phys. D.* **1980**, *13*, 1267.

24.   Ausloos, P. *J. Am. Chem. Soc.* **1981**, *103*, 3931.

25.   Arnold, S. T.; Williams, S.; Dotan, I.; Midey, A. J.; Morris, R. A.; Viggiano, A. A. *J. Phys. Chem. A* **1999**, *103*, 8421.

26.   Jiao, C. Q.; DeJoseph Jr., C. A.; Lee, R.; Garscadden, A. *Int J. Mass Spectrom.* **2006**, *257*, 34.

27.   Jonsson, B. O.; Lindholm, E.; Skerbele, A. *Int. J. Mass Spectrom. Ion Phys.* **1969**, *3*, 385.

28.   Asbrink, L.; Fridh, C.; Jonsson, B. O.; Lindholm, E. *Int. J. Mass Spectrom. Ion Phys.* **1971**, *8*, 215.

29.   Milligan, D. B.; Wilson, P. F.; Freeman, C. G.; Meot-Ner, M.; McEwan, M. J. *J. Phys. Chem. A* **2002**, *106*, 9745.

30.   Wang, T.; Spanel, P.; Smith, D. *Int. J. Mass Spectrom* **2004**, *237*, 167.

31.   McLafferty, F. W.; Turecek, F. *Interpretation of Mass Spectra*, 4th ed.; University Science Books: Sausalito, 1993.

32.   M. J. Frisch, G. W. T., H. B. Schlegel, G. E. Scuseria, M. A. Robb, J. R. Cheeseman, J. A. Montgomery, Jr., T. Vreven, K. N. Kudin, J. C. Burant, J. M. Millam, S. S. Iyengar, J. Tomasi, V. Barone, B. Mennucci, M. Cossi, G. Scalmani, N. Rega, G. A. Petersson, H. Nakatsuji, M. Hada, M. Ehara, K. Toyota, R. Fukuda, J. Hasegawa, M. Ishida, T. Nakajima, Y. Honda, O. Kitao, H. Nakai, M. Klene, X. Li, J. E. Knox, H. P. Hratchian, J. B. Cross, V. Bakken, C. Adamo, J. Jaramillo, R. Gomperts, R. E. Stratmann, O. Yazyev, A. J. Austin, R. Cammi, C. Pomelli, J. W. Ochterski, P. Y. Ayala, K. Morokuma, G. A. Voth, P. Salvador, J. J. Dannenberg, V. G. Zakrzewski, S. Dapprich, A. D. Daniels, M. C. Strain, O. Farkas, D. K. Malick, A. D. Rabuck, K. Raghavachari, J. B. Foresman, J. V. Ortiz, Q. Cui, A. G. Baboul, S. Clifford, J. Cioslowski, B. B. Stefanov, G. Liu, A. Liashenko, P. Piskorz, I. Komaromi, R. L. Martin, D. J. Fox, T. Keith, M. A. Al-Laham, C. Y. Peng, A. Nanayakkara, M. Challacombe, P. M. W. Gill, B. Johnson, W. Chen, M. W. Wong, C. Gonzalez, and J. A. Pople. Gaussian 03, Revision C.02; Gaussian, Inc: Wallingford CT, 2004.

CHAPTER 4

ION-NEUTRAL REACTIONS OF $C_4H_4^+$

4.1 INTRODUCTION

The formation of cyclic species in the interstellar medium (ISM) and the atmosphere of Titan is under investigation. Benzene has been detected in the ISM[1] and two nitrogen analogues, pyridine and pyrimidine, were searched for without positive identification[2-5]. Data from the Cassini orbiter indicates that benzene is present in the atmosphere of Titan[6-8]. It also detected an abundance of nitrogen containing molecules which was unexpected[9]. Peaks at both m/z 79 and 80 could indicate the presence of charged and/or protonated pyridine. It is likely that m/z 79 is protonated benzene but the possibility of pyridine cannot be ruled out until spectroscopic data are collected in Titan's atmosphere. The m/z at 80 is given the chemical formula $C_5H_5NH^+$ which correlates to protonated pyridine. The ion neutral mass spectrometer (INMS) aboard Cassini was only able to detect positive ions up to 99 amu. However, the CAPS Ion Beam Spectrometer was able to detect positive ions in the range of 100-350 amu and negative ions up to a mass of 8000 amu[10-13]. Note that this instrument was not originally designed for this type of experiment and therefore has a lower resolution than the

INMS. However, the abundance of very large negative molecules bodes well for the formation and stability of very large positive ions and neutrals.

The formation of benzene in the interstellar medium is thought to occur through the polymerization of acetylene[1,4]. Subsequent additions of C_2H_2 could lead to large polycyclic aromatic hydrocarbons (PAHs)[4] where additions of HCN could lead to the incorporation of nitrogen in the ring. In fact, polyaromatic nitrogen heterocycles (PANHs) along with PAHs are thought to be responsible for the unidentified infrared emission spectrum[14,15] in the ISM. In Titan's atmosphere, the primary mechanism of benzene formation is thought to be the recombination of the propargyl radical (C_3H_3)[8], although, it appears that ion molecule reactions play an important role in benzene production. A model by Vuitton et al.[7] identified 13 ion-neutral reactions that are important for the formation of benzene. Without the ion-molecule reactions, the model underestimates the density of benzene in the upper atmosphere by a factor of 3. Benzene is also considered to play an important role in the formation of larger, multi-ring molecules in Titan's atmosphere and with the large abundance of nitrogen in the atmosphere large nitrogen containing ring molecules are likely to be formed. The simplest of the nitrogen aromatic cyclic species is pyridine. With only one nitrogen in the 6-membered ring, it is more likely to be formed and detected than the larger multi-ring systems so it is important to determine how it is formed. Knowledge of its production mechanisms might provide clues to the formation mechanisms of larger nitrogen containing rings, should they exist.

A previous study has investigated the reaction of pyridine with a series of ions with differing recombination energies. The major ion product of these reactions is $C_4H_4^+$. Reactive and non-reactive isomers could be distinguished in many of the reactions producing this species. Interestingly, the neutral product when $C_4H_4^+$ is produced from reaction with pyridine is HCN, which is very abundant in both the ISM and in Titan's atmosphere. An m/z= 52 that could correspond with $C_4H_4^+$ is also present in Titan's atmosphere, though at present it is being attributed mainly to HC_3NH^+. If pyridine is present in Titan's atmosphere there is probably more than one reaction that will contribute to its formation (much like benzene). Since both HCN and $C_4H_4^+$ are possibly present in Titan's atmosphere it is interesting to consider if the ion-neutral reaction between the two could be a reaction that result in pyridine. $C_4H_4^+$ has not been identified in the ISM so this reaction may not be relevant to formation of pyridine there.

4.2 EXPERIMENTAL

A selected ion flow tube (SIFT) was used to study the reaction of $C_4H_4^+$ with HCN. The technique has been described in detail previously and will not be discussed here[16,17]. $C_4H_4^+$ was produced in several ways. First, it was created by ionizing pyridine in a low pressure electron impact ionization source (LPIS) and was mass selected before injection into the flow tube. However, once in the flow tube this ion underwent two parallel metastable unimolecular decompositions to form $C_4H_3^+$ and $C_4H_2^+$ both in the same relative intensities[18]. Therefore, it was not possible to isolate $C_4H_4^+$ through EI of pyridine. However, $Kr^+ + C_5H_5N$ was previously shown to produce only $C_4H_4^+$ as the

product ion. Thus, this reaction was carried out by injecting Kr^+ into the flow tube to react with the pyridine which was introduced through the long neutral reactant port. This created $C_4H_4^+$ which was then reacted with the HCN that was introduced in the middle neutral reactant port. Unfortunately, a closer look at this reaction revealed two minor products ($C_3H_3^+$ and $C_4H_5^+$)that were not observed previously and a myriad of secondary reactions made the mass spectrum difficult to interpret.   Because of the inability to selectively isolate $C_4H_4^+$ for reaction with HCN, product distributions could not be determined; however, the ion products resulting from the reaction were identified. In the case of the injected $C_4H_4^+$ the separate contributions of the three primary ions to the product ions are not defined and this prevented detailed product distributions from being obtained. Several additional reactions were also studied to determine how charged pyridine reacts with HCN and O_2. The charged pyridine was created by reaction of injected O_2^+, Xe^+, and NH_3^+ with neutral pyridine. Details for these reactions are given below.

Pyridine was obtained from Sigma Aldrich as a liquid with a manufactured purity of 99.9+%. It was further purified by several cycles of freeze-pump-thaw before use, in order to eliminate dissolved gases. When pyridine was used as the neutral reactant, a 1% mix in helium was prepared. This helped eliminate problems establishing a stable neutral flow due to the pyridine sticking to the walls of the capillary system and the flow tube. The rate coefficients for all primary ions were determined at 298K. The rate coefficients have an error of $\pm$ 30% associated with them.

Hydrogen cyanide was synthesized in house by slight modifications to a known synthesis method[19]. The apparatus used for the synthesis is shown in Figure 4.1. Sulfuric acid was reacted drop wise onto dissolved aqueous sodium cyanide to evolve gaseous HCN. A flow of helium gas carried the HCN from the reaction zone through a reflux condenser. The HCN then passed through calcium chloride pellets to remove moisture. It was then frozen in a cold finger cooled by liquid nitrogen while the helium traveled through to a beaker filled with sodium hydroxide to destroy any residual HCN. When the solid HCN filled most of the cold finger the addition of H_2SO_4 was halted and the helium flow stopped. The cold finger was then isolated from all of the system except an evacuated gas storage bottle that was cooled by dry ice. The cold finger was removed from the liquid nitrogen and as the solid HCN in the cold finger gasified it transferred to the gas storage bottle and was refrozen. After the HCN was transferred, the gas bottle was closed from the system and any remaining gas evacuated from the system. The flow of H_2SO_4 was restarted and this procedure was repeated several times until adequate HCN had been obtained. At this point, all reaction was quenched by adding excess NaOH to the mixture of H_2SO_4 and NaCN. The helium was then allowed to flow for some time to carry the last of the HCN to the beaker of NaOH.

The HCN stored in the tank was allowed to come to room temperature and the pressure was determined with a thermocouple pressure gauge. Enough helium was then added to the gas tank to make a ~ 12-15% mix. This mixture was ionized and the resulting mass spectrum analyzed to ensure that only helium and HCN were present. When there were impurities, the tank was chilled again by dry ice to selectively freeze
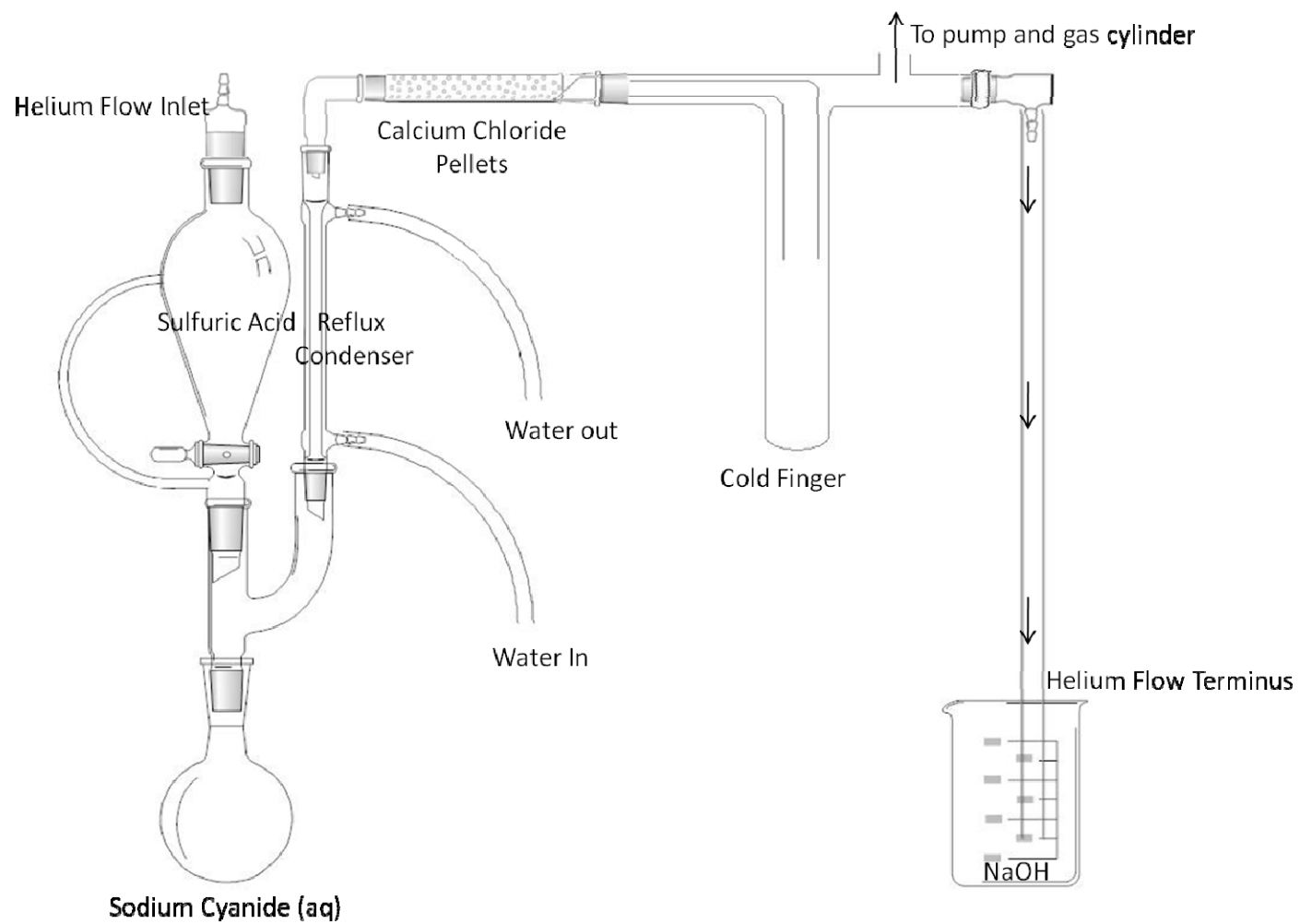
Figure 4.1 Apparatus used to synthesize HCN.

the HCN while gaseous impurities were removed by evacuation. A more accurate percentage of HCN in helium was determined by studying the reaction of HCN with Kr^+, which has a well known rate coefficient.

4.3 RESULTS AND DISCUSSION

The structure of the $C_4H_4^+$ radical cation has been investigated in some depth and reported in the literature. $C_4H_4^+$ is a common product formed in the unimolecular dissociation of ionized unsaturated/cyclic hydrocarbons[20]. It was first noted by Rosenstock that more than one isomer of $C_4H_4^+$ might be formed by the ionization of benzene[21]. Subsequent work by Ausloos on the fragmentation of benzene and pyridine proved that both a reactive isomer and an unreactive isomer of $C_4H_4^+$ were present in the dissociation of both neutral molecules[22]. The reactive isomer reacted with benzene by charge transfer and the only isomer with a large enough recombination energy for this product channel is vinyl acetylene. Several more reactions with neutrals of varying ionization energies determined that the unreactive portion was methylene cyclopropene. Subsequent work determined that of the four stable $C_4H_4^+$ isomers accessible, that of methylene cyclopropene has the lowest heat of formation followed by vinyl acetylene[23]. Several other studies confirmed the identity of the reactive and unreactive isomers of $C_4H_4^{+18,20,24,25}$. In the present study, the $C_4H_4^+$ produced in the LPIS was reacted with benzene to confirm that the reactive isomer is linear vinyl acetylene and the unreactive isomer is assumed to be the cyclic methylene cyclopropene (identified as l-$C_4H_4^+$ and c-$C_4H_4^+$, respectively).

In a previous study[26], the dissociative charge transfer between several rare gas ions and molecular ions with pyridine resulted mainly in the formation of the $C_4H_4^+$ ion product and the HCN neutral product. On the basis of microreversibility the reaction of $C_4H_4^+$ + HCN is expected to form pyridine barring any activation energy barriers. Before this reaction was investigated, it was informative to determine if $C_4H_4^+$ isomers of differing reactivity were created by EI on pyridine in a LPIS. To determine the isomer contributions $C_4H_4^+$ was reacted with benzene where it was determined that 60% linear and 40% cyclic isomers were present. The rate coefficient for the linear isomer is 1.2×10^{-9} cm^3 s^{-1} and that of the cyclic isomer is $\leq 3.4 \times 10^{-13}$ cm^3 s^{-1}. The ratio of reactive to nonreactive isomer agrees well with that obtained in the literature[22]. There is some conflict in the literature concerning the rate of l- $C_4H_4^{+}$[18,22,24,27,28] , however, the value obtained in the present study agrees well with the gas kinetic rate of 1.3×10^{-9} cm^3 s^{-1}. The ion products indicated charged benzene and protonated benzene as the only two products but a product distribution was not obtained since three primary ions were present; $C_4H_4^+$, $C_4H_3^+$ and $C_4H_2^+$.

The reaction of $C_4H_4^+$ with HCN was studied using two different techniques to create the ion. This was done because EI of pyridine created $C_4H_4^+$ which after injected into the flow tube dissociates to some extent to $C_4H_2^+$ and $C_4H_3^+$. To counter this problem, the chemical ionization of pyridine by Kr^+ was used since a previous study showed that $C_4H_4^+$ was the only product[26]. However, closer inspection determined that $C_4H_4^+$ was produced with an 88% abundance with small amounts of $C_3H_3^+$ and $C_4H_5^+$. These minor products and several secondary reactions involving $C_4H_4^+$ complicated the

mass spectrum. At high neutral flows, $C_4H_4^+$ reacts rapidly with pyridine by association.

Also, charged pyridine is produced from a secondary reaction. This is unfortunate because the goal of the study was to determine if this product is formed in the association of $C_4H_4^+$ and HCN. Since this mass is already present in the flow tube before HCN is added to the reaction zone it becomes difficult to determine if it is also produced by association. Thus, this reaction was studied at a low pyridine flow (to avoid secondary association reactions of $C_4H_4^+$ with pyridine) to determine the portion of $C_4H_4^+$ that reacts with HCN. Rate coefficients for both linear and cyclic isomers were also determined. The products could not be determined in detailed so the following ions signals were followed: HCN^+, $HCNH^+$, $C_4H_4^+$, $C_5H_5N^+$, $C_5H_5NH^+$, $C_9H_8N^+$, $C_9H_9N^+$ and the proton bound pyridine dimer. 67% of the $C_4H_4^+$ reacted with a rate coefficient of 3.6 x 10^{-10} cm^3 s^{-1} and 33% of the $C_4H_4^+$ was less reactive with an upper limit rate coefficient of $\leq$ 3.9 x 10^{-12} cm^3 s^{-1}.

Because the pyridine chemical ionization spectrum proved to be too complicated the electron impact of pyridine in the LPIS was revisited. The three primary ions, $C_4H_4^+$, $C_4H_3^+$ and $C_4H_2^+$, were present in approximately equal abundances. Once HCN was added, reaction with all three ions was evident by the decay of the three ions and the emergence of three primary products and two secondary products. The product masses and rate coefficients for this reaction can be found in Table 4.1. HCN appears to associate with each of the primary ions producing $C_4H_2^{+\bullet}$HCN ($C_5H_3N^+$), $C_4H_3^{+\bullet}$HCN ($C_5H_4N^+$) and $C_4H_4^{+\bullet}$HCN ($C_5H_5N^+$). Both $C_4H_2^{+\bullet}$HCN and $C_4H_3^{+\bullet}$HCN react further with

Table 4.1 Data obtained for the reactions investigated in the present study are listed here. Rate coefficients for the primary ion under investigation are given with units of cm^3 s^{-1}. When two primary ion isomers are evident percent ratios and rate coefficients are given for both.

Reactions Studied

$C_4H_4^+$ + C_6H_6

    kl= 1.2 x 10^{-9} 60% linear $C_4H_4^+$

    kc=3.4 x 10^{-13} 40% cyclic $C_4H_4^+$

$C_4H_4^+$ + HCN

    kl= 1.2 X 10^{-10} 62% linear $C_4H_4^+$

    kc= 1.3 x 10^{-12} 38% cyclic $C_4H_4^+$

Product Ions

$C_5H_3N^+$ $C_5H_3N^+$ •HCN

$C_5H_4N^+$ $C_5H_4N^+$ •HCN

$C_5H_5N^+$

$C_4H_2^+$ + HCN

    k=5.1 x 10^{-10}

$C_4H_3^+$ + HCN

    k=6.8 x 10^{-10}

Kr^+ + C_5H_5N →

     $C_4H_4^+$ + HCN

    $k_{l-C4H4+}$= 3.6 X 10^{-10} 67% linear $C_4H_4^+$

    $k_{c-C4H4+}$ ≤ 3.9 x 10^{-12} 33% cyclic $C_4H_4^+$

O_2^+ + C_5H_5N →

    $C_5H_5N^+$ + HCN

   k_{C5H5N+}= 1.1 x 10^{-11}

Xe^+ + C_5H_5N →

    $C_5H_5N^+$ + O_2

   k_{C5H5N+}= 9.6 x 10^{-13}

NH_3^+ + C_5H_5N →

    $C_5H_5N^+$ + O_2

   k_{C5H5N+}= 1.2 x 10^{-12}

---

the neutral gas to create the secondary products $C_4H_2^{+\bullet}(HCN)_2$ and $C_4H_3^{+\bullet}(HCN)_2$, respectively. $C_4H_4^{+\bullet}HCN$ does not appear to react further as no secondary association product was detected and the counts of the product does not decrease as more HCN is added, as can be seen from Figure 4.2. An attempt to model the data assuming that there was no further reaction resulted in a poor fit. This is most likely due to the low counts of the $C_4H_4^{+\bullet}HCN$ product that are close to the limit of detection of the apparatus. $C_4H_2^+$ and $C_4H_3^+$ react more rapidly with HCN (5.1 and 6.8 x 10^{-10} cm^3s^{-1}, respectively) and 100% of both ions reacts unlike only the ~60% of $C_4H_4^+$ that reacts more slowly (1.2 x 10^{-10} cm^3 s^{-1}). The other two products formed are assumed to result from the association of $C_4H_2^+$ and $C_4H_3^+$ with HCN and they have significantly higher count rates than the product attributed to $C_4H_4^+$. This emphasizes how important it is to create a situation in the flow tube where only $C_4H_4^+$ is present to react with HCN.

In spite of the complications, the formation of a product with the chemical formula $C_5H_5N^+$ is encouraging; however, the structure of the product is unknown. Both the reactive $C_4H_4^+$ isomer and HCN neutral are known to be linear. Whether the association product isomerizes to a cyclic structure to create charged pyridine has yet to be determined. To determine if the association product has the same structure as charged pyridine it is advantageous to compare the reactivity of the two. As mentioned above, $C_4H_4^{+\bullet}HCN$ does not appear to react further with HCN. However, a rate coefficient for the reaction cannot be reliably determined from the data available. It is
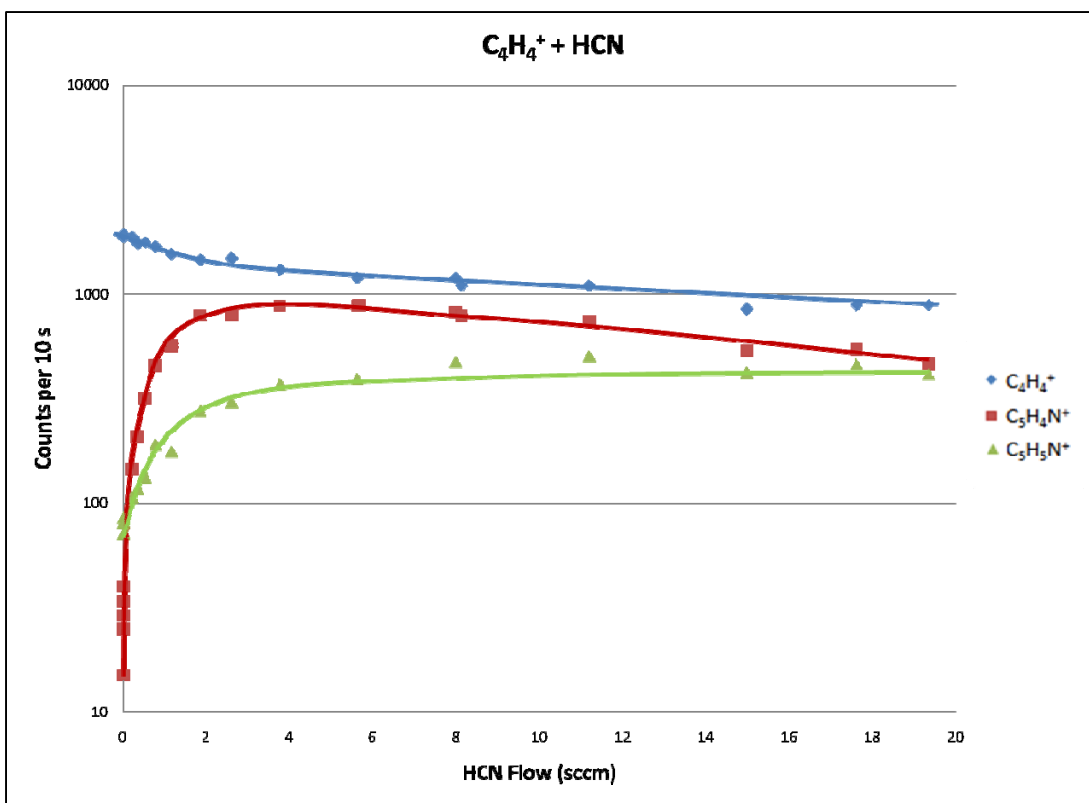
Figure 4.2 The decay of the primary ion $C_4H_4^+$ as it reacts with HCN. The rise of two of the products are shown here. The $C_5H_3N^+$ product is not shown for the sake of clarity. Notice that $C_5H_4N^+$ begins to react with HCN as the flow increases while $C_5H_5N^+$ does not.

necessary to repeat the reaction when $C_4H_4^+$ can be isolated as the lone primary ion and the reaction can be followed to higher HCN flows.

In the meantime, the reactivity of charged pyridine with HCN has been studied to compare with the reactivity of $C_4H_4^{+\bullet}HCN$ with HCN. O_2^+ was created with a LPIS and reacted with pyridine to produce 100% $C_5H_5N^+$. Pyridine was introduced into the flow tube through the long port (83.6 cm reaction length) at a constant flow large enough to produce the maximum amount of $C_5H_5N^+$. HCN was injected through the middle port (59.6 cm reaction length) and its flow was varied while the signal of $C_5H_5N^+$ was monitored. The $C_5H_5N^+$ reacted with a rate coefficient of 1.1 x 10^{-11} cm^3 s^{-1}.

In a second experiment $C_5H_5N^+$ underwent reaction with O_2. $C_5H_5N^+$ was created by chemical ionization from Xe^+ and NH_3^+, where the two primary ions were created in a LPIS. Pyridine was injected into the long port and oxygen in the middle port for both reactions. $C_5H_5N^+$ was produced by two different chemical ionization reactions to determine if the ionization method created $C_5H_5N^+$ with different structures which could be evident by two different rate coefficients. The recombination energy of Xe^+ is 12.1 ev compared to that of NH_3^+ which is 10.07 eV. The ionization energy of pyridine is 9.26 eV. The $C_5H_5N^+$ created from Xe^+ chemical ionization reacted with O_2 with a rate coefficient of 9.6 x 10^{-13} cm^3 s^{-1}. The $C_5H_5N^+$ created from NH_3^+ chemical ionization reacted with O_2 with a rate coefficient of 1.2 x 10^{-12} cm^3 s^{-1}. These two values agree within the ±30% error associated with the measurements. This suggests that the $C_5H_5N^+$ created in each reaction are similar. Furthermore, the $C_5H_5N^+$ is assumed to by a cyclic

ion because ionization of an aromatic cyclic molecule that doesn't result in fragmentation of the ring is expected to retain a cyclic structure for the parent ion.

4.4 CONCLUSIONS

A study was undertaken to determine if the reaction of $C_4H_4^+$ with HCN results in the formation of charged pyridine. The reaction of linear $C_4H_4^+$ does result in a product at an m/z corresponding with charged pyridine. However, there is no theoretical data available detailing the potential energy surface of this reaction so there is no way to know if the formation of a cyclic structure from two associated linear structures is energetically favorable. Instead, the reactivity of charged pyridine with HCN and O_2 was studied to compare to the reactivity of the $C_4H_4^{+\bullet}HCN$ association product. The reaction with O_2 proceeds slower than the HCN reaction. The reaction of $C_4H_4^{+\bullet}HCN$ with both O_2 and HCN needs to be studied to determine the rate coefficients and compare them with the reactions of charged pyridine. If the two molecules show similar reactivity to the same neutrals it could indicate that they have the same structure. However, more reactions need to be studied to determine the approximate recombination energy of the $C_4H_4^{+\bullet}HCN$ so it can be compared with that of charged pyridine. Ultimately, theoretical and spectroscopic data would help confirm if the structures are the same.

The reaction of l-$C_4H_4^+$ and HCN proceeds via an association complex in the flow tube. This is a possible formation route for the formation of charged pyridine in the atmosphere of Titan. The pressures in certain regions of Titan's atmosphere are high

69

enough to effectively stabilize an association complex such as this. Also, HCN is a very abundant neutral and the mass of $C_4H_4^+$ has been identified in the mass spectra obtained by the Cassini orbiter. Work is needed to determine the structure of the association complex but preliminary results indicate the structure could be similar to charged pyridine.

4.5 REFERENCES

1. Cernicharo, J.; Heras, A. M.; M., T. A. G. G.; Pardo, J. R.; Herpin, F.; Guelin, M.; Waters, L. B. F. M. *Ap. J.* **2001**, *546*, L123.

2. Kuan, Y.-J.; Charnley, S. B.; Huang, H.-C.; Kisiel, Z.; Ehrenfreund, P.; Tseng, W.-L.; Yan, C.-H. *Adv. Space Res.* **2004**, *33*, 31.

3. Simon, M. N.; Simon, M. *Ap. J.* **1973**, *184*, 757.

4. Kuan, Y.-J.; Yan, C.-H.; Charnley, S. B.; Kisiel, Z.; Ehrenfreund, P.; Huang, H.-C. *Mon. Not. Roy. Astr. Soc.* **2003**, *345*, 650.

5. Peeters, E.; Mattioda, A. L.; Hudgins, D. M.; Allamandola, L. J. *Ap. J.* **2004**, *617*, L65.

6. Coustenis, A.; Salama, A.; Schultz, B.; Lellouch, E.; Encrenaz, T.; Gautier, D.; Feuchtgruber, H. *Icarus* **2003**, *161*, 383.

7. Vuitton, V.; Yelle, R. V.; Cui, J. *Journal of Geophysical Research* **2008**, *113*, E05007(1.

8. Wilson, E. H.; Atreya, S. K.; Coustenis, A. *J. Geophys. Res.* **2003**, *108(E2)*, 5014.

9. Vuitton, V.; Yelle, R. V. *ApJ* **2006**, *647*, L175.

10. Coates, A.; Wellbrock, A.; Lewis, G. R.; Jones, G. H.; Young, D. T.; Crary, F. J.; Waite, J. H. *Planet. Space Sci.* **2009**, *doi:10.1016/j.pss.2009.05.05.009*.

11. Coates, A. J.; Crary, F. J.; Lewis, G. R.; Young, G. T.; Waite, J. H.; Sittler, E. C. *Geophys. Res. Letts.* **2007**, *34*, L22103.

12. Vuitton, V.; Lavvas, P.; Yelle, R. V.; Galand, M.; Wellbrock, A.; Lewis, G. R.; Coates, A. J.; Wahlund, J.-E. *Planet. Space Sci.* **2009**, *57*, 1558.

13. Wahlund, J.-E.; Galand, M.; Mueller-Wodarg, I.; Cui, J.; Yelle, R. V.; Crary, F. J.; Mandt, K.; Magee, B.; Waite Jr., J. H.; Young, D. T.; Coates, A. J.; Garnier, P.; Aagren, K.; Andre, M.; Eriksson, A. I.; Cravens, T. E.; Vuitton, V.; Gurnett, D. A.; Kurth, W. S. *Planet. Space Sci.* **2009**, *57*, 1857.

14. Allamandola, L. J.; Hudgins, D. M.; Sandford, S. A. *Ap. J.* **1999**, *511*, L115.

15. Hudgins, D. M.; Bauschlicher, C. W.; Allamandola, L. J. *Ap. J.* **2005**, *632*, 316.

16. Adams, N. G.; Smith, D. *Int. J. Mass Spectrom. Ion Phys.* **1976**, *21*, 349.

17. Adams, N. G.; Smith, D. Flowing Afterglow and SIFT. In *Techniques for the Study of Ion-Molecule Reactions*; Farrar, J. M., Saunders, J. W. H., Eds.; Wiley Interscience: New York, 1988; pp 165.

18. Lifshitz, C.; Gibson, D. L.; Levsen, K.; Dotan, I. *International Journal Of Mass Spectrometry and Ion Physics* **1981**, *40*, 157.

19. Ziegler, K. *Organic Syntheses* **1941**, *1*, 314.

20. Zhang, M.-Y.; Carpenter, B. K.; McLafferty, F. W. *J. Am. Chem. Soc.* **1991**, *113*, 9499.

21. Rosenstock, H. M.; McCulloh, K. E. *International Journal Of Mass Spectrometry and Ion Physics* **1977**, *25*, 327.

22. Ausloos, P. *J. Am. Chem. Soc.* **1981**, *103*, 3931.

23. Zhang, M.-Y.; Wesdemiotis, C.; Marchetti, M.; Danis, P. O.; Ray, J. C.; Carpenter, B. K.; McLafferty, F. W. *J. Am. Chem. Soc.* **1989**, *111*, 8341.

24. Wagner-Redeker, W.; Illies, A. J.; Kemper, P. R.; Bowers, M. T. *J. Am. Chem. Soc.* **1983**, *105*.

25. Arnold, S. T.; Williams, S.; Dotan, I.; Midey, A. J.; Morris, R. A.; Viggiano, A. A. *J. Phys. Chem. A* **1999**, *103*, 8421.

26. Fondren, L. D.; McLain, J. L.; Jackson, D. M.; Adams, N. G.; Babcock , L. M. *Int. J. Mass Spectrom.* **2007**, *265*, 60.

27. Field, F. H.; Hamlet, P.; Libby, W. F. *J. Am. Chem. Soc.* **1967**, *89*, 6035.

28.	Lifshitz, C.; Reuben, B. G. *J. Chem. Phys.* **1969**, *50*, 951.

CHAPTER 5

GAS PHASE REACTIONS OF CH_3^+ WITH A SERIES OF HOMO- AND HETEROCYCLIC

MOLECULES

5.1 ABSTRACT

In gas phase ion chemistry, the growth of larger molecules is known to occur through association of ions and neutrals. Where the ion attaches to the neutral is important because it can influence the possibility of additional associations, effectively enabling or terminating further molecular growth. This was investigated using a Selected Ion Flow Tube (SIFT) at 300 K to study the reactions of CH_3^+ with the following series of single ring homocyclic and heterocyclic molecules: benzene (C_6H_6), cyclohexane (C_6H_{12}), pyridine (C_5H_5N), pyrimidine ($C_4H_4N_2$), piperidine ($C_5H_{11}N$), 1,4-dioxane ($C_4H_8O_2$), furan (C_4H_4O), pyrrole (C_4H_5N), and pyrrolidine(C_4H_9N). Most of the reactions, except 1,4-dioxane, pyrrole and pyrrolidine, proceed at the gas kinetic rate. In the ion product distributions, charge transfer, hydride ion abstraction, proton transfer, fragmentation and association were observed. In particular, proton transfer is seen to be small in all cases even though these channels are energetically favorable. Association is appreciable when the molecules are aromatic (except for furan) and nonexistent when there are no π electrons in the ring. CH_3^+ ions are an important intermediate in molecular synthesis in interstellar clouds and in the Titan ionosphere and ring molecules have also been detected in these media. The significance of the studied reactions to these media is discussed.

5.2 INTRODUCTION

In gas phase ion chemistry, the growth of larger molecules occurs mainly through association of the ions and neutrals. Where the ion attaches to the neutral is important

because it can affect the possibility of additional associations, effectively enabling or terminating further molecule growth. Association reactions are important in the interstellar medium (radiative association[1]) and the ionosphere of Titan (collisional association[2]) where ion-neutral associations are thought to lead to the formation of benzene and PAHs[3-5].

There is a lack of experimental data exploring association reactions of larger hydrocarbons and because of this, the possible importance of association in models of Titan's atmosphere has been under explored. In this work, a series of reactions of the methyl cation, CH_3^+, with homo- and hetero-cyclic neutral molecules is investigated. The structures of neutral molecules are shown in Figure 5.1. The association product channel is explored as a function of the presence of π electrons and the type and/or
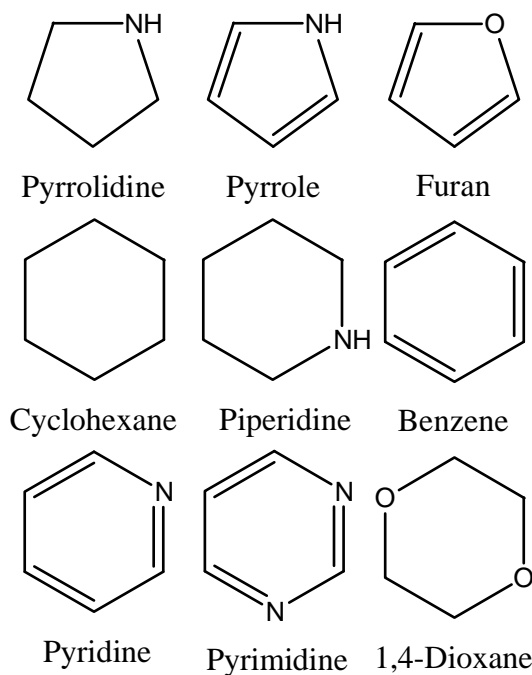
Figure 5.1. Structural diagrams of the cyclic neutrals used in this study.

amount of heterocyclic substitution. CH_3^+ is an important ion in Titan's ionosphere and the interstellar medium and reactions involving this ion figure significantly in insuring the thorough modeling of the chemistry occurring in these regions. Association of CH_3^+ to any of these molecules would be of interest as a mechanism for creating more massive molecules.

5.3 EXPERIMENTAL

A selected ion flow tube (SIFT) was used to study this series of ion-neutral reactions between CH_3^+ and benzene (C_6H_6), cyclohexane (C_6H_{12}), pyridine (C_5H_5N), pyrimidine ($C_4H_4N_2$), piperidine ($C_5H_{11}N$), 1,4-dioxane ($C_4H_8O_2$), furan (C_4H_4O), pyrrole (C_4H_5N), and pyrrolidine (C_4H_9N).   The SIFT method has been described extensively in the literature[6-8] and this will not be repeated here. Specific to this experiment, the CH_3^+ was formed by injecting methane into a low pressure ionization source. After mass selection in a quadrupole mass filter, the ions were injected into the flow tube at an ion energy of ~20 V to minimize fragmentation of the CH_3^+. Although a low ion injection energy was used it was not possible to completely eliminate further fragmentation of CH_3^+ and because of that the following ions were present in the flow tube at the average indicated percentage when compared to CH_3^+: C^+ (3%), CH^+ (5%), CH_2^+ (7%), and CH_4^+ (6%). Pyridine, pyrrole, pyrrolidine, furan, 1,4 dioxane, benzene and cyclohexane were obtained from Sigma-Aldrich with purities of >99.9%, 98%, 99.5+%, 99+%, 99.5%, 99.5%, and 99% respectively. Pyrimidine and piperidine were obtained from Alfa Aesar with manufactured purities of 99%. Benzene was obtained from Fisher Scientific with a purity of 99.5%. To eliminate dissolved gases, the liquids were further purified before use by

several cycles of freeze-pump-thaw. The neat vapors proved difficult to work with due

to condensation of the vapors in the neutral reactant system and on the flow tube walls,

so a 1% mixture of the reactant neutral in helium was used. This dilution was accounted

for when determining the rate coefficients. Ion product distributions and rate

coefficients were determined in the usual way[6,7,9]. The ion product distributions are

accurate to ± 5 in the percentage and the rate coefficients are accurate to $\pm 30\%$ due to

the sticky nature of these gases.   All reactions were studied at 298K.   Mass

discrimination in the detection quadrupole was corrected as before[8].

5.4 RESULTS

The rate coefficients for all reactions studied are given in Table 5.1. While it can

be seen that most of the reactions occur within experimental error of the gas kinetic

rate there is a tendency for the experimental rates to be less than gas kinetic. This

feature has not been seen in reactions of other ions involving the same neutrals. The

1,4-dioxane and pyrrolidine reactions are significantly slower than the gas kinetic rate.

The reason for this is not clear at present. A sample of the data is shown in Figure 5.2.

Note that the decay of the primary ion is linear over two orders of magnitude. This

provides increased confidence in the rate coefficients experimentally derived. Figure 5.2

will be discussed in more detail later.

The product distributions obtained for the reactions are listed in Table 5.2. The

recombination energy for the methyl cation is given in the table together with the

ionization energies and proton affinities for the reactant neutrals. All of the neutrals,

with the exception of cyclohexane, have smaller ionization energies than the

Table 5.1 Experimental rate coefficients, k_{exp}, for the reactions between CH_3^+ and the indicated neutrals are listed followed by the theoretical rate coefficients, $k_{theor}{}^{a}$, calculated using combined variational transition state theory and classical trajectory theory [10].

Neutral Molecule	k_{exp} (10^{-9} cm^3 s^{-1})	k_{theor} (10^{-9} cm^3 s^{-1})	*Efficiency[b]
Cyclohexane	1.87	2.18	0.86
Piperidine	1.86	2.30	0.81
1,4-Dioxane	1.73	3.44	0.50
Pyrrolidine	1.60	2.97	0.54
Benzene	1.88	2.12	0.89
Pyridine	3.14	3.55	0.88
Pyrimidine	2.71	3.76	0.72
Pyrrole	2.23	3.21	0.70
Furan	1.83	2.16	0.85

[a] Data needed to calculate the theoretical rate coefficients were obtained from the CRC Handbook and the literature [11-14]. [b] The reaction efficiency, k_{exp}/k_{theor}, is also included. All rate coefficients are expressed in units of 10^{-9} cm^3 s^{-1}.
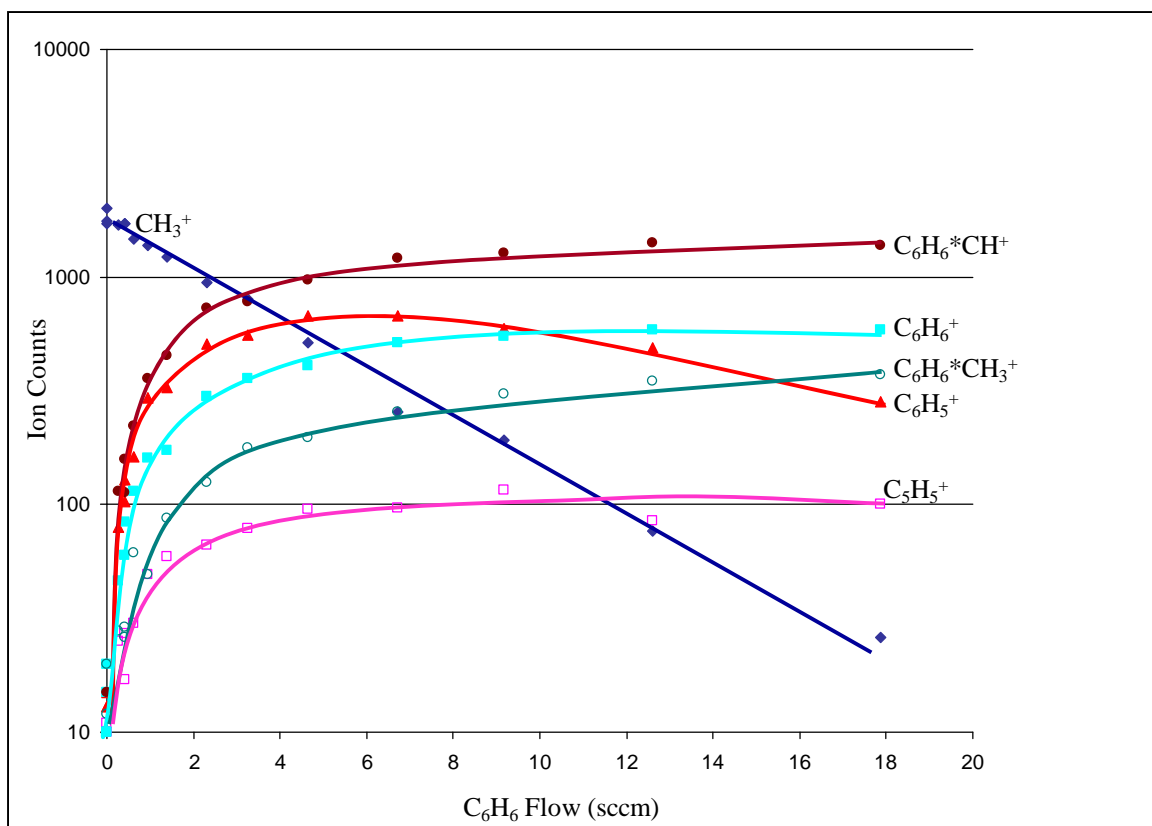
Figure 5.2 Decay of CH_3^+ and the rise of the product ions for the CH_3^+ reaction with benzene. Notice that the association product, $C_6H_6 \cdot CH_3^+$ increases and shows no secondary reaction.

Table 5.2 Product distribution (%) for the reactions of CH_3^+ with the listed neutral molecules[a]

Neutral Molecule	Ion Product	Product Channel*	%	Neutral Molecule	Ion Product	Product Channel*	%
Non-Aromatic							
Cyclohexane	$C_4H_7^+$	F	7%	Pyrrolidine	$C_2H_6N^+$	F	46%
C_6H_{12}	$C_4H_8^+$	F	7%	C_4H_9N	$C_4H_8N^+$	HA	32%
9.88 eV	$C_6H_{11}^+$	HA	68%	8.41 eV	$C_4H_9N^+$	CT	18%
164.2 kcal/mol	$C_6H_{12}^+$	CT	18%	226.6 kcal/mol	$C_4H_9NH^+$	PT	4%
Piperidine	$C_2H_6N^+$	F	21%	1,4- Dioxane	$C_2H_5^+$, CHO^+	F	11%
$C_5H_{11}N$	$C_4H_7^+$, $C_3H_5N^+$	F	6%	$C_4H_8O_2$	$C_2H_7^+$, CH_3O^+	F	18%
8.03 eV	$C_5H_9^+$, $C_4H_7N^+$	F	7%	9.19 eV	$C_3H_7^+$, $C_2H_3O^+$	F	5%
228.0 kcal/mol	$C_5H_{10}^+$	F	6%	190.6 kcal/mol	$C_2H_5O^+$,CHO_2^+	F	5%
	$C_5H_{10}N^+$	HA	34%		$C_3H_7O^+$,$C_2H_3O_2^+$	F	28%
	$C_5H_{11}N^+$	CT	22%		$C_4H_7O_2^+$	HA	14%
	$C_5H_{11}NH^+$	PT	4%		$C_4H_8O_2^+$	CT	19%
Aromatic							
Benzene	$C_5H_5^+$	F	5%	Pyridine	$C_5H_4N^+$	HA	20%
C_6H_6	$C_6H_5^+$	HA	31%	C_5H_5N	$C_5H_5N^+$	CT	21%
9.24 eV	$C_6H_6^+$	CT	17%	9.26 eV	$C_5H_5NH^+$	PT	9%
179.4 kcal/mol	$C_6H_{6*}CH^+$	AF	39%	222.3 kcal/mol	$C_5H_5N_*CH_3^+$	A	50%
	$C_6H_{6*}CH_3^+$	A	8%				
Pyrimidine	$C_3H_3^+$, C_2HN^+	F	6%	Pyrrole	$C_3H_5^+$, $C_2H_3N^+$	F	3%
$C_4H_4N_2$	$C_3H_3N_2^+$	F	8%	C_4H_5N	$C_2H_4N^+$	F	5%
9.33 eV	$C_4H_2N_2^+$	F	9%	8.21 eV	$C_3H_5N^+$	F	13%
211.7 kcal/mol	$C_4H_3N_2^+$	HA	19%	209.2 kcal/mol	$C_4H_5N^+$	CT	64%
	$C_4H_4N_2^+$	CT	25%		$C_4H_5NH^+$	PT	7%
	$C_4H_4N_2H^+$	PT	9%		$C_4H_5N_*CH_3^+$	A	8%
	$C_4H_4N_{2*}CH_3^+$	A	24%				
Furan	HCO^+	F	9%				
C_4H_4O	$C_3H_3^+$	F	4%				
8.88 eV	$C_2H_3O^+$	F	5%				
194.0 kcal/mol	$C_3H_3O^+$	F	56%				
	$C_4H_4O^+$	CT	26%				

[a] Ionization energies and proton affinities are given below each neutral molecular species[15]. The recombination energy of CH_3^+ is given at 9.84 eV[15] and the proton affinity of CH_2 is used is 207 kcal/mol[16]. [b] Product channels are indicated in the following manner: fragment (F), hydride abstraction (HA), charge transfer (CT), proton transfer (PT) association (A), and association with concerted fragmentation (AF).

recombination energy of CH_3^+, therefore charge transfer is expected in these cases. Charge transfer is a product channel in all reactions studied. The proton affinity of CH_2, 207 kcal/mol[16], was used to determine if proton transfer was energetically favorable. For pyridine, pyrimidine, pyrrole, piperidine and pyrrolidine, proton transfer is energetically possible and was seen as a product channel. Proton transfer is endothermic for furan, benzene, 1,4-dioxane and cyclohexane and was not observed.

In all but two of the reactions, hydride abstraction was a significant product channel. The two neutrals that did not experience hydride abstraction were pyrrole and furan, the aromatic five membered rings. By comparing the hydride ion affinities (HIA) of each species to that of CH_3^+ one can determine if the hydride abstraction channel is energetically favorable. The hydride ion affinity of CH_3^+ is well known in the literature[17] with a value of 313 kcal mol^{-1}. However, values for the species investigated in this study are not available. Since these values are unknown, it is logical to assume that the HIA of the species that have hydride abstraction as a product channel must be lower than that of CH_3^+, which indicates an exothermic reaction. In the case of pyrrole and furan, where no hydride abstraction is observed, an HIA value greater than CH_3^+ could explain the lack of this product channel. The HIA for furan was calculated[18] at the G3 level of and determined to be larger than 313 kcal mol^{-1} and therefore hydride abstraction is not energetically favorable for this reaction. Hydride abstraction for pyrrole was also calculated and is determined to be exothermic by 8.75 kcal mol^{-1}. Therefore, while hydride abstraction is energetically favorable it might not be seen due to competition from more favorable product channels.

An association product channel was observed in many of the reactions. Particularly, in the reactions involving pyridine and pyrimidine, it was surprising to see that association was very competitive with the other product channels such as proton transfer and charge transfer. There are some cases in the literature where this has occurred for instance where association was competitive with charge transfer and hydride abstraction in reactions involving NO^+[19] and where association was competitive with proton transfer in a reaction involving H_3O^+[20] as the primary ion. However, it is generally known, that when proton transfer is energetically favorable, it is a very efficient process and occurs rapidly[21]. Mechanistically, proton transfer must occur through a close encounter and usually it is only when proton transfer starts to become thermoneutral or endothermic that association is observed[22]. Because of this, it is not expected for proton transfer and association to be competitive product channels. The observation of association in this study suggests another process is taking place that can overcome or inhibit rapid proton transfer. Interestingly, for almost all of the neutral molecules that possess π electrons, association is a product channel while the neutral molecules without these π electrons show no association.

5.5 DISCUSSION

Of the neutrals in this study, five (benzene, pyridine, pyrimidine pyrrole and furan) are aromatic and therefore possess π electrons. Association occurred with all these aromatic neutrals except furan. There was no association with saturated neutrals and thus the π electrons appear to promote association. This seems a natural conclusion considering CH_3^+ is an electron deficient species and therefore will act as an

electrophile and be strongly attracted to the concentrated density of negative charge that is easily accessible in aromatic molecules. Several theoretical studies have investigated the interaction between cations and aromatic compounds. The studies use species such as Na^+, Mg^+, Al^+ and other main group metal ions[23], NH_4^+ and $CH_3NH_3^{+}$[24] and it was determined how they interact with the π electrons. The conclusion was that the cation usually forms a π-complex with the aromatic molecule with the binding energy being dependent on several factors. In particular, one study looked at the differences in binding energies of a Na^+ cation with 11 cyclic molecules containing varying amounts heteroatoms and substituents[25]. That study determined that the cation-π interaction most strongly depends on the electrostatic interaction and inspection of the electrostatic potential surface of the neutral molecule gives a good indication of the strength of cation-π bonding. In a further study, the number of cyclic molecules studied was expanded to include five membered rings and several more polycyclic aromatic molecules[26]. The authors were able to conclude that they could use a lower level of theory to generate the electrostatic potential surfaces and still have the ability to predict the strength of the cation-π interaction. This enables the electrostatic maps of even large molecules to be generated with ease.

While the cation-π interaction is responsible for the increased association with aromatic molecules it is not an accurate way to describe the structure of the associated complex when dealing with CH_3^+ as the cation. Several theoretical calculations involving CH_3^+ with various aromatic molecules have been undertaken[27-30] and show that CH_3^+ does not have a long lived π interaction with benzene; instead the σ interaction is more

energetically favorable. A molecular dynamics study determined that the reactants were brought together by cation-π electron attraction, however, at a certain intermolecular separation, the CH_3^+, regardless of the initial approach, quickly forms a σ complex with a carbon in the ring[29]. This fast forming complex rapidly isomerizes to give the final stable σ complex where the hydrogen attached to the same carbon as the newly attached methyl cation shifts to the para position. Miklis et al. explained the difference in reactivity of the CH_3^+ ion to ions that form π complexes (such as metal ions and the NH_4^+ ammonium ion) by pointing out that the unsaturated nature of the ion can promote different reactions[28]. It is likely that the interaction of an unsaturated species is not as strongly dependent on electrostatic forces as saturated species. Therefore, describing such interactions as cation-π is misleading. Hence, the term cation-π interaction will not be invoked and all associations of CH_3^+ with the aromatic neutrals studied in this paper are believed to result in a σ interaction.

Fragmentation product channels were also of great interest in this study. In an attempt to understand how each fragment was formed, it was necessary to study known fragmentation procedures in the literature. Rules governing unimolecular dissociation, used most widely in interpreting electron impact (EI), are well known[31], however, there is less information available on how the internal energy imparted during an ion-molecule reaction will be distributed and which bonds will break. One area of the literature where this is considered is chemical ionization mass spectrometry (CI). Fundamentally, CI occurs through ion-molecule reactions and though the reason CI is used differs from the reason ion-molecule reactions are investigated in this study, the

basic principles are the same for both. If the reactions in this study are considered in terms of chemical ionization then information about fragmentation mechanisms becomes available[17].

In these studies there are several product channels that do not involve fragmentation but might be the starting point for fragmentation. These are hydride abstraction, charge transfer, proton transfer and association. By investigating the fragments formed, it is possible to identify the starting point as one of the four listed above. It is known in CI, that if there is internal energy left over after a charge transfer reaction, then fragmentation reactions will resemble those observed in EI[17]. Some differences between the spectrums of CI versus EI relating to the relative abundances of the fragment ions formed are likely to occur. This arises because, in EI, a wide range of internal energy is imparted to the molecule upon ionization while in CI the energy imparted is restricted by the difference in the recombination energy of the primary ion and the ionization energy of the neutral. This allows for different fragmentation mechanisms to be favored in the two situations. Therefore, a major product ion in one process may only be a minor product ion in the other process. If the starting point for fragmentation is proton transfer then it is possible that the internal energy will be localized around the point of proton attachment, however, it is also possible for the internal energy to randomize throughout the molecule and break the weakest bond. It is likely that the fragmentation product of the proton transfer will be the result of the elimination of an even-electron stable molecule resulting in an even electron product ion[17]. The fragmentation that occurs if the starting point is hydride abstraction or

association is not well known. In the case of hydride abstraction while it seems logical that the atom at which the H$^-$ is lost will be the starting point for fragmentation, it is also possible for the internal energy to break the weakest bond just as with proton transfer.

The EI spectrum of each neutral, obtained from the NIST website, was compared to the fragments formed in each reaction.   Fragmentation peaks seen in both spectra indicate that the fragment formed in our reactions could be initiated via charge transfer and if the peaks were not seen in both spectra then the fragment was not formed via charge transfer. In some cases, the fragments formed in our reactions, but not seen in the EI spectrum, only differ by an H-atom. It is possible that these fragments are created by unimolecular dissociation mechanisms, but with a starting point that has one extra hydrogen such as proton transfer, or a starting point with one less hydrogen such as hydride abstraction. In discussing each neutral in detail, an attempt has been made to determine the starting point of each fragmentation channel and how it was formed.

5.5.1 Saturated Neutrals

Cyclohexane. The major product (68%) in the reaction with cyclohexane (C_6H_{12}) is hydride abstraction and is much larger than in any other reactions. There is a small amount of charge transfer present although the reaction is slightly endothermic (0.04 eV endothermic at 298K). However, when considering the errors associated with the ionization/recombination energies involved, the reaction could actually be thermoneutral or be driven by the fraction of the interactions that are energetically allowed by kinetic energy in a Maxwell-Boltzmann distribution and by internal energy in a Boltzmann distribution. Hence, the 18% charge transfer channel does not seem

unreasonable. The two remaining product channels are fragmentations and each represents 7% of the product distribution. Both of the fragments, m/z 56 ($C_4H_8^+$), and m/z 55 ($C_4H_7^+$), are present in the EI spectrum of cyclohexane . It is most likely these fragments are from the dissociation of the charge transfer product. While $C_4H_7^+$ is a product of EI unimolecular dissociation, it is also possible it could be formed after hydride abstraction followed by two inductive cleavages (charge initiated bond dissociation) to give the loss of neutral C_2H_4.

Piperidine. Piperidine ($C_5H_{11}N$) has a significantly lower IE than cyclohexane; therefore more fragmentation is expected and is seen. The lone pair of electrons on the nitrogen in the piperidine ring provides an additional reaction site. In fact, this site would be an ideal place for CH_3^+ to associate because the availability of two electrons should be very attractive to the methyl cation. However, association was not a product of the reaction. Instead hydride abstraction was again the largest product channel followed closely by charge transfer. Several fragmentation products were observed along with a very small amount of proton transfer. Of the four fragmentation channels, three had the possibility of being assigned more than one unique molecular formula. By calculating the reaction enthalpies, ΔH_{rxn}, we were able to determine that the product at m/z 44 is $C_2H_6N^+$ (ΔH_{rxn}= -87.15 kcal mol^{-1}) rather than $C_3H_8^+$ (ΔH_{rxn}= 122.75) since the latter is very endothermic. Unfortunately, there was not enough information to give a definite assignment to the m/z at 55 or 69 so the two possible molecular formulas are listed in the table. In many of the reactions, the thermodynamic data were not available to make a distinction between two possible ions of the same mass. In

these cases, the ions are not identified definitively. Identification by isotopic labeling

was not within the scope of this study.

Of the four fragment products present, $C_2H_6N^+$, $C_4H_7^+$ /$C_3H_5N^+$, and $C_5H_{10}^+$ are

also present in the EI spectrum of piperidine. These fragments are likely formed from

unimolecular decomposition of charged piperidine. The remaining fragment,

$C_5H_9^+$/$C_4H_7N^+$ could originate from either the proton transfer by a loss of NH_3/CH_5

(unlikely) or from the hydride abstraction by a loss of NH/CH_3.

1,4-Dioxane. In 1,4-Dioxane ($C_4H_8O_2$), the addition of two oxygen atoms

compared to cyclohexane again provides two very reactive sites. The availability of two

lone pairs of electrons on each oxygen would again suggest an ideal place for CH_3^+ to

react. However, this reaction produced a large number of fragment ions and no

association. The ionization energy of 1,4-dioxane is 9.19 eV. Upon ionization, only ~0.65

eV remains for bond dissociation so it was surprising to observe the large amount of

fragmentation. Unfortunately, detailed thermodynamic information is not available for

these channels.   All five of the fragment ions are present in the EI spectrum of 1,4-

Dioxane and suggest these fragments originate from the charged parent ion. Charge

transfer and hydride abstraction product channels are also present.

Pyrrolidine. Pyrrolidine (C_4H_9N), the only five membered saturated ring studied,

showed only one fragmentation product.   The fragment is at m/z 44 and the major

product with 46% abundance. This peak is identified as $C_2H_6N^+$ by thermodynamic

consideration. The main peak in the EI spectrum of pyrrolidine is at m/z 43 but there is

a small peak at m/z 44. This reversal in peak intensity can be explained by looking at the

differences between EI and CI. When comparing the fragmentation of EI to CI, the major difference is in the relative abundances of the fragments[17]. This arises because, in EI, a wide range of internal energy is imparted to the molecule upon ionization, while in CI the energy imparted is restricted by the difference in the recombination energy of the primary ion and the ionization energy of the neutral. This allows for different fragmentation mechanisms to be favored in the two situations. Worth noting is the ability of $C_2H_6N^+$ to form from the protonated form of pyrrolidine. Assuming protonation happens on the carbon next to the nitrogen, as it does in pyrrole[32], the ring can open by an inductive cleavage to the cation site and then an additional inductive cleavage to eliminate C_2H_4 leaving the $C_2H_6N^+$ product ion. Utilizing this mechanism in addition to the charge transfer mechanism, might help explain why the $C_2H_6N^+$ is such a large product percentage.

5.5.2 Aromatic Neutrals

Benzene. The reaction of CH_3^+ with the prototype aromatic compound, benzene (C_6H_6), resulted in several product channels. As suggested by theory, and similar reactions, the association between the two species was observed, however, it is only an 8% product channel. This was a little unexpected since the association process for CH_3^+ and benzene is theoretically proven to be very rapid[30]. There is also a product at m/z 91, which can only correspond to the molecular formula $C_7H_7^+$. This is the dominant product of the reaction with a 39% product channel. It is not possible that this product is formed via association with injected CH^+ because CH^+ is not present in the flow tube in sufficient concentration to form such a major product. Nor can it be attributed to a

secondary product where the first reaction is association of CH_3^+ with benzene and then a second reaction with another species in the flow tube to give rise to loss of H_2 from the association complex. Inspection of Figure 5.2 reveals that the product ion of $C_6H_6 \cdot CH_3^+$ increases, but never decreases as the concentration of benzene increases, thereby indicating that the association ion product is not involved in any secondary reaction processes with benzene. Figure 5.3 confirms that, when plotting the product distribution, the behavior usually associated with a secondary reaction is not present for m/z 91. If it were a secondary product, the fraction would be zero at low neutral flow and increase as the flow increased. In light of this information, the product ion most likely is formed through a concerted reaction that adds CH_3^+ to the benzene ring and subsequently eliminates an H_2 molecule forming the $C_7H_7^+$ product. There has been much discussion in the literature concerning the structure of the $C_7H_7^+$ ion[33-36]. It is well known that the lowest energy form is the tropylium ion, a seven membered ring. In this study, the H_2 can be eliminated in several ways with the most likely eliminations coming from the ring to give $C_6H_4 \cdot CH_2^+$, the tolyl ion, or from the ring and the CH_3^+ to give $C_6H_5 \cdot CH_2^+$, the benzyl ion. The tolyl ion can isomerize to the benzyl ion providing the 26.3 kcal/mol[35] activation energy is overcome. Ultimately, the tropylium ion can be reached by the isomerisation of the benzyl ion providing the activation energy of 32.7 kcal/mol[33] is surmounted. This reaction is energetically driven because the tropylium ion is 24.8 kcal/mol[33] lower in energy than the benzyl ion. While it is known that the benzyl ion reacts rapidly with aromatic compounds, the rate coefficient for the reaction of the benzyl ion with benzene is not known. If the aforementioned reaction was
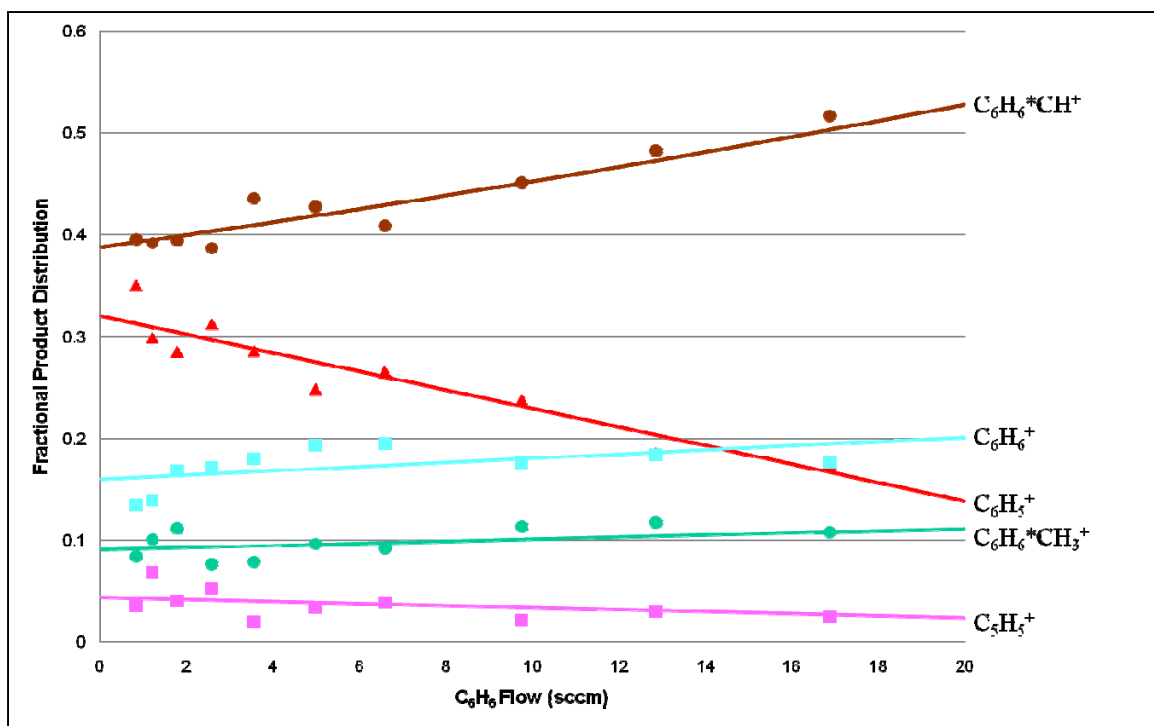
Figure 5.3 Fractional product distribution for the reaction of CH_3^+ with C_6H_6. If $C_6H_6 \bullet CH^+$ were a secondary product it would be evident in this plot because the line going through those points would be zero at low flow and increase sharply as the flow increased. Points at flows less than 0.5 sccm have been omitted from the plot since with sticky gases, such as benzene, the time to equilibrate prevents accurate measurements.

sufficiently slower than the gas kinetic rate of the CH_3^+ reaction then it would not be evident from the data collected if m/z 91 reacted further. Therefore, we are unable to say definitively that m/z 91 does not react further and therefore it is not clear whether the tolyl ion, benzyl ion, tropylium ion or a mixture of these three are present.

Other products include a fragment at m/z 65, H-abstraction and charge transfer. This fragment can only be $C_5H_5^+$. This mass in not present in the EI spectrum of benzene and is not attributed to fragmentation of the charge transfer product. Intuitively, it seems unlikely to come from the hydride abstraction because it would require the loss of a bare carbon. It is more likely that it forms via dissociation of the association ion by the concerted loss of a C_2H_4 neutral to once again give a primary product ion.

Pyridine. The addition of nitrogen to the aromatic ring seems to have a large affect on the amount of association evident by the 50% association product channel. Since it has already been determined that CH_3^+ does not form π complexes, the CH_3^+ can either interact with a carbon on the ring or the nitrogen. Interaction with the nitrogen is more probable because the lone pair offers an attractive binding site. Also, theoretical calculations involving Na^+ and pyridine (C_5H_5N) showed that only binding to the nitrogen represented a minimum on the potential energy surface[26].

Proton transfer is another product channel for this reaction. However, it is only present at 9%. Proton transfer is usually a very efficient and rapid process when energetically possible, as it is in this case. Since proton transfer, like association, must happen at very close intermolecular distances, it seems likely that the presence of π electrons stabilizes the initial complex long enough for CH_3^+ to form a strong interaction

with the nitrogen lone pair. Without this stabilizing presence, the pyridine would quickly remove a proton from the CH_3^+ and any further interaction between the two species would cease. The other two products are charge transfer and hydride abstraction. There is no further fragmentation of the ring.

Pyrimidine. Reaction with pyrimidine resulted in three fragmentation products, as well as hydride abstraction, charge transfer, proton transfer and association. The amount of association is only half of the amount observed in the pyridine reaction. This seems counterintuitive if the presence of nitrogen in the ring encourages a larger amount of association, as shown with pyridine. Having two sites at which association is possible should increase the amount of association. However, the fact that the opposite occurs indicates that the addition of a second nitrogen reduces the efficiency of the association channel. Once again there is only a 9% proton transfer channel even though the process is exothermic. The fragments observed are $C_3H_3^+/C_2HN^+$, $C_3H_3N_2^+$, and $C_4H_2N_2^+$. A peak at m/z 39 ($C_3H_3^+/C_2HN^+$) is present in the EI spectrum but only at a 1% intensity of the major peak. Also, in this study the product at m/z 39 is a minor product and it is likely it is formed via charge transfer dissociation. The other two fragments were not seen in the EI spectrum of pyrimidine and it is doubtful that these fragments were formed via the charge transfer product.   They could be formed via dissociation of hydride abstraction, proton transfer or association. If $C_3H_3N_2^+$ and $C_4H_2N_2^+$ were formed via proton transfer then neutral CH_2 and H_3 would have to be eliminated, respectively. If $C_3H_3N_2^+$ and $C_4H_2N_2^+$ were formed via hydride abstraction then neutral C (unlikely) and H would have to be eliminated, respectively. If $C_3H_3N^+$ and $C_4H_2N_2^+$ were formed via

association then neutral C_2H_4 and CH_5 (unlikely) would have to be eliminated, respectively. It is not clear at this point which mechanisms created $C_3H_3N^+$ and $C_4H_2N_2^+$.

Pyrrole. Pyrrole is a five membered heterocyclic molecule. Like the other heterocycles mentioned above it also has nitrogen in the ring. The nitrogen in pyrrole must donate the lone pair of electrons to the π system for the molecule to be aromatic so this lone pair is not as easily available for bonding as in pyridine and pyrimidine. Also, unlike the two species mentioned above, the nitrogen in pyrrole has a hydrogen atom attached, which uses the remaining electron. Because of these issues, it is not likely that the nitrogen atom will be as reactive as before. This is evident in the decreased amount of association. There is only an 8% product channel for association with pyrrole. Another reason for lower association might be attributed to the smaller ring size leading to more steric strain. Charge transfer is the major ion product with a channel of 64%. Since charge transfer can occur at a distance, it is possible that this occurs before CH_3^+ can get close enough to be stabilized by the π electrons and therefore decreasing the association product. Fragmentation accounts for 21% of the products and it is spread among 3 products. The smallest fragment, at m/z 41, can either be $C_3H_5^+$ or $C_2H_3N^+$ and is seen in the EI spectrum of pyrrole. $C_2H_4N^+$ is also a peak in the EI spectrum although it is very small. Therefore, these two ions are likely formed via dissociation of the charge transfer product. The remaining fragment, $C_3H_5N^+$, is not in the EI spectrum and must come from dissociation of either the proton transfer (by loss of a CH) or association (by a loss of C_2H_3) of pyrrole.

Furan. Furan is a five membered ring that contains an oxygen atom. Oxygen has two lone pairs of electrons, one of which participates in the π system, allowing the molecule to be aromatic, and leaving the remaining lone pair available for reaction. This made the results of this reaction even more puzzling. Furan is the only aromatic molecule that does not undergo association with CH_3^+. The same stabilization of the ion by π electrons should occur and, once stabilized, the electrophilic nature of CH_3^+ should promote binding with the free electrons. In fact, association of the CH_3^+ to the lone pair on the oxygen does not require the loss of aromaticity like it does in pyrrole, the other five membered ring. An IR study of the protonation site of furan, showed that the proton is located on the carbon next to the heteroatom (C_α)[32]. Using this information, and assuming that the CH_3^+ will also bind to the C_α, this situation closely resembles the intermediate in an electrophilic aromatic substitution (EAS) reaction that occurs with all aromatic species. In EAS reactions, pyrrole is more reactive than furan because the nitrogen atom has a lower electronegativity and is able to stabilize the cation more effectively[37]. Therefore the small amount of association seen in pyrrole is lost when going to furan because the more electronegative oxygen atom holds its electrons strongly and allows for less stabilization of the cation.

It is evident from the cases presented above that π electrons promote association by stabilizing the cation as it draws near the neutral molecule. In the case of furan, the σ complex is destabilized by the presence of the oxygen in the ring. Due to this, the complex can follow a number of reaction pathways such as fragmentation, hydride abstract, proton transfer, or charge transfer. Neither proton transfer nor

hydride abstraction was energetically allowed nor were they observed as a product channel. Charge transfer was favorable and did occur. Fragmentation of the complex did occur to form the major product ion, $C_3H_3O^+$. This ion is not present in the EI spectrum of furan and thus cannot be attributed to the charge transfer, the only non-fragmented product ion. It is possible to envision $C_3H_3O^+$ being produced by several inductive cleavages of the unstable association complex ending with CH_3CH neutral eliminated from the ring. The three other fragments, HCO^+, $C_3H_3^+$ and $C_2H_3O^+$, are all present in the EI spectrum of furan and are most likely formed via dissociation of the charge transfer species.

5.6 CONCLUSION

The association of CH_3^+ to these 9 simple cyclic molecules seems to depend strongly on the availability of π electrons. The substitution of nitrogen into the ring increases the amount of association when compared to benzene. Inclusion of two nitrogen atoms decreases the amount of association compared to pyridine but still gives more association than benzene. The aromatic five membered rings showed little to no association even though π electrons are available to facilitate the association. Steric hindrance could be partially responsible along with the lack of availability of suitable association sites. The saturated ring compounds demonstrated no association.

Association is an important chemical process. The reactions of CH_3^+ also have a particular importance to the ionosphere of Titan. CH_3^+ is one of the major ions in this ionosphere and plays an important role in the chemistry. It is usually believed that when proton transfer can take place it will and CH_3^+ is largely considered to proton

transfer in the reactions it is involved with in the ionosphere. However, these data

suggest that proton transfer should not be the only product channel assumed to result

from reactions with the methyl cation. Association products should also be included in

chemical models of the Titan ionosphere and the importance of proton transfer should

be diminished.

5.7 AKNOWLEDGEMENTS

5.8 REFERENCES

1. Herbst, E. *Chem. Soc. Revs.* **2001**, *30*, 168.

2. Anicich, V.; Milligan, D. B.; Fairley, D. A.; McEwan, M. J. *Icarus* **2000**, *146*, 118.

3. McEwan, M. J.; Scott, G. B. I.; Adams, N. G.; Babcock, L. M.; Terzieva, R.; Herbst, E. *Ap. J.* **1999**, *513*, 287.

4. Woods, P. M.; Willacy, K. *Astrophys. J.* **2007**, *655*, L49.

5. Vuitton, V.; Yelle, R. V.; Cui, J. *Journal of Geophysical Research* **2008**, *113*, E05007(1.

6. Adams, N. G.; Smith, D. *Int. J. Mass Spectrom. Ion Phys.* **1976**, *21*, 349.

7. Adams, N. G.; Smith, A. D. Flowing Afterglow and SIFT. In *Techniques for the Study of Ion-Neutral Reactions* Farrar, J. M., Saunders, J. W. H., Eds.; Wiley-Interscience: New York, 1988; pp 165.

8. Fondren, L. D.; McLain, J. L.; Jackson, D. M.; Adams, N. G.; Babcock , L. M. *Int. J. Mass Spectrom* **2007**, *265*, 60.

9. Adams, N. G.; Smith, D. *J. Phys. B.* **1976**, *9*, 1439.

10.   Su, T.; Chesnavich, W. J. *J. Chem. Phys.* **1982**, *76*, 5183.

11.   *CRC Handbook of Chemistry and Physics*; 77 ed.; Lide, D. R., Ed.; CRC Press, Inc.: New York, 1996-1997.

12.   Rodgers, M. T., Wayne State University.

13.   Sun, J.; Bohme , D. K. *Int. J. Mass Spectrom.* **2000**, *195/196*, 401.

14.   http://www.chemspider.com. Building a Structure Centric Community for Chemists, 2008.

15.   Linstrom, P. J.; Mallard, W. G. NIST Chemistry WebBook. In *NIST Standard Database 69*; National Institute of Standards and Technology: Gaithersburg MD, 20899, August 2008.

16.   Pliego, J. R.; De Almeida, W. B. *J. Chem. Soc., Faraday Trans.* **1997**, *93*, 1881.

17.   Harrison, A. G. *Chemical Ionization Mass Spectrometry*, 2 ed.; CRC Press: Boca Raton, 1992.

18.   Mckee, C., Personal Communication.

19.   Wang, T.; Spanel, P.; Smith, D. *Int. J. Mass Spectrom* **2004**, *237*, 167.

20.   Kennedy, R. A.; Mayhew, C. A.; Thomas, R.; Watts, P. *Int J. Mass Spectrom.* **2003**, *223-224*, 627.

21.   Bohme , D. K. The Kinetics and Energetics of Proton Transfer. In *Interaction Between Ions and Molecules*; Ausloos, P., Ed.; Plenum Press: New York, 1975; Vol. 6; pp 489.

22.   Adams, N. G.; Williams, T. L.; Babcock, L. M.; Decker, B. K. Recent Studies of Thermal Charge (Electron) and Proton Transfer in the Gas Phase. In *Recent Research Developments in Physical Chemistry*; Pandalai, S. G., Ed., 1999; Vol. 3; pp 191.

23.   Petrie, S. *Int. J. Mass Spectrom.* **2003**, *227*, 33.

24.   Deakyne, C. A.; Meotner, M. *J. Am. Chem. Soc.* **1985**, *107*, 474.

25.   Mecozzi, S.; West, A. P.; Dougherty, D. A. *J. Am. Chem. Soc.* **1996**, *118*, 2307.

26. Mecozzi, S.; West, A. P.; Dougherty, D. A. *Proc. Natl. Acad. Sci.* **1996**, *93*, 10566.

27. Raos, G.; Astorri, L.; Raimondi, M.; Cooper, D. L.; Gerratt, J.; Karadakov, P. B. *J.Phys.Chem.A* **1997**, *101*, 2886.

28. Miklis, P. C.; Ditchfield, R.; Spencer, T. A. *J.Am.Chem.Soc.* **1998**, *120*, 10482.

29. Ishikawa, Y.; Yilmaz, H.; Yanai, T.; Nakajima, T.; Hirao, K. *Chem. Phys. Lett.* **2004**, *396*, 16.

30. Zheng, F.; Sa, R.; Cheng, J.; Jiang, H.; Shen, J. *Chem. Phys. Lett.* **2007**, *435*, 24.

31. McLafferty, F. W.; Turecek, F. *Interpretation of Mass Spectra*, Fourth ed.; University Science Books: Sausalito, 1993.

32. Lorenz, U. J.; Lemaire, J.; Maitre, P.; Crestoni, M. E.; Fornarini, S.; Dopfer, O. *International Journal of Mass Spectrometry* **2007**, *267*, 43.

33. Cone, C.; Dewar, M. J. S.; Landman, D. *J. Am. Chem. Soc.* **1975**, *99*, 372.

34. Ausloos, P. *J. Am. Chem. Soc.* **1982**, *104*, 5259.

35. Ignatyev, I. S.; Sundius, T. *Chem. Phys. Lett.* **2000**, *326*, 100.

36. Sorrilha, A.; Santos, L.; Gozzo, G.; Sparrapan, R.; Augusti, R.; Eberlin, M. *J. Phys. Chem. A* **2004**, *108*, 7009.

37. Bruice, P. Y. More About Amines and Heterocyclic Compounds. In *Organic Chemistry*; 4th ed.; Pearson Education, Inc.: Upper Saddle River, 2004; pp 883.

CHAPTER 6

ION CHEMISTRY OF $C_3H_3^+$ WITH SEVERAL CYCLIC MOLECULES

_____

6.1 ABSTRACT

Rate coefficients and ion product distributions have been determined for the gas phase reactions of $C_3H_3^+$ with several homocyclic and heterocyclic molecules in a Selected Ion Flow Tube (SIFT) at 298K. The rate coefficients for both the linear and cyclic isomers of $C_3H_3^+$ are given. l-$C_3H_3^+$ reacts by association with the neutral cyclic in the majority of the reactions. c-$C_3H_3^+$ is shown to be more reactive than previously considered in low pressure experiments. In fact, the cyclic isomer reacts at the gas kinetic rate when the reaction involves a nitrogen containing cyclic but not with hydrocarbon and oxygen containing cyclic compounds. This reactivity of both the cyclic and linear isomer should be included when modeling the atmosphere of Titan due to the large number of nitrogen containing molecules that are implied to be present because of the large concentration of nitrogen. Currently, the models consider electron recombination to be the only loss channel of c-$C_3H_3^{+}$.[1]

6.2 INTRODUCTION

The $C_3H_3^+$ molecule has been studied for many different reasons. In the late 1950's Ronald Breslow was the first to successfully synthesize a derivative of the cyclic form of this molecule[2] thus demonstrating an aromatic system with only 2 π electrons, i.e. the first member of the 2 + 4n aromatic series. $C_3H_3^+$ is also often seen in the mass spectrum of organic compounds[3] and there have been many experimental and theoretical studies to determine whether the linear or cyclic isomer is the structure of lower energy and it has been determined that the cyclic isomer, cyclopropenyl cation, is the most stable form. The linear isomer, propargyl cation, is the next most stable

isomer with a heat of formation approximately 26 kcal/mol greater than that of the cyclic isomer[4-6]. $C_3H_3^+$ also has a strong connection to combustion chemistry. It is the most abundant ion observed in many fuel rich flames and was once thought to be the starting point for soot formation. However, it is now widely believed that the neutral radical C_3H_3 and other small resonantly stabilized radicals are responsible for the buildup of carbon in soot formation[7-10].

In addition to fundamental studies and combustion chemistry, $C_3H_3^+$ is thought to exist in the interstellar medium. The first cyclic molecule discovered in interstellar clouds was c-C_3H_2[11,12]. It is believed to be formed by electron recombination of $C_3H_3^+$, after $C_3H_3^+$ is formed by radiative association of C_3H^+ with the abundant H_2.[13] In studies of the analogous laboratory collisionally stabilized association reactions, it is concluded that equal quantities of the cyclic and linear isomer are formed by this process. However, because of the greater reactivity of l-$C_3H_3^+$ (see later), this will be removed rapidly from interstellar clouds through ion-molecule reactions while c-$C_3H_3^+$ is mainly removed via dissociative electron recombination.

Recently a mass of 39 amu has been detected in the ionosphere of Titan by the Ion Neutral Mass Spectrometer (INMS) onboard the Cassini spacecraft. The possible identities of this include both linear and cyclic $C_3H_3^+$ as well as HC_2N^+. Modeled densities of these three species show that c-$C_3H_3^+$ is most abundant followed by l-$C_3H_3^+$ and then HC_2N^+. The current assumption for the Titan atmosphere is that odd masses are hydrocarbons while even masses are nitrogen containing species. So for mass 39,

HC_2N^+ is of less interest as the possible identity, at least until a more definite identification is obtained. Much is known about the two isomers[3,14] of $C_3H_3^+$ and shows that $c\text{-}C_3H_3^+$ is less reactive than the linear isomer. Indeed, $c\text{-}C_3H_3^+$ is known to have no discernable reaction with small linear or branched hydrocarbons while $l\text{-}C_3H_3^+$ is known to react quite rapidly. Therefore, it is easy to identifiy the isomer in a gas phase reaction by choosing an appropriate neutral reactant. For example, $l\text{-}C_3H_3^+$ reacts with benzene at the gas kinetic rate while $c\text{-}C_3H_3^+$ does not react ($\leq 10^{-13}\, cm^3\, s^{-1}$). Also, depending on the method used to form the molecular ion, it is possible to obtain different ratios of the linear to cyclic isomer. Impact of 70 eV electrons on propyne (C_3H_4) produces a majority of cyclic $C_3H_3^+$ and only ~ 30% linear $C_3H_3^+$[14] while electron impact on ethane in a high pressure ionization source creates 40% cyclic and 60% linear isomers[15]. Some ion molecule reactions that produce only the cyclic form of $C_3H_3^+$ include the reaction of CH_3^+ with C_2H_2 to give 100% $c\text{-}C_3H_3^+$ as well as the reaction of C^+ with C_2H_4 to give 80% $c\text{-}C_3H_3^+$ and a 20% mix of linear and cyclic $C_3H_2^+$.[13]

Although there has been much investigation of the different isomers of $C_3H_3^+$ with small neutrals, there is little in the literature about ion-molecule reactions of $C_3H_3^+$ with cyclic molecules. As the picture of Titan's atmosphere evolves, it is becoming evident that many more complex species are present. It is known that the haze surrounding Titan is organic in nature and most likely is due to tholins, polycyclic aromatic hydrocarbons (PAHs) and other organic macromolecules. These PAHs are thought to form by successive acetylene additions to benzene. The concentration of benzene in Titan's atmosphere is much higher than once predicted and it is known that

benzene is formed not only by recombination of the propargyl molecule (C_3H_3)[16] but also by ion-neutral molecule reactions. Since benzene is formed in the ionosphere it has the possibility of reacting with the many ion species present. Also, the possibility of nitrogen containing heterocyclics in Titan's atmosphere is great since the atmosphere is mainly N_2 (98%). Studying the reactivity of $C_3H_3^+$ with both benzene and nitrogen heterocyclic species is thus very important.

This current study is an extension of earlier work (Chapter 5) involving the reactions of CH_3^+ with the same neutral ring molecules. The data from this previous study indicated that association was a major product in reactions with aromatic rings, even when competing with proton transfer. This association provides a mechanism for creating larger molecules in ion-molecule reactions. In the interest of making larger association complexes in less steps the previous study was extend to include the larger $C_3H_3^+$ ion.

6.3 EXPERIMENTAL

A selected ion flow tube was used to study a series of ion-neutral reactions between $C_3H_3^+$ and the neutrals benzene (C_6H_6), cyclohexane (C_6H_{12}), toluene (C_7H_8) pyridine (C_5H_5N), pyrimidine $(C_4H_4N_2)$, piperidine $(C_5H_{11}N)$, 1,4-dioxane $(C_4H_8O_2)$, furan (C_4H_4O), tetrahydrofuran (C_4H_8O), pyrrole (C_4H_5N), and pyrrolidine(C_4H_9N). The SIFT method has been described extensively in the literature[17-19] so only a brief overview will be given here. The ion of interest was selected from an ion source using a quadrupole mass filter and focused through a 1 mm orifice into the flow tube. Then the ions were

carried downstream in a helium gas flow injected supersonically into the tube through a venturi type inlet. The pressure in the flow tube was maintained at ~0.5 torr by the helium flow (~200 Tls^{-1}), which was exhausted from the flow tube by a Roots pump. Downstream of the ion injection port, and after the thermalization of the ions, the reactant neutrals were introduced into the flow tube. A small portion of the reactant and product ions was then sampled at the end of the reaction region through a pinhole orifice in the detection nose cone, while the rest was evacuated by the Roots pump. A quadrupole mass filter and an electron multiplier counting system located after the nose cone were used to quantitatively identify the ions by their mass to charge ratios. Specific to this experiment, $C_3H_3^+$ was created by injected propyne (C_3H_4) into a low pressure electron impact ionization source. Due to limitations of the mass filter and collision breakup of $C_3H_3^+$ upon entering the flow tube, it was not possible to completely isolate $C_3H_3^+$. Here the following ions were present in the flow tube at the average indicated percentage relative to $C_3H_3^+$: $C_3H_4^+$ (6%), $C_3H_2^+$ (10%), C_3H^+(4%). The presence of these unwanted ions possibly contribute to the products formed but we expect the effect to be small because of the ions are not present in a very large quantites.

Pyridine, pyrrole, pyrrolidine, furan, tetrahydrofuran, 1,4-dioxane, toluene and cyclohexane were obtained from Sigma-Aldrich with purities of >99.9%, 98%, 99.5+%, 99+%, ≥99.9%, 99.5%, 99.8% and 99% respectively. Pyrimidine and piperidine were obtained from Alfa Aesar both with manufactured purities of 99%. Benzene was obtained from Fisher Scientific with a purity of 99.5%. To eliminate dissolved gases, the liquids were further purified before use by several cycles of freeze-pump-thaw. The

neat vapors proved difficult to work with due to their sticky nature with condensation in the neutral reactant system and on the flow tube walls. To minimize this, a 1% mixture of the reactant neutral in helium was used. This dilution was accounted for when determining the rate coefficients. Ion product distributions and rate coefficients were determined in the usual way[17,18,20]. The ion product distributions are accurate to ±5 in the percentage and the rate coefficients are accurate to only ±30% due to the sticky nature of these gases. All reactions were studied at 298K. Mass discrimination in the detection quadrupole was corrected for as before[19].

6.4 RESULTS

6.4.1 Rate Coefficients

$C_3H_3^+$ can be produced in many ways producing different ratios of cyclic to linear isomers[3,4,14,15,21-25]. In this study, the primary ion was produced by electron impact on propyne and from the literature, a cyclic to linear isomer ratio of 70:30 was expected. This ratio was confirmed in the present study by reaction of the $C_3H_3^+$ (produced in our low pressure source) with benzene.   This is a well known reaction in which c-$C_3H_3^+$ undergoes no reaction[3,25]. Therefore, the reactive portion of the primary ion decay is attributed to l-$C_3H_3^+$. To accurately determine both the percent of reactive isomer and the rate coefficient for each isomer it was necessary to model the data. In the experiment, the counts of the primary ion mass are obtained as a function of the number density of neutral reactant [NR]. This relationship is given by

$$[c\text{-}C_3H_3^+] = [c\text{-}C_3H_3^+]_o \exp{-k_c [NR]t} \qquad (6.1)$$

and

$$[l\text{-}C_3H_3^+] = [l\text{-}C_3H_3^+]_o \exp -k_l [NR]t \qquad (6.2)$$

where $[c\text{-}C_3H_3^+]$ and $[l\text{-}C_3H_3^+]$ are the amounts of cyclic and linear isomer present at a particular neutral reactant flow (NR), while $[c\text{-}C_3H_3^+]_o$ and $[l\text{-}C_3H_3^+]_o$ represents the initial amounts of each isomer. k_c and k_l are the rate coefficients for the cyclic and linear isomers, respectfully. Since the experiment measures the combined amount of cyclic and linear isomer at each neutral reactant the experimental data is modeled by

$$[c\text{-}C_3H_3^+] + [l\text{-}C_3H_3^+] = [c\text{-}C_3H_3^+]_o \exp -k_c [NR]t + [l\text{-}C_3H_3^+]_o \exp -k_l [NR]t \qquad (6.3)$$

which is the sum of equations (6.1) and (6.2). The rate coefficient for each isomer can then be determined by adjusting k_c and k_l to fit the data and the ratio of each isomer initially present can be determined by adjusting $[c\text{-}C_3H_3^+]_o$ and $[l\text{-}C_3H_3^+]_o$. An example of this model applied can be seen in Figure 6.1.

The rate coefficients for each reaction are listed in Table 6.1. The model was only applied to reactions that clearly had a reactive and non-reactive region on the primary ion decay and made it possible to obtain values of rate coefficients for both isomers. So in addition to the rate coefficients of l- $C_3H_3^+$ the rate coefficients for c- $C_3H_3^+$ are also listed. In many reactions it appears that $c\text{-}C_3H_3^+$ was not reacting but a closer look at the primary ion decay revealed that c- $C_3H_3^+$ was reacting, albeit slowly, with several of the neutrals. The efficiency listed is determined for the reaction involving the linear isomer.
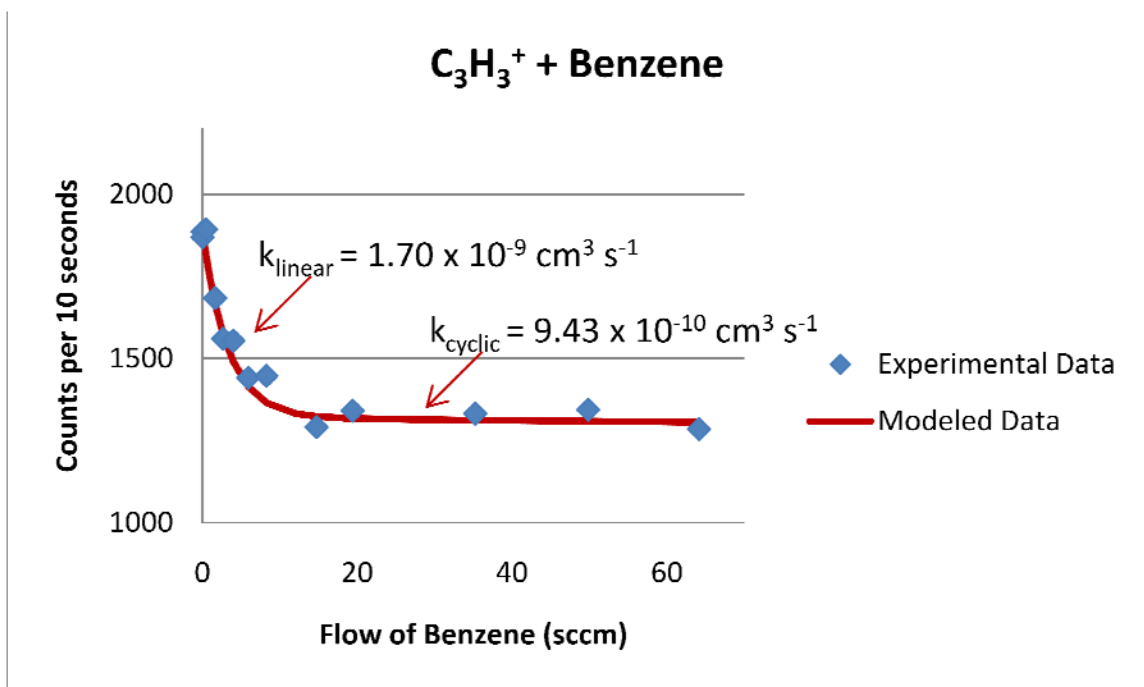
Figure 6.1 Modeling of the rate coefficients of both the linear and cyclic isomers of $C_3H_3^+$ in reaction with benzene. The modeled line was fit by varying the initial concentrations of the two isomers as well as varying their rate coefficients.

Table 6.1 Experimental rate coefficients, k_{exp}, for the reactions between $C_3H_3^+$ and the indicated neutrals followed by the theoretical rate coefficients, k_{theor},[a] calculated using combined variation transition state theory and classical trajectory theory[26]. The available experimental values in the literature are indicated underneath the values obtained in the present study in italic and are agreement to within error.

Neutral Molecule	l-$C_3H_3^+$ k_{exp} (10^{-9} cm^3 s^{-1})	c-$C_3H_3^+$ k_{exp} (cm^3 s^{-1})	k_{Theory} (cm^3 s^{-1})	Efficiency (l-$C_3H_3^+$)
Cyclohexane	1. 7(-9)	1.3(-11)	1.5(-9)	1.1
Benzene	1.7(-9) *1.40(-9)[27]*	≤ 5(-13)	1.5(-9)	1.1
Toluene	1.9(-9) *1.75(-9)[27]*	3.8(-11) *1.70(-11)[27]*	1.7(-9)	1.1
Piperidine	2.1(-9)	2.1(-9)	1.7(-9)	1.2
Pyridine	2.2(-9)	2.2(-9)	2.6(-9)	0.85
Pyrimidine	1.8(-9)	1.8(-9)	2.6(-9)	0.69
Pyrrolidine	1.2(-9)	1.2(-9)	2.1(-9)	0.57
Pyrrole	~1.4(-10)	~1.4(-10)	2.2(-9)	0.06
Tetrahydrofuran	~2.3(-10)	~2.3(-10)	2.3(-9)	0.10
Furan	1.4(-9)	4.0(-12)	1.5(-9)	0.93
1,4-Dioxane	2.4(-9)	2.9(-11)	2.4(-9)	1.0

[a] Data needed to calculate the theoretical rate coefficients were obtained from the CRC handbook and the literature[28,29]. The reaction efficiency, k_{exp}/k_{theor}, is included and calculated using the values for the linear isomer.

Suffice to say the efficiencies of the cyclic isomer reactions are often much smaller than those of the linear isomer.

Most of the reactions of l-$C_3H_3^+$ proceed at the gas kinetic rate to within experimental error. However, l-$C_3H_3^+$ reacts with, pyrimidine, pyrrole, pyrrolidine and tetrahydrofuran slower than this but there is no clear reason at this time for this. However, it is also interesting to note that, in the case of the nitrogen heterocycles, the cyclic isomer appears to react at the same rate as the linear isomer so it was not possible to distinguish between them as can be seen in Figure 6.2. The linear and the cyclic isomer also react at the same rate in the case of tetrahydrofuran, albeit slowly. An approximate value is given for the rate coefficients for both pyrrole and tetrahydrofuran. Very little of the $C_3H_3^+$ reacts over the flow rate covered in the reaction. Due to this and the sticky nature of both gases, the rate coefficients reported for these two reactions are approximate values.

6.4.2 ION PRODUCT DISTRIBUTIONS

<u>Hydrocarbon Rings</u>. The product distributions for the reactions involving cyclohexane, benzene and toluene are listed in Table 6.2. $C_3H_3^+$ reacts with cyclohexane only by abstracting a hydride ion. It is evident from looking at the decay of the primary ion that only one $C_3H_3^+$ isomer reacts rapidly with cyclohexane. The reaction of $C_3H_3^+$ with benzene has been studied before and was repeated here to determine the percentage of each $C_3H_3^+$ isomer produced in our ion source. As in the literature, we only observed the linear isomer reacting at an appreciable rate. In fact, of all the c-$C_3H_3^+$ rate coefficients that we measured this one was the slowest at $< 10^{-13}$ cm^3 s^{-1}. This
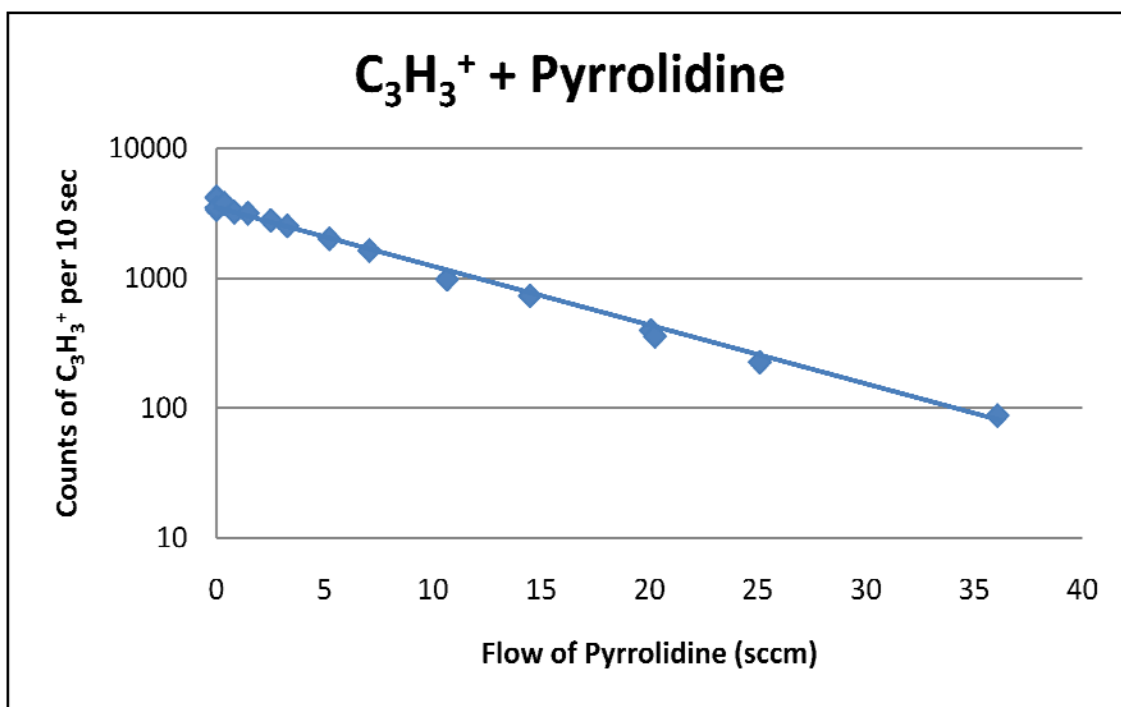
Figure 6.2 The decay of the primary ion, $C_3H_3^+$, as it reacts with pyrrolidine is shown here as the log(counts of $C_3H_3^+$) versus the flow of neutral pyrrolidine. This data is representative of the $C_3H_3^+$ reactions with nitrogen heterocyclic molecules. The only exception to this situation is the reaction involving pyrrole. Both linear and cyclic isomers react at the same rate but this is much slower than the other nitrogen heterocyclic reactions.

Table 6.2 Percentage ion product distributions for the reactions of linear $C_3H_3^+$ with the listed cyclic hydrocarbons

Neutral Reactant	Ion Products	Product Channel	Yield
Cyclohexane C_6H_{12} 686.9 kJ/mol 9.88 eV	$C_6H_{11}^+$	HA	100%
Benzene[a] C_6H_6 750.4 kJ/mol 9.24 eV	$C_6H_6{*}C_3H_3^+$ $C_6H_7^+$	A PT	84% 16%
Toluene C_7H_8 784 kJ/mol 8.83 eV	$C_7H_8{*}C_3H_3^+$ $C_9H_7^+$ $C_{10}H_9^+$ $C_{10}H_8^+$	A AF AF AF	43% 28% 17% 12%

[a]The reaction of $C_3H_3^+$ and benzene in the literature where the products in an ICR study are reported as $C_7H_7^+$ and $C_9H_7^+$.[25] No branching ratio was given. Ionization energies (eV) and proton affinities (kJ/mol) are given below each neutral molecular species. The recombination energy of linear $C_3H_3^+$ is given as 8.67 eV. The recombination energy of cyclic $C_3H_3^+$ is given as 6.6 eV and the proton affinity of $c\text{-}C_3H_2$ used is 941 kJ/mol. Product channels are indicated in the following manner: hydride ion abstraction (HA), charge transfer (CT), proton transfer (PT), association with fragmentation (AF), and association (A).

value is at the limit of our apparatus and thus only an upper limit of the reaction can be reported. Here the major product channel is the association complex formed between the ion and neutral. Also, a small proton transfer channel is observed. The products given in the literature[25] are $C_7H_7^+$ and $C_9H_7^+$. These are fragments that must result from the fragmentation of the association ion. It is not surprising that these ions are not seen in the present study since the previous study was conducted in an ICR at low pressure. Therefore the colllisional stabilization of association complexes cannot occur in the ICR as it does in the SIFT. However, it was surprising that no proton transfer was observed in the ICR study since a discernable channel was detected in the present study. The reaction with toluene results mainly in the association complex. However, it appears that the association complex is less stable than that formed in the benzene reaction since the association product channel is much smaller and there are several product masses that are attributed to the fragmentation of the association complex. Apparently, after the ion and the neutral come together, rearrangements occur that result in the loss of small stable molecules like CH_4 and H_2. Note though that 100% of the product distribution involves the association complex. Like the other two hydrocarbon rings, only l- $C_3H_3^+$ reacts with toluene at the gas kinetic rate.

Nitrogen Heterocycles. Five ring compounds containing at least one nitrogen atom were studied. The product distributions for pyridine, pyrimidine, piperidine, pyrrole and pyrrolidine are given in Table 6.3. Each reaction exhibits a large amount of association. The largest association product channel occurs in the reaction with

Table 6. 3 Percentage ion product distributions for the reactions of $C_3H_3^+$ with the listed nitrogen heterocyclic molecules. Since c-$C_3H_3^+$ reacts with all of the nitrogen compounds, these product distributions listed are for a 70:30 ratio of cyclic to linear isomer.

Neutral Reactant	Ion Products	Product Channel	Yield
Piperidine	$C_5H_{11}N*C_3H_3^+$	A	76%
$C_5H_{11}N$	$C_5H_{11}NH^+$	PT	24%
954 kJ/mol			
8.03 eV			
Pyridine	$C_5H_5N*C_3H_3^+$	A	80%
C_5H_5N	$C_5H_5NH^+$	PT	20%
930 kJ/mol			
9.26 eV			
Pyrimidine	$C_4H_4N_2*C_3H_3^+$	A	89%
$C_4H_4N_2$	$C_4H_4N_2H^+$	PT	11%
885.8 kJ/mol			
9.33 eV			
Pyrrolidine	$C_4H_9N*C_3H_3^+$	A	69%
C_4H_9N	$C_4H_8N^+$	HA	13%
948.3 kJ/mol	$C_4H_9NH^+$	PT	12%
8.77 eV	$C_4H_9N^+$	CT	6%
Pyrrole	$C_4H_5N*C_3H_3^+$	A	84%
C_4H_5N	$C_4H_5N^+$	CT	16%
875.4 kJ/mol			
8.21 eV			

Additional information is as in Table 2

pyrimidine with an 89% abundance. The least amount of association involves pyrrolidine but still with a substantial abundance of 69%. Unlike the hydrocarbon rings, both isomers of $C_3H_3^+$ react with the nitrogen containing rings. This is not unexpected since c- $C_3H_3^+$ is known to react rapidly with nitrogen containing compounds like CH_3CN^{24} and amines[3] through several mechanisms including hydride abstraction and association. In addition to association, the reactions of pyridine, piperidine, and pyrimidine also show a small product channel of proton transfer. The pyrrole reaction has a small charge transfer product channel along with the association product. The pyrrolidine reaction with $C_3H_3^+$ results not only in association but also in proton transfer, charge transfer and hydride abstraction.

Oxygen Heterocycles. Three oxygen containing rings, dioxane, furan and tetrahydrofuran, were studied and the product ion distributions of these are given in Table 6.4. The amount of association is much less in these compounds relative to the cyclic hydrocarbons and the nitrogen heterocycles. Dioxane only has a 37% association channel followed by two fragmentation channels, hydride abstraction, and proton transfer. Furan has an even smaller association channel at only 5%. However, the two most abundant channels are due to fragmentation of the association complex and together they account for 83% of the products. Proton transfer is present in a small abundance. In reactions involving tetrahydrofuran, the major product is hydride ion abstraction with an abundance of 40%. The association channel is the next most abundant at 36% which is very similar to the amount of association in the dioxane reaction. Proton transfer accounts for the remaining 24% of the product abundance.

Table 6.4 Percentage ion product distributions for the reactions of $C_3H_3^+$ with the listed oxygen heterocyclic molecules.   In the reaction involving tetrahydrofuran, both $C_3H_3^+$ isomers react so the product distribution is for a 70:30 cyclic to linear ratio.

Neutral Reactant	Ion Products	Product Channel	Yield
Tetrahydrofuran	$C_4H_7O^+$	HA	40%
C_4H_8O	$C_4H_8O*C_3H_3^+$	A	36%
822 kJ/mol	$C_4H_8OH^+$	CT	24%
9.4 eV			
Furan	$C_5H_2O^+$, $C_6H_6^+$	AF	42%
C_4H_4O	$C_5H_3O^+$, $C_6H_7^+$	AF	41%
803.4 kJ/mol	$C_4H_4OH^+$	PT	12%
8.88 eV	$C_4H_4O*C_3H_3^+$	A	5%
1,4-Dioxane	$C_4H_8O_2*C_3H_3^+$	A	37%
$C_4H_8O_2$	$C_4H_9O^+$, $C_3H_5O_2^+$	AF/F	17%
797.4 kJ/mol	$C_4H_7O_2^+$	HA	18%
9.19 eV	$C_5H_7O^+$, $C_4H_3O_2^+$, $C_6H_{11}^+$	AF/F	14%
	$C_4H_8O_2H^+$	PT	14%

Additional information is as in Table 2

6.5 DISCUSSION

As noted in the introduction, the $C_3H_3^+$ ion has undergone much scrutiny. There are several instances in the literature where the reactions of the $C_3H_3^+$ isomers with small acyclic hydrocarbon, nitrogen containing and oxygen containing molecules have been studied[15,21,24,30]. In the majority of these cases only l-$C_3H_3^+$ was seen to react and the dominant reaction mechanism is association. c- $C_3H_3^+$ is known to be unreactive with most species but was shown previously to react with NO[15], CH_3CN[24], and C_2H_5CN[31] and in all cases the product channel was association. The present study is the first of its kind that involves the reaction of $C_3H_3^+$ with such a diverse and extensive number of cyclic compounds. Firstly, both five membered and six membered are present. Secondly, both homocyclic and heterocyclic molecules are represented with both nitrogen and oxygen present as the heteroatom. Lastly, the molecules can also be labeled as aromatic and non-aromatic and this difference in stability and availability of π electrons may affect the reactivity of the rings as was seen in the CH_3^+ study.

In the present study, the major product channel is association in 6 of the 11 reactions (piperidine (76%), pyridine (80%), pyrimidine (89%), pyrrolidine (69%), pyrrole (84%), benzene (84%)). In three of the remaining five reactions there is a large amount of association with concerted fragmented. This can be determined because the product mass has a higher mass than either the neutral or ion separately. If the association with fragmentation and the association products channels are summed, it accounts for the majority of the product distribution in these three reactions (furan (88%), 1,4-dioxane (68%), and Toluene (100%). In only two reactions is association or fragmentation

related to the association not the dominate product channel; cyclohexane (0%) and

tetrahydrofuran (36%). In the cases where both isomers react we were not able to

isolate the isomers so the product distribution includes contributions from both isomer

(in the 70:30 cyclic to linear ratio). Evidently, l-$C_3H_3^+$ reacts very similarly with rings as it

does with acyclic species. Since association seems to be large in most reactions, the

availability of π electrons, the presence of a heteroatom and the two different ring sizes

does not seem to have much of an effect on the product distributions.

The biggest effect is seen in the rate coefficients for c- $C_3H_3^+$. It was noted by

Ausloos et. al. that c- $C_3H_3^+$ reacts with unsaturated molecules having four or more

carbon atoms (excluding linear or branched hydrocarbons) as well as aldehydes and

amines by association and in some cases hydride transfer.   Some of the neutrals

appeared, at first glance, to undergo no reaction with c- $C_3H_3^+$. A closer inspection, and

with the help of the model described earlier, it became apparent that c- $C_3H_3^+$ was

reacting very slowly ($\sim 10^{-11}$ cm^3 s^{-1}) with cyclohexane, toluene, and 1,4-dioxane. The

cyclic isomer reacted even more slowly with furan ($\sim 10^{-12}$ cm^3 s^{-1}). There was essentially

no reaction between benzene and the cyclic isomer ($\leq 10^{-13}$ cm^3 s^{-1}). When comparing

the reactions in the present study to those in the literature, c- $C_3H_3^+$ is much more

reactive with the cyclic molecules. This could be due to the fact that most of the

previous reactions were studied using an ICR. If c- $C_3H_3^+$ is reacting via an association

complex, the higher pressures of a SIFT would afford more stabilization making the

complex less likely dissociate to reactants. Also, the c- $C_3H_3^+$ is sure to be in its ground

vibrational state before it comes in contact with the neutral gas by undergoing

approximately 10^7 collisions with the carrier gas and this would increase the stabilization of the association complex.

In addition to this general reactivity with the ring compounds, we observed c-$C_3H_3^+$ reacting rapidly (10^{-9} cm^3s^{-1}) with the nitrogen heterocyclic molecules pyridine, pyrimidine, piperidine, and pyrrolidine. In the reactions with pyridine and piperidine $C_3H_3^+$ reacts very close to the collision rate. In the reactions of pyrrolidine and pyrimidine, l- $C_3H_3^+$ reacts at a comparatively rapid rate but not as fast as the gas kinetic limit. In the reaction with pyrrole both isomers react with the same rate coefficient (1.4 x 10^{-10} cm^3s^{-1}). However, unlike the other nitrogen heterocycles the reaction does not proceed even close to the gas kinetic rate. The reaction is only 6% efficient when compared to the theoretical collisional value. The same situation occurs in the tetrahydrofuran reaction. Both isomers react with the same rate coefficient (2.3 x 10^{-10} cm^3s^{-1}) but the reaction is much slower than in the other oxygen heterocyclic reactions. This reaction is an order of magnitude lower than the upper limit theoretical value. This is the only reaction of those involving an oxygen heteroatom where the cyclic isomer reacts this rapidly with a rate coefficient on the order of 10^{-10} cm^3s^{-1}. Conversely, it is also the only one of the three reactions that the linear isomer reacts so slowly.

In a previous study, we noted that association was competing with proton transfer even when proton transfer was energetically favorable[32]. In the present study, the proton transfer product channel is present in most of the reactions but in a much smaller abundance compared to association. Analysis of the energetics of proton transfer was hampered by the lack of key thermodynamic information. The proton

affinity of the cyclic isomer of C_3H_2 is given as 941 kJ/mol[33]. This proton affinity is larger than the proton affinities of all of the rings except for piperidine. No value for the proton affinity of the linear isomer of C_3H_2 is available but there were several cases where l- $C_3H_3^+$ reacts with molecules with proton affinities lower than those of the rings used in this study and proton transfer was observed. For instance, reactions with H_2O (PA= 691 kJ/mol)[24], NH_3(853.6 kJ/mol)[24], CH_3OH (754.3 kJ/mol)[34], C_2H_5OH (776 kJ/mol)[27] all had a proton transfer product channel. This indicates that proton transfer is an energetically accessible product channel in all of the reactions studied here.

6.6 COMPARISON TO CH_3^+ PRODUCTS

A comparison with products from our previous CH_3^+ study[32] to the products obtained in the present study is given in Table 6.5. In the CH_3^+ reactions, only those involving an aromatic ring resulted in the association of the ion and neutral. In contrast, the present study shows association as a product channel for every ring except cyclohexane. The availability of π electrons does not seem to be necessary to form an association complex with $C_3H_3^+$. Also, overall in the reactions of $C_3H_3^+$, the amount of fragmentation of the rings is very low. This could be explained by considering the recombination energies (RE) of each ion. CH_3^+ has an RE of 9.84 eV while l- $C_3H_3^+$ has an RE of only 8.67 eV. In the CH_3^+ study, charge transfer was expected and was seen as a product channel. Excess energy left over from the charge transfer is likely contributed to the fragmentation of the ring. While with reactions involving l- $C_3H_3^+$, charge transfer is energetically favorable with only two neutral species and the reactions are close to

Table 6.5 A comparison of percentage ion product distributions for the reactions of CH_3^+ and $C_3H_3^+$ with the indicated neutrals.

	CH_3^{+32}						$C_3H_3^+$					
	F	HA	CT	PT	AF	A	F	HA	CT	PT	AF	A
Cyclohexane	14%	68%	18%					100%				
Piperidine	40%	34%	22%	4%						24%		76%
Pyrrolidine	46%	32%	18%	4%				13%	6%	12%		69%
1,4-Dioxane	67%	14%	19%					18%		14%	31%	37%
Tetrahydrofuran								40%		24%		36%
Benzene	5%	31%	17%		39%	8%				16%		84%
Toluene											57%	43%
Pyridine		20%	21%	9%		50%				20%		80%
Pyrimidine	24%	19%	25%	9%		24%				11%		89%
Pyrrole	21%		64%	7%		8%			16%			84%
Furan		74%	26%							12%	83%	5%

Product channels are indicated in the following manner: fragment (F), hydride abstraction (HA), charge transfer (CT), proton transfer (PT), association with fragmentation (AF), and association (A).

thermoneutral. In fact, the only reaction that has product masses possibly identified as

fragmentation of the ring is the 1,4-dioxane reaction. However, it is most likely that the

fragmentation is due to the breakup of the association complex. Because the ring has

two heteroatoms one mass can often be identified by several different molecular

formulas. For example, the product mass peak at 73 amu could be identified as either

of the following

$$C_3H_3^+ + C_4H_8O_2 \rightarrow C_4H_9O^+ + C_3H_2O \qquad (6.4)$$

or

$$C_3H_3^+ + C_4H_8O_2 \rightarrow C_3H_5O_2^+ + C_4H_6 \qquad (6.5)$$

Reaction 6.4 requires the loss of an oxygen atom and the acquisition of a hydrogen atom

to the dioxane molecule while reaction 6.5 requires the loss of a CH_3 neutral.

Fragmentation is not expected to occur considering charge transfer is not favorable in

this reaction so neither of these processes are likely to occur without an intermediate

association complex to assist in rearrangement and fragmentation. Unfortunately,

there was no way to calculate which product is more energetically favorable due to

insufficient data in the literature. In the case of CH_3^+ versus $C_3H_3^+$ reactions resulting in

fragmentation, the reactions of the latter does not have enough energy to drive

fragmentation with the studied rings. Instead, the low energy of the system translates

into a very stable association complex that does not require the presence of π electrons

to stabilize the complex as is required in the case of CH_3^+ associations with the same

neutrals.

Proton transfer and hydride abstraction are product channels seen in both studies. However, there was not as much proton transfer for the CH_3^+ reactions as for the $C_3H_3^+$ reactions. As stated above, there is incomplete data in the literature concerning the PA of l- $C_3H_3^+$ so the driving force of this reaction and the presence of a proton transfer product channel in all but three reactions cannot be discussed in depth. Hydride abstraction is only observed in four of the reactions with $C_3H_3^+$ whereas all but one reaction with CH_3^+ shows hydride abstraction as a product channel. Consequently, hydride abstraction in the CH_3^+ reactions results in the very stable neutral CH_4 molecule. The hydride ion affinities (HIA) of cyclohexane, pyrrolidine, 1,4-dioxane, and tetrahydrofuran are all lower than that of $C_3H_3^+$ and thus accounts for the observations of this product channel[35].

6.7 CONCLUSIONS

The reactivity of both linear and cyclic $C_3H_3^+$ with several linear molecules has previously been studied in some depth, mostly using an ICR. The present study involves the reactivity of both isomers with several different type of cyclic molecules in the higher pressure environment of the SIFT. The major products in all but two reactions was the association or association with concerted fragmentation. l- $C_3H_3^+$ tends to react at or near the gas kinetic rate except for the reaction involving pyridine, pyrimidine, pyrrolidine, pyrrole and tetrahydrofuran where it reacts more than 30% lower than the theoretical upper limit. The c- $C_3H_3^+$ isomer proves to be slowly reactive with all of the hydrocarbon homocyclic and oxygen heterocyclic species studied except benzene with

which it is nonreactive. The cyclic isomer proves to be very reactive with the nitrogen heterocyclic species.

These data have implications to the much scrutinized atmosphere of Titan. A peak corresponding to the mass of $C_3H_3^+$ has been identified in the mass scans taken of Titan's ionosphere. It is one of the most abundant peaks in the scan with a density approximately 90 cm^{-3}. A recent model calculated the cyclic and linear $C_3H_3^+$ densities as 34 cm^{-3} and 1.8 cm^{-3}, respectively[1]. Here the only loss channel for c-$C_3H_3^+$ is the electron recombination. However, the present study shows that in the high pressure (0.5 torr) environment of the SIFT, c-$C_3H_3^+$ has the possibility of reacting with ring compounds at an appreciable rate, especially those containing nitrogen. The total number density in Titan's atmosphere ranges from ~10^{10} cm^3 s^{-1} at an altitude of 1000 km[36] to and nitrogen containing ring compounds are likely to exist so these association reactions should be considered when forming models that include c-$C_3H_3^+$. This becomes especially true as models for lower altitudes are developed where pressure increases closer to Titan's surface. It must be noted that the information collected in this study does not explain why the model mentioned above underestimates the abundance of the peak at m/z 39 by a factor of 3. In fact, increased reactivity of c- $C_3H_3^+$ in the model would decrease the density calculated as this additional loss channel is introduced making the agreement even worse.

The data received from the extended Cassini Mission have transformed the old perceptions and models of Titan due to the complex organic compounds, nitrogen

containing species, and large negative ions indicated by the myriad of instruments aboard the Cassini Orbiter. In spite of all of the new data, there is still a lot of uncertainty about Titan's atmosphere since the identities of most of the chemical species have not been established. The models created must assume chemical formulas dependant on the information known such as the neutral composition and the ionization of these neutrals. The models build up the larger masses from this starting point through various reaction pathways. However, if a reaction pathway is missed this could affect the entire model. This emphasizes how important it is for each reaction possible to take place in Titan's atmosphere be studied in the laboratory. The data collected in the present study identifies reaction pathways that have not been considered but given the conditions of Titan's atmosphere might very well be important.

6.8 ACKNOWLEDGEMENT

6. 9 REFERENCES

1.   Vuitton, V.; Yelle, R. V.; McEwan, M. J. *Icarus* **2007**, *191*, 722.

2.   Breslow, R.; Yuan, C. *J.Am.Chem.Soc.* **1958**, *80*, 5991.

3.   Ausloos, P.; Lias, E. S. G. *J. Am. Chem. Soc.* **1981**, *103*, 6505.

4.   Burgers, P. C.; Homes, J. L.; Mommers, A. A.; Szulejko, J. E. *J. Am. Chem. Soc.* **1984**, *106*, 521.

5.   Radom, L.; Hariharan, P.; Pople, J. A.; Schleyer, P. v. R. *J. Am. Chem. Soc.* **1976**, *98*, 10.

6.   Cameron, A.; Leszczynski, J.; Zerner, M. C. *J. Phys. Chem.* **1989**, *93*, 139.

7.   Richter, H.; Howard, J. B. *Prog. Energy Combust. Sci.* **2000**, *26*, 565.

8.   Miller, J. A.; Pilling, M. J.; Troe, J. *Proc. Combust. Inst.* **2005**, *30*, 43.

9.   Hall-Roberts, V. J.; Hayhurst, A. N.; Knight, D. E.; Taylor, S. G. *Combust. Flame* **2000**, *120*, 578.

10.   Wheeler, S. E.; Robertson, K. A.; Allen, W. D.; Schaefer III, H. F.; Bomble, Y. J.; Stanton, J. F. *J. Phys. Chem. A* **2007**, *111*, 3819.

11.   Matthews, H. E.; Irvine, W. M. *Ap. J.* **1985**, *298*, L61.

12.   Thaddeus, P.; Vrtilek, J. M.; Gottlieb, C. A. *Ap. J.* **1985**, *299*, L63.

13.   Adams, N. G.; Smith, D. *Ap. J.* **1987**, *317*, L25.

14.   Smith, D.; Adams, N. G. *Int. J. Mass Spectrom. Ion Proc.* **1987**, *76*, 307.

15.   Scott, G. B. I.; Milligan, D. B.; Fairley, D. A.; Freeman, C. G.; McEwan, M. J. *Journal of Chemical Physics* **2000**, *112*, 4959.

16.   Atreya, S. *Science* **2007**, *316*, 843.

17.   Adams, N. G.; Smith, D. *Int. J. Mass Spectrom. Ion Phys.* **1976**, *21*, 349.

18.   Adams, N. G.; Smith, A. D. Flowing Afterglow and SIFT. In *Techniques for the Study of Ion-Neutral Reactions* Farrar, J. M., Saunders, J. W. H., Eds.; Wiley-Interscience: New York, 1988; pp 165.

19.   Fondren, L. D.; McLain, J. L.; Jackson, D. M.; Adams, N. G.; Babcock , L. M. *Int. J. Mass Spectrom.* **2007**, *265*, 60.

20.   Adams, N. G.; Smith, D. *J. Phys. B* **1976**, *9*, 1439.

21.   Scott, G. B. I.; Fairley, D. A.; Freeman, C. G.; McEwan, M. J.; Anicich, V. G. *J. Phys. Chem. A* **1999**, *103*, 1073.

22.   Anicich, V.; Blake, G.; Kim, J. K.; McEwan, M. J.; Huntress, W. T. *J. Phys. Chem.* **1984**, *88*, 4608.

23.   Bone, L. I.; Futrell, J. *Journal of Chemical Physics*
       1967, *47*, 4366.

24.   McEwan, M. J.; McConnell, C. L.; Freeman, C. G.; Anicich, V. *J. Phys. Chem.* **1994**, *98*, 5068.

25.   Smyth, K. C.; Lias, E. S. G.; Ausloos, P. *Combustion Science and Technology* **1982**, *28*, 147.

26.   Su, T.; Chesnavich, W. J. *J. Chem. Phys.* **1982**, *76*, 5183.

27.   Anicich, V. *An Index of the Literature for Bimolecular Gas Phase Cation-Molecule Reaction Kinetics: JPL Publication 03-19*; Jet Propulsion Laboratory: Pasadena, 2003.

28.   *CRC Handbook of Chemistry and Physics*; 77 ed.; Lide, D. R., Ed.; CRC Press, Inc.: New York, 1996-1997.

29.   Sun, J.; Bohme , D. K. *Int. J. Mass Spectrom.* **2000**, *195/196*, 401.

30.   Scott, G. B. I.; Fairley, D. A.; Freeman, C. G.; McEwan, M. J.; Adams, N. G.; Babcock, L. M. *J. Phys. Chem. A* **1997**, *107*, 4973.

31.   Edwards, S. J.; Freeman, C. G.; McEwan, M. J. *International Journal of Mass Spectrometry* **2008**, *272*, 86.

32.   Fondren, L. D.; Adams, N. G.; Stavish, L. *J. Phys. Chem. A* **2009**, *113*, 592.

33.   Maclagan, G. A. R. *Theochem* **1992**, *258*, 175.

34.   Prodnuk, S. D.; Gronert, S.; Bierbaum, V. M.; DePuy, C. H. *Org. Mass Spectrom.* **1992**, *27*, 416.

35.   Mckee, C., Personal Communication.

36.   Cravens, T. E.; Yelle, R. V.; Wahlund, J.-E.; Shemansky, D. E.; Nagy, A. F. Composition and Structure of the Ionosphere and Thermosphere. In *Titan from Cassini-Huygens*; Brown, R. H., Lebreton, J.-P., Waite, J. H., Eds.; Springer: Dordrecht, 2009; pp 259.

CHAPTER 7

REACTIONS OF CH_3^+ AND $C_3H_3^+$ OF RELEVANCE TO THE TITAN ATMOSPHERE[1]

7.1 INTRODUCTION

The formation of large, multi-ring molecules in the atmosphere of Titan is thought to start with the formation of benzene and continue by the successive H atom removal and acetylene addition[2] to the neutral benzene.   Benzene, in turn, is proposed to form through the recombination of propargyl radicals, C_3H_3. Just recently it was proposed that benzene must also be formed through several ion-neutral reactions[3] to account for the larger than expected number density detected by the INMS aboard the Cassini orbiter. A model by Vuitton details thirteen ion-neutral reactions that could be involved in the formation of benzene[3]. Since neutral benzene is so abundant and is believed to play such an important role in formation of larger and multi-ring compounds, reactions of benzene with abundant Titan hydrocarbon ions should be investigated. If the reaction between ions and benzene can form a stable association complex this could indicate an alternative pathway to building larger molecules. Interestingly, a mass corresponding to toluene (a benzene with a CH_3 group substituent, $C_6H_5CH_3$) has been recently discovered[3,4] in Titan's atmosphere. Models have suggested that toluene is formed by the radical reactions

$$C_3H_3 + C_4H_5 + M \rightarrow C_7H_8 + M \tag{7.1}$$

or

$$C_6H_5 + CH_3 + M \rightarrow C_7H_8 + M \tag{7.2}$$

However, a previous SIFT study by our group (Chapter 5) shows that the following ion-neutral reaction

$$CH_3^+ + C_6H_6 \rightarrow C_7H_9^+ \tag{7.3}$$

is quite rapid. This gives protonated toluene which could then undergo dissociative electron recombination or a proton transfer reaction to a molecule with a higher proton affinity to form C_7H_8. CH_3^+ is known to be an abundant ion in the Titan ionosphere being formed via the prolific methane chemistry. So considering the availability of the two reactants and the high number densities in Titan's atmosphere (10^{10} cm^{-3}), the probability of this collisionally stabilized association reaction taking place is favorable. Note it was originally believed radical recombination reactions were the only source of benzene and this has now been disproved. In light of this, it is possible that toluene can be formed through ion-molecule chemistry. If this is the case, then there is the possibility that larger, multi-ring species could also be formed through ion-molecule reactions involving benzene as the neutral.

Another recent study (Chapter 6) has shown that neutral benzene will react with $C_3H_3^+$ to form the $C_6H_6 \bullet C_3H_3^+$ association complex. $C_3H_3^+$ has been shown to exist in the mass spectra obtained by the Ion-Neutral Mass Spectrometer aboard the Cassini Orbiter

by the presence of a peak at m/z 39. Consequently, this is one of the most abundant ion peaks detected. Interestingly, the resulting ion product has a chemical formula of $C_9H_9^+$. This formula could correspond with the protonated form of one of the eight structures listed in the NIST WebBook or even a structure not yet considered. However, it is worth noting that one of the structures listed is the multi-ring species indene.

Due to the importance of both CH_3^+ and $C_3H_3^+$ in Titan's atmosphere several ion-neutral reactions between these ions and cyclic species have been studied previously. In this study, the reactions of CH_3^+ with benzene and CH_3^+ with pyridine have been studied in more depth. The products formed from these two reactions have been reacted further with the three most abundant neutral species in Titan's atmosphere; N_2, CH_4 and H_2. The information gathered from these studies help determine if the number density of the products will be large enough to facilitate detection in Titan's atmosphere. Reactions with pyridine are considered because of the possible mass identification of this nitrogen containing cyclic species. Knowing that cyclic species are present in Titan's atmosphere and that both HCN and $HCNH^+$ are very abundant increases the probability that nitrogen containing cyclic species, such as pyridine, are also formed.

In addition to the reactions mentioned above, it is important to determine how competitive the ion-neutral reaction will be in Titan's ionosphere. If the ion involved in reaction is removed via electron recombination before it has the chance to react with neutrals then looking for products of the reaction will not be successful. So here we

provide a numerical analysis of the rate equations that govern the kinetics of each reaction. The analysis will consider the competition between a generic association product channel formed with a ring neutral (such as occurs during the reactions of CH_3^+ and $C_3H_3^+$ with benzene) and the electron recombination of the same ion.

7.2 EXPERIMENTAL

A selected ion flow tube (SIFT) was used to study the following reaction sequences with CH_3^+: $CH_3^++C_6H_6+N_2$, $CH_3^++C_6H_6+CH_4$, $CH_3^++C_6H_6+H_2$, $CH_3^++C_5H_5N+N_2$, $CH_3^++C_5H_5N+CH_4$, and $CH_3^++C_5H_5N+H_2$. The CH_3^+ was created by electron impact on methane gas in a low pressure ionization source. The SIFT technique has been discussed in detail previously and will not be repeated here[5,6]. Specific to this experiment, benzene neutral gas was injected into the flow tube at the long injection port corresponding to a reaction length of 83.6 cm. The second neutral gas, N_2, CH_4 or H_2, was injected in the short injection port which is 53.8 cm downstream of the long port. This gave the most time possible to allow CH_3^+ to react with benzene. The benzene neutral gas flow was kept constant at a value that reacted away most of the CH_3^+ present. The masses of the products of the CH_3^+/benzene reaction were followed as a function of the second neutral flow. Rate coefficients were determined for these reactions. The same procedure was followed for the reactions of CH_3^+ with pyridine.

Pyridine was obtained from Sigma Aldrich with a manufactured purity of 99.9+% and benzene was obtained from Fisher Scientific with a purity of 99.5%. To eliminate dissolved gases, the liquids were further purified before use by several cycles of freeze-

pump-thaw. The neat vapors proved difficult to work with due to condensation of the vapors in the neutral reactant flow system and on the flow tube walls, so a 1% mixture of the reactant neutral in helium was used. Nitrogen was obtained from BOC Gases with a purity of 99.999%. Methane and hydrogen were obtained from National Specialty Gases with purities of 99.997% and 99.999%, respectively.

7.3 RESULTS

7.3.1 Further Reactivity of the Products of CH_3^+ and Benzene

The reaction between CH_3^+ and benzene has been previously studied and has the following product channels: association (8%), association with fragmentation ($C_7H_7^+$,39%), charge transfer (17%), hydride abstraction (31%) and one fragmentation product ($C_5H_5^+$, 5%). The most abundant product was association with fragmentation and the reaction proceeded at the gas kinetic rate (1.9 x 10^{-9} cm^3 s^{-1}). In order to determine the ions and ion abundances present in Titan's atmosphere due to the reaction of CH_3^+ plus benzene the products of that reaction were reacted further with the most abundant neutral constituents on Titan. The rate coefficients determined for the reactions of the product ions with N_2, CH_4 and H_2 are given in Table 7.1.

The reactivity of the CH_3^+/benzene product ions with molecular nitrogen was monitored for a large flow of nitrogen. $C_5H_5^+$ and $C_6H_6^+$ did not react with the nitrogen; however, $C_6H_5^+$ reacted slightly with a rate coefficient of 1.2 x 10^{-11} cm^3 s^{-1}. The rate coefficients for $C_6H_6\bullet CH^+$ and $C_6H_6\bullet CH_3^+$ were not obtained because the

Table 7.1 The rate coefficients for the ion products formed in the CH_3^+ + Benzene reactions with the three listed neutrals. The products from the reaction are listed on the left side of the table. The rate coefficients are given in cm^3 s^{-1}.

	CH_3^+ + Benzene (C_6H_6)		
	N_2	CH_4	H_2
$C_5H_5^+$	≤1.4(-13)	≤4.1(-13)	<1(-13)
$C_6H_5^+$	1.2(-11)	2.6(-10)	4.1(-11)
$C_6H_6^+$	≤5.1(-13)	≤1.4(-13)	≤4.4(-13)
$C_7H_7^+$	--------	<1(-13)	≤1.7(-13)
$C_7H_9^+$	--------	--------	≤2.4(-13)

concentration of both of these products increased when nitrogen was first introduced to the flow tube. After ~ 50 sccm of nitrogen was added, the concentration of the two products began to decrease slightly. The uncertainty in the reason for this increase made it difficult to estimate the best rate equation to use in modeling the situation and prevented the determination of the rate coefficients. The addition of nitrogen to the flow tube could have caused an increase in product concentration in two different ways. First, the addition of large amounts of nitrogen increases the pressure in the flow tube. The association complex between CH_3^+ and benzene is collisionally stabilized by the helium bath gas in the system. The association product channel is due to a three body reaction and if this product channel has not reached a maximum then the increase in pressure would facilitate the additional formation of the association product. Alternatively, N_2 has been known to participate in switching reactions that promote the formation of association complexes. So for this case, if any CH_3^+ is still present in the ion swarm when it reaches the nitrogen injection port then a reaction of this with N_2 could occur. Thus, if the reaction results in the association complex $N_2 \bullet CH_3^+$ there is the possibility then that a switching reaction could occur that replaces the N_2 with a benzene neutral.

In the reactions of the CH_3^+/benzene products with methane, the reactivity was monitored throughout a large methane flow. Again the concentration of the association product increased with the addition of the neutral gas. However, in this case the concentration stayed constant after the initial increase. Interestingly, the association with fragmentation product was not affected and the concentration was constant

indicating no reaction with the neutral methane. $C_5H_5^+$ and $C_6H_6^+$ also appeared to be unreactive with methane. Conversely, $C_6H_5^+$ proved to be very reactive with methane and reacted with a rate coefficient of 2.6 x 10^{-10} cm^3 s^{-1}.

The last reaction involving benzene followed the reactivity of the products of the CH_3^+/Benzene reaction with hydrogen gas. Once again $C_6H_5^+$ proved to be reactive with the neutral gas and a rate coefficient of 4.1 x 10^{-11} cm^3 s^{-1} was obtained.   The other four products were unreactive with hydrogen. The $C_7H_7^+$ and $C_7H_9^+$ products did not increase in concentration as they did previously therefore rate coefficients for these are given. This gives some doubt that the pressure increase alone was the reason for the increase in the ion signals in the other reactions.

7.3.2 Further Reactivity of the Products of CH_3^+ and Pyridine

The reaction between CH_3^+ and pyridine was previously studied and was shown to have the product channels: association (50%), proton transfer (9%), charge transfer (21%), and hydride abstraction (20%). The most abundant product was the association complex and the reaction proceeded at the gas kinetic rate (3.1 x 10^{-9} cm^{-3} s^{-1}). These products were reacted further with nitrogen, methane and hydrogen to determine the fate of these ions in Titan's atmosphere should they exist. The rate coefficients for each reaction are given in Table 7.2. The counts of the product ions were followed over large neutral flow ranges. With nitrogen and hydrogen no reaction occurred and the rate

135

Table 7.2 The rate coefficients for the ion products formed in the CH_3^+ + Pyridine reactions with the three listed neutrals. The products from the reaction are listed on the left side of the table. The rate coefficients are given in $cm^3 s^{-1}$.

	CH_3^+ + Pyridine (C_5H_5N)		
	N_2	CH_4	H_2
$C_5H_4N^+$	≤5.8(-13)	1.6(-11)	≤2.4(-13)
$C_5H_5N^+$	<1(-13)	2.2(-11)	≤2.4(-13)
$C_5H_5NH^+$	≤1.6(-13)	<1(-13)	<1(-13)
$C_6H_9N^+$	≤5.0(-13)	≤1.7(-13)	<1(-13)

coefficients were all on the order of $\leq 10^{-13}$ cm^3 s^{-1}. For methane, both $C_5H_4N^+$ and

$C_5H_5N^+$ reacted to some extent. Rate coefficients of 1.6 and 2.2 10^{-11} cm^3 s^{-1} were
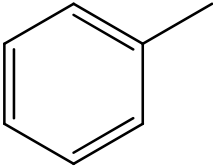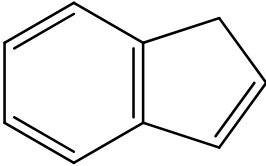
obtained.

7.4 DISCUSSION
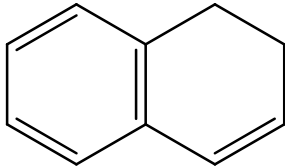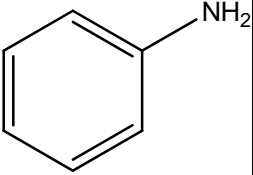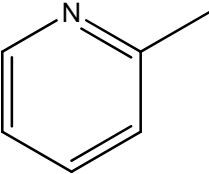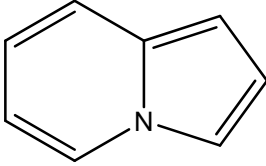
7.4.1 Fate of Products

The Cassini orbiter has flown through the Titan atmosphere more than 60 times

and each time collecting an abundance of data. One of the parameters routinely

measured is the total number density of the neutral atmosphere. As noted before, the

three most abundant neutrals are nitrogen, methane and hydrogen. To determine if the

products of a particular reaction will be present in Titan's atmosphere it is important to

determine how they interact with the neutral atmosphere. In the present study, the

reaction of CH_3^+, one of the more abundant ions present in Titan's atmosphere, with

both benzene and pyridine has been investigated. The products of both reactions are

then further reacted with each of the three most abundant neutral species. The rate

coefficient for each reaction was obtained to determine if the species would survive in

Titan's atmosphere. Of course, reactions with other neutrals present are possible but

are of less significance since the number density of the other neutrals are so much

smaller than those of nitrogen, methane and hydrogen. The $C_6H_5^+$ product arising from

the reaction of CH_3^+ with benzene reacted with all three neutrals with the greatest

reactivity occurring with methane. Therefore the concentration of $C_6H_5^+$ would be very

small compared to the other two ions. There was no reaction with $C_5H_5^+$ and $C_6H_6^+$ with

any of the three neutrals and these ions would build up to an appreciable amount facilitating detection. The situation is the same for the association complex and the fragmented association complex. In the reactions involving the products of the CH_3^+/pyridine reaction both $C_5H_4N^+$ and $C_5H_5N^+$ reacted moderately with methane with rate coefficients on the order of 10^{-11} cm^3 s^{-1}. The proton transfer and association products did not react with methane. None of the products react with either nitrogen or hydrogen. The lack of reaction with nitrogen will prolong the life of the ions since nitrogen is by far the most abundant neutral. Overall, the products of the reaction of CH_3^+ with both benzene and pyridine are not very reactive with the major constituents of Titan's neutral atmosphere. Therefore, detection of these ions should not be hampered by such reactivity.

7.4.2 Competition of Ion-Molecule Reactions with Electron Recombination

When determining the likelihood of detection of product ions of an ion-neutral reactions it is necessary to determine if ion-neutral reaction will be competitive with the electron recombination of the ion. Of most interest here are ion-neutral reactions involving cyclic species that create larger, more massive species. For this to occur the ion and neutral must form a stable association complex. The association complexes formed between CH_3^+ and $C_3H_3^+$ with benzene and with pyridine, and $C_3H_3^+$ with toluene are of the most interest since these neutral rings are of the most importance to the Titan atmosphere. Table 7.3 gives the abundance of each of these association channels and also identifies possible structures for the chemical formula of the association

Table 7.3 Percentage association channels for reactions of CH_3^+ and $C_3H_3^+$ with the three single ring compounds indicated. Product neutral structures are suggested assuming the product ion is the protonated form of each neutral. In some cases many isomer can be assigned to one chemical formula. Listed are the structures containing cyclic species since these are of most interest to this study. Additional isomers can be found in the NIST WebBook[7].

Reactant Neutral	CH_3^+		$C_3H_3^+$	
	% Association	Neutral Product Possibility	% Association	Neutral Product Possibility
Benzene C_6H_6	$C_7H_9^+$ 8%	toluene	$C_9H_9^+$ 84%	Indene
Toluene C_7H_8	-----	-----	$C_{10}H_{11}^+$ 100%	Naphthalene, 1,2-dihydro-
Pyridine C_5H_5N	$C_6H_8N^+$ 50%	aniline methyl pyridine	$C_8H_8N^+$ 80%	Indolizine

complex. Of particular interest is the association complex of CH_3^+ and benzene. This formula could correspond with protonated toluene which has been indicated to be present in Titan's ionosphere by the presence of a peak at m/z 93[3,4]. Theory has shown that CH_3^+ initially interacts with the π electrons in the benzene ring. However, as the CH_3^+ moves closer to the ring it shifts to interact with a carbon in a σ bond[8]. This structure is the same as protonated toluene. In Titan's ionosphere the protonated toluene could undergo electron recombination that results in the ejection of an H-atom to form neutral toluene. This toluene could then react with another CH_3^+ to produce protonated dimethyl, or ethyl, benzene. Successive recombination and association could produce ethyl methyl benzene and diethyl benzene and could possibly lead to the closing of the ring giving a two ring hydrocarbon. Also, the reaction between $C_3H_3^+$ and toluene has been observed to result in an association complex that has a chemical formula that corresponds to 1,2-dihydronapthalene. This type of reaction generates larger molecules with less reaction steps and also provides a route for ring growth by converting single ring compounds to multi-ring compounds.

Detailed modeling is beyond the scope of this chapter, but greater insight can be gained by considering reactions likely to be in competition in Titan's ionosphere and comparing the rate equations that govern these reactions. Solar photoionization and ionization by Saturn's magnetosphere electrons initiates hydrocarbon chemistry that leads to the formation of ions such as CH_3^+ and $C_3H_3^+$. These ions can then react with neutral cyclic species in Titan's atmosphere such as benzene, toluene and pyridine. The

association reactions between the ion and neutral will be stabilized by the very abundant N_2

$$I^+ + Ring + N_2 \underset{k_d}{\overset{k_a}{\leftarrow\rightarrow}} I^+\bullet Ring + N_2 \qquad (7.4)$$

where I^+ is a generic representation for the ion and Ring is a generic representation for the neutral cyclic species, k_a is the forward association rate coefficient and k_d is the reverse collisional dissociation. During this process, the association will compete with dissociative electron recombination of I^+

$$I^+ + e \overset{\alpha_e}{\rightarrow} products \qquad (7.5)$$

where α_e is the electron recombination rate coefficient. For reactions in which association occurs, the product ion, $I^+\bullet Ring$, can then recombine as

$$I^+\bullet Ring + e \overset{\alpha_a}{\rightarrow} products \qquad (7.6)$$

where α_a is the recombination rate coefficient for the association complex. Association will increase in raqpidity when it involves dominant constituents such as N_2,

$$I^+ + 2N_2 \underset{k_d'}{\overset{k_a'}{\leftarrow\rightarrow}} I^+\bullet N_2 + N_2 \qquad (7.7)$$

with forward k_a' and reverse k_d' rate coefficient followed by the exchange of the N_2 molecule for the ring

$$I^+\bullet N_2 + Ring \overset{k_s}{\rightarrow} I^+\bullet Ring + N_2 \qquad (7.8)$$

where k_s is the rate coefficient for this switching reaction. Since the abundant N_2 is involved, the sequential reactions (7.7) and (7.8) are a much more rapid possibility than the direct association reaction (7.4). Kinetic equations can be written for each of these reactions, for example, reaction (7.4) gives

$$\frac{d[I^+]}{dt} = -k_a[Ring][N_2][I^+] \tag{7.9}$$

and reaction (3) gives

$$\frac{d[I^+]}{dt} = -\propto_e [e][I^+] \tag{7.10}$$

To evaluate the competition between the various reactions, the equations can be written in the form of the normalized rates such as

$$\frac{1}{[I^+]}\frac{d[I^+]}{dt} = -k_a[Ring][N_2] \tag{7.11}$$

and

$$\frac{1}{[I^+]}\frac{d[I^+]}{dt} = -\alpha_e[e] \tag{7.12}$$

The rate coefficients and electron recombination rates for each reaction are estimated using values obtained from the literature. The value used for k_a, 2×10^{-26} cm^6 s^{-1}, is taken from an experiment involving the HCN system in which the rate of a three body association was determined[9]. There is no value available for k_d so this reaction will not be evaluated. The value used for α_e, 2×10^{-7} cm^3 s^{-1}, is estimated from the electron recombination rates of small hydrocarbon ions[10]. The electron recombination rate of an

association complex involving a hydrocarbon ion and cyclic species has not been measured. However, the recombination rates of proton bound dimers have been studied and are a suitable approximation for the association complex because a proton bound dimer is likely to compare more closely to the structure of the association complex. Therefore, a value of 10^{-6} cm^3 s^{-1} is estimated for α_a which was averaged from the α_e values obtained for some hydrocarbon proton bound dimers[11]. $k_a{}'$ is estimated as k_a reduced by a factor of 2 to account for the less efficient association of I$^+$ with the more abundant N$_2$. The switching reaction is assumed to react at the gas kinetic rate and thus 10^{-9} cm^3 s^{-1} is used for k_s.

Table 7.4 lists the normalized rates for all of the reactions mentioned above. The concentrations needed to evaluate the rate equations have been obtained from the data collected in the Cassini Mission. Concentrations are estimated for an altitude of 1,000 km which corresponds with Titan's ionosphere[12]. The values used are [N$_2$]= 1 x 10^{10} cm^{-3}, [e]= 10^2 10^3 cm^{-3}, and [Ring]= 10^4 cm^{-3} where [benzene]=[Ring]. Concentrations of neutral toluene and pyridine are not available but will most likely be smaller than the concentration of benzene. So use of the benzene concentration gives us the best set of conditions. Evaluation of the normalized rates shows that the direct association of the ion and ring in reaction (7.4) is not competitive with the electron recombination reaction (7.5). However, a much more competitive process occurs if the ion associates with the abundant N$_2$ present (7.7) and then undergoes a switching reaction (7.8) to replace the N$_2$ with the Ring. If the [N$_2$] and [Ring] are an order of

Table 7.4 Approximate normalized rates, e.g. $\frac{1}{[I+]}\frac{d[I^+]}{dt}$, for reactions (7.4) to (7.8) at the conditions for 1,000 km altitude in the Titan atmosphere. It can be seen that for the higher rates of $[N_2]$ and [Ring], association (reaction (7.7)) is more competitive with recombination (reaction (7.5))

Reaction from text	Normalized Rate s^{-1}	Normalized rates (s^{-1}) at 1,000 km	Rates for $[N_2]$ and [Ring] Increased by 10
(7.4)	$\frac{1}{[I^+]}\frac{d[I^+]}{dt} = -k_a[Ring][N_2]$	2 x 10^{-12}	2 x 10^{-10}
(7.4)*	$\frac{1}{[I^+.Ring]}\frac{d[I^+.Ring]}{dt} = -k_d[N_2]$	---	---
(7.5)	$\frac{1}{[I^+]}\frac{d[I^+]}{dt} = -\alpha_e[e]$	2 x 10^{-5} to 2 x 10^{-4}	2 x 10^{-4} to 2 x 10^{-3}
(7.6)	$\frac{1}{[I^+.Ring]}\frac{d[I^+.Ring]}{dt} = -\alpha_a[e]$	1 x 10^{-4} to 1 x 10^{-3}	1 x 10^{-4} to 1 x 10^{-3}
(7.7)	$\frac{1}{[I^+]}\frac{d[I^+]}{dt} = -k_a'[N_2]^2$	1 x 10^{-6}	1 x 10^{-4}
(7.7)*	$\frac{1}{[I^+.N_2]}\frac{d[I^+.N_2]}{dt} = -k_d'[N_2]$	---	---
(7.8)	$\frac{1}{[I^+.N_2]}\frac{d[I^+.N_2]}{dt} = k_s[Ring]$	1 x 10^{-5}	1 x 10^{-4}

* Indicates the reverse reaction of reactions (7.4) and (7.7).

magnitude larger then reaction sequence (7.7) and (7.8) become comparable with the recombination reactions (7.5) and (7.6). This increase in concentration would still not make the direct association reaction (7.4) competitive with the electron recombination reactions. The reaction sequence of (7.5) and (7.6) will become more dominant with decreasing altitude and the electron recombination of the association complex in reaction (7.6) will be the main channel for loss of ionization. The recombination of the larger species are expected to result in less fragmentation since there will be ample modes to distribute any excess energy remaining from the recombination process. Clearly, these conclusions are only semi-quantitative. An abundance of chemical reactions are likely to be occurring at the same time in Titan's atmosphere and more detailed chemical modeling is necessary to determine exactly which reactions will take place. However, this analysis can act as a guide into directions that the models should explore.

7.5 CONCLUSIONS

The atmosphere of Titan is an intriguing study of simply hydrocarbon chemistry working in tandem with complex chemical reactions producing massive positive, negative and neutral species. The presence of so many chemical species and the inaccessibility of Titan because of its distance from Earth make it difficult to model this environment. However, laboratory experiments are providing the data needed to turn the mass spectra obtained by the INMS aboard Cassini into the identity of the chemical compounds present in the atmosphere. The laboratory data also provide information

on the types of reactions expected to form these compounds. Much of the focus now is on the formation of large ring and multi-ring compounds. The mechanism for this formation is still in debate. The data in the present study provides information on three body association reactions and the conditions needed for this type of reaction to be competitive with the very fast electron ion recombination. However, this study does not address any possible temperature dependence nor does it determine if a saturated three body reaction is occurring. Both temperature and pressure dependant reactions need to be investigated to answer these questions.

7.6 REFERENCES

1.   Adams, N. G.; Mathews, L. D. *Farad. Disc.* **2010**, *Submitted*.

2.   Atreya, S. *Science* **2007**, *316*, 843.

3.   Vuitton, V.; Yelle, R. V.; McEwan, M. J. *Icarus* **2007**, *191*, 722.

4.   Vuitton, V.; Yelle, R. V.; Cui, J. *Journal of Geophysical Research* **2008**, *113*, E05007(1.

5.   Adams, N. G.; Smith, D. *Int. J. Mass Spectrom. Ion Phys.* **1976**, *21*, 349.

6.   Adams, N. G.; Smith, D. Flowing Afterglow and SIFT. In *Techniques for the Study of Ion-Molecule Reactions*; Farrar, J. M., Saunders, J. W. H., Eds.; Wiley Interscience: New York, 1988; pp 165.

7.   http://webbook.nist.gov/chemistry. NIST Chemistry WebBook NIST Standard Database 69 Vol. March 2010.

8.   Ishikawa, Y.; Yilmaz, H.; Yanai, T.; Nakajima, T.; Hirao, K. *Chem. Phys. Lett.* **2004**, *396*, 16.

9.   McLain, J. L.; Molek, C. D.; Osbourne, D.; Adams, N. G. *Int J. Mass Spectrom.* **2009**, *282*, 85.

10.   McLain, J. L.; Poterya, V.; Molek, C. D.; Babcock, L. M.; Adams, N. G. *J. Phys. Chem. A* **2004**, *108*, 6704.

11.   Osborne, D. S.; Adams, N. G. **2010**.

12.   Waite, J. H., Jr.; Young, D. T.; Cravens, T. E.; Coates, A. J.; Crary, F. J.; Magee, B.; Westlake, J. *Science* **2007**, *316*, 870.

CHAPTER 8

CONCLUSIONS AND FUTURE DIRECTIONS

8.1 CONCLUSIONS

Our solar system, and therefore Earth, was formed from a large rotating cloud of interstellar gas and dust. The chemistry occurring in the interstellar medium, where the gas and dust were formed, is intriguing because it provides information about the chemical processes that prompted the formation of life on Earth. Since the development of microwave telescopes, scientists have been searching the skies to determine what chemicals are present. Over 150 chemical species have been discovered to date in the ISM and circumstellar shells[1]! Of particular interest is the discovery of benzene, a 6 carbon aromatic ring compound[2,3]. The formation of ring compounds is important since many biologically active molecules contain cyclic species. For example, thymine ($C_5H_6N_2O_2$), cytosine ($C_4H_5N_3O$) and uracil ($C_4H_4N_2O_2$), three of the nucleotides of DNA and RNA are composed partially of the heterocyclic base pyrimidine ($C_4H_4N_2$), which is a nitrogen containing analogue of benzene. The formation of multi-ring compounds is also under investigation since they are suspected to be responsible for some unidentified diffuse interstellar absorption bands[4-6]. These multi-ring compounds are proposed to be formed through sequential acetylene additions to

benzene. Nitrogen could be incorporated into the ring by the addition of hydrogen cyanide, a common interstellar species. Once these ring systems grow large enough they can start to form particulate matter such as dust and aerosols.

The formation of aerosols and large carbon and nitrogen molecules is especially important when considering the atmosphere of Titan.   Titan has long been of interest to astronomers, partially because it is surrounded by a hazy orange layer that obscures the surface. The recent Cassini mission has penetrated the atmosphere of Titan and discovered that this haze is organic in nature and likely composed of thiolins and polycyclic aromatic hydrocarbons. Titan is of interest to scientists because, like Earth, it has an atmosphere composed mainly of nitrogen (~98% to Earth's ~78%). Therefore, Titan is considered to be a possible model for pre-biotic Earth. The chemistry occurring on Titan centers on the ionization and subsequent reactions of nitrogen and methane (which is the second most abundant neutral in the atmosphere). Titan has been found to have a meteorological cycle similar to that of rain on earth with the water being replaced by methane[7]. Large rivers of methane are purported to exist below Titan's surface[8]. The surface itself is covered over 6 feet deep in organic molecules that are transported from the ionosphere where they are formed, to the lower atmosphere where they condense as snow. The methane rain likely transports these chemicals to the rivers of methane where they can mix freely and possible create more exotic species such as pre-biotic or even biotic molecules. Because of this possibility the identity of the compounds formed in the ionosphere are under intense investigation.   The Cassini orbiter has confirmed the presence of a large number of chemical species through the

use of mass spectrometry, infrared spectroscopy and a plasma spectrometer. Because most of the species were identified with mass spectrometry the identity of the chemical formula and molecular composition of these species is left largely up to educated conjecture and complex models. Because so many chemical species have been detected these models are based on a large number of chemical reactions. Each of these reactions requires a determination of rate coefficients and product distributions that can only be obtained through laboratory experiments, such as the ones presented here. The chemical processes that form Titan's intriguing atmosphere continue to be studied and revised as new data come in from the Cassini Orbiter and from the laboratory. Fortunately, because of its success the Cassini mission has been extended to 2017[9] and an additional 54 flybys of Titan are planned. This will keep both modelers and laboratory chemist busy for years to come.

8.2 FUTURE DIRECTIONS

There are several different directions that need to be followed in the continued investigation of Titan's atmosphere. The reaction of important ions with relevant cyclic species should be completed to aid the models. Two important ions that need to be studied are $C_2H_5^+$ and $HCNH^+$; both are very abundant Titian ions. It will be very interesting to determine if either of these ion associate with benzene, pyridine or pyrimidine. A second area of interest is the completion of the $C_4H_4^+$ + HCN study to determine if this is a viable formation route to pyridine. Identifying other reactions that could lead to the formation of pyridine on Titan is also important. More than one ion-

neutral reaction is thought to contribute to the formation of benzene and the same could apply to pyridine. In addition to single ring molecules, pathways to formation of positive, negative and neutral PAH and PANH need to be studied. The buildup of these larger molecules plays an important role in creating the haze surrounding Titan. The identities of the large molecules present needs to be established and reactions with abundant neutral and ion species in Titan's atmosphere investigated. The difficulty with studying this in the laboratory is the tendency for the molecule to go from liquids with appreciable vapor pressures to a solid when going from a single cyclic rings to multi-ring compounds. Getting these solids in the gas phase is difficult. One of the most common ways is to heat the molecule but this must be done gently lest the compound is fragmented or destroyed. A heated neutral gas source has been built by this laboratory and is awaiting preliminary test. The source is shown in Figure 8.1. One concern about using this source to create the neutral gas is the probability of the heated gas condensing on the flow tube walls (298 K) and clogging the small orifices that are necessary for a successful experiment. Removing clogs, especially hydrocarbon residue, from sub millimeter sized orifices will be difficult, to say the least. A variable temperature SIFT could help overcome some of these problems.

8.3 REFERENCES

1.   Institut, P. Molecules in Space; http://www.astro.uni-koeln.de/cdms/molecules, 2010.

2.   Cernicharo, J.; Heras, A. M.; M., T. A. G. G.; Pardo, J. R.; Herpin, F.; Guelin, M.; Waters, L. B. F. M. *Ap. J.* **2001**, *546*, L123.

3.   Kuan, Y.-J.; Yan, C.-H.; Charnley, S. B.; Kisiel, Z.; Ehrenfreund, P.; Huang, H.-C. *Mon. Not. Roy. Astr. Soc.* **2003**, *345*, 650.

4.   Hudgins, D. M.; Bauschlicher, C. W.; Allamandola, L. J. *Ap. J.* **2005**, *632*, 316.

5.   Leger, A.; d'Hendecourt, L. *Astron. Astrophys.* **1985**, *146*, 81.

6.   Leger, A.; Puget, J. L. *Astron. Astrophys.* **1984**, *137*, L5.

7.   Atreya, S. K.; Lorenz, R. D.; Waite Jr., J. H. Volatile Origin and Cycles: Nitrogen and Methane. In *Titan from Cassini-Huygens*; Brown, R. H., Lebreton, J.-P., Waite Jr., J. H., Eds.; Springer: New York, 2009; pp 177.

8.   Lorenz, R. D.; Stiles, B. W.; Kirk, R. L.; Allison, M. D.; Persi del Marmo, P.; Less, L.; Lunine, J. I.; Ostro, S. J.; Hensley, S. *Science* **2008**, *319*, 1649.

9.   Brown, D. NASA Extends Cassini's Tour of Saturn, Continuing International Cooperation for World Class Science, 2010.
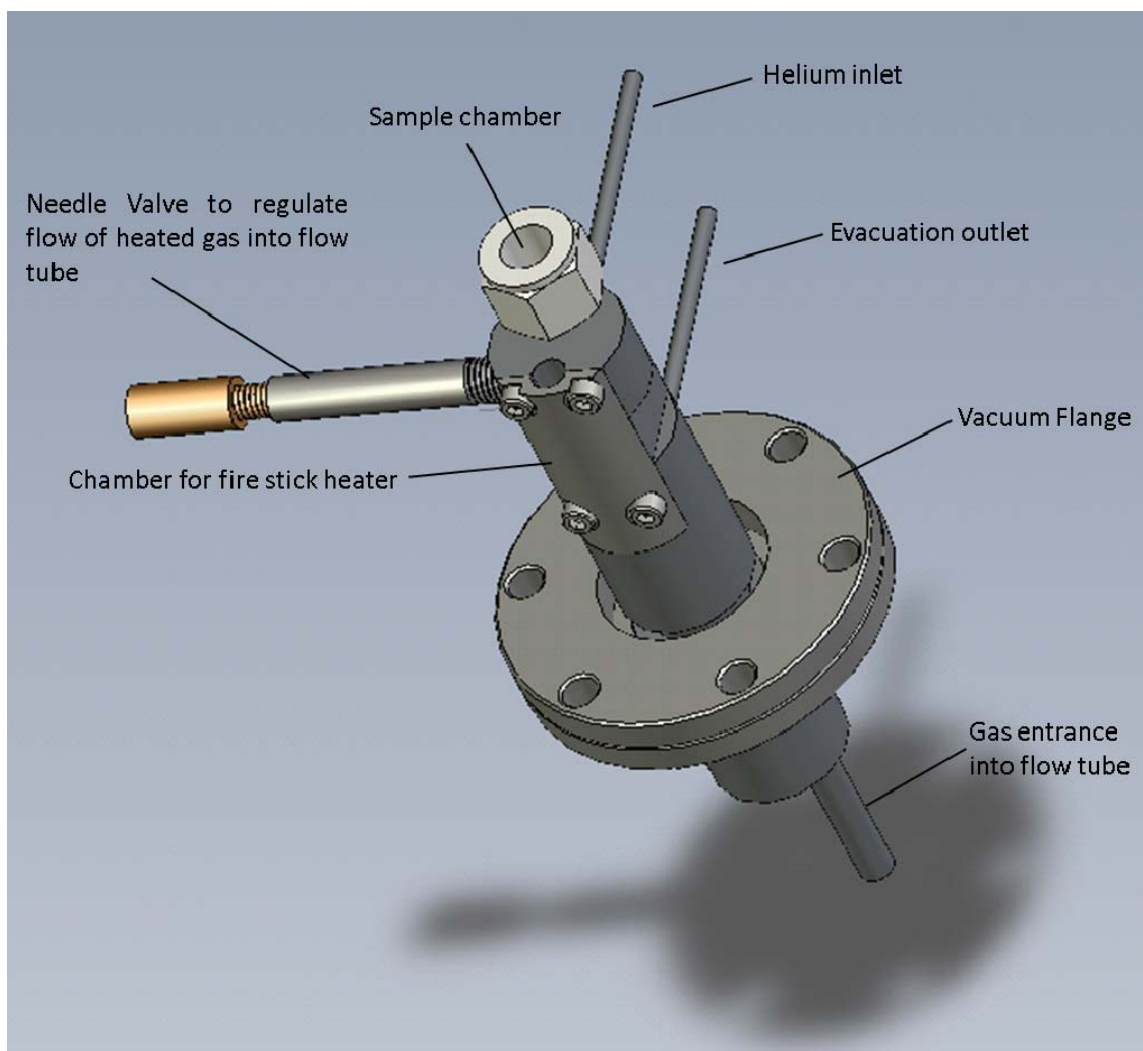
Figure 8.1 A heated neutral gas source. The solid sample is placed in the sample chamber which is enclosed on top by a glass cap. The sample is heated by a resistive fire rod heater which heats up the entire source. When the needle valve is open a small flow of helium carries the gas vapors through an opening within the body of the source. The source is connected to the flow tube with a vacuum flange.